2013

Environmentally persistent free radicals (EPFRs) in $PM_{2.5}$: their contribution to hydroxyl radical formation and atmospheric transformation

William Micheal Gehling, Jr.
Louisiana State University and Agricultural and Mechanical College

Recommended Citation

Gehling, Jr., William Micheal, "Environmentally persistent free radicals (EPFRs) in $PM_{2.5}$: their contribution to hydroxyl radical formation and atmospheric transformation" (2013). *LSU Doctoral Dissertations*. 3291.
https://digitalcommons.lsu.edu/gradschool_dissertations/3291

ENVIRONMENTALLY PERSISTENT FREE RADICALS (EPFRS) IN $PM_{2.5}$: THEIR CONTRIBUTION TO HYDROXYL RADICAL FORMATION AND ATMOSPHERIC TRANSFORMATION

A Dissertation

Submitted to the Graduate Faculty of the
Louisiana State University and
Agricultural and Mechanical College
In partial fulfillment of
the requirements for the degree of
Doctorate of Philosophy

in

The Department of Chemistry

by

William M. Gehling, Jr.
B.S. , Northwestern State University, Natchitoches, LA, 2003
May 2013

To my wife, Jolie Gehling, for all the support and patience

And my son, William Gia Binh Gehling

ACKNOWLEDGEMENTS

Accomplishing my goals of graduate school studies could not have been done alone. Only through the skills, wisdom, and compassion of others could I realize my goals here. Therefore, I would like to send my all my appreciation to them.

At the top of the list, I would like to thank my wife and family for all their support and encouragement throughout my entire graduate career. Without them, I would not have made it this far. I would like to extend my gratitude to my advisor, Dr. Barry Dellinger, for allowing me to join his research group and learn about the fascinating research performed over the years. His scientific achievements in addition to the breadth and depth of knowledge he possesses are an inspiration for me. I am very appreciative for all the help I received from Dr. Slawomir Lomnicki, Dr. Mikhail Bryukov, and Dr. Zofia Maskos. I am deeply indebted to Dr. Lavrent Khachatryan and sincerely appreciate all the time and assistance he has provided me.

I would also like to thank my previous group members Dr. Albert de la Cruz, Dr. Eric Vejerano, and Dr. Hongyi Wu for all the wonderful discussions and assistance in furthering my abilities as a researcher. I thank members of the Dellinger research group, Lucy Kiruri, Joshua Kibet, and Cholena Russo, for all their support and assistance. In addition to my fellow researchers, I would like to acknowledge the moral support Ms. Tina Black has given me over the years.

TABLE OF CONTENTS

LIST OF TABLES

LIST OF FIGURES

LIST OF ABBREVIATIONS

AM	air mass
BSTFA	N,O-bis(trimethylsilyl)trifluoroacetamide
DETAPAC	diethylenetriaminepentaacetic acid
DEP	diesel exhaust particles
DFO	deferoxamine mesylate
DPPH	2,2-diphenyl-1-picryhydrazyl
DMPO	5,5-dimethyl-1-pyroline-N-oxide
EPFR	environmentally persistent free radicals
EPR	electron paramagnetic resonance (spectroscopy)
GC/MS	gas chromatography / mass spectrometry
GF/A	binder free glass fiber filter
ICP-AES	inductively coupled plasma – atomic emission spectroscopy
LDEQ	Louisiana department of environmental quality
NADPH	nicotinamide adenine dinucleotide phosphate
NMOC	nonmethane organic carbon
NO_x	nitrogen oxides

OC	organic carbon
PAH	polycyclic aromatic hydrocarbons
PBS	phosphate buffered saline solution
PCDD/F	polychlorinated dibenzo-p-dioxin/furan
PCP	pentachlorophenol
PM	particulate matter (general)
$PM_{2.5}$	particulate matter of 2.5 μm aerodynamic radius
PM_{10}	particulate matter of 10 μm aerodynamic radius
PTFE	polytetrafluoroethylene
RH	relative humidity
ROS	reactive oxygen species
SOA	secondary organic aerosol
TBME	tert-butyl methyl ether
THC	total hydrocarbons
TSP	total suspended particles
UFPM	ultrafine particulate matter
UHP	ultra high purity

UP H_2O	ultrapure water
UV-Vis-NIR	ultraviolet visible near infrared (spectroscopy)
VOC	volatile organic compounds

ABSTRACT

Previous research demonstrated environmentally persistent free radicals (EPFRs) will form on particulate surfaces under combustion conditions (temperature range of 150-400 °C) from reactions of organic precursors with redox-active transition metals. With an understanding of how these EPFRs form, it is necessary to determine how they behave in a natural environment after emission. To better understand this, the nature of EPFRs in ambient $PM_{2.5}$ under simulated atmospheric conditions was investigated.

Ambient $PM_{2.5}$ samples were collected at a roadside ambient monitoring site near heavy interstate traffic and major industrial activity. The EPFR concentration and general radical structure were determined with EPR spectroscopy. Studies of EPFR decay in ambient air demonstrated four decay patterns to emerge from analysis: a fast followed by a slow decay (47% of samples), a slow decay (24% of samples), no decay (18% of samples), and a fast decay followed by no decay (11% of samples) with half-lives for the decays lasting from several days to several months. All decays were suggested to result from reaction with oxygen and strengthened from an overall shift in the EPR g-factor. This shift implied an increased presence of oxygen centered radicals.

The negative health impacts of $PM_{2.5}$ were studied by the generation of hydroxyl radicals. These studies revealed dissolved oxygen coupled with the presence of $PM_{2.5}$ necessary to generate significant levels of hydroxyl radicals without the addition of H_2O_2.

Exposure of $PM_{2.5}$ to ozone and NO revealed no effect on the organic radical (EPFR) signal, while NO_2 exhibited a 5-8 time increase. When these exposed EPFRs were evaluated by hydroxyl radical generation, the NO and ozone exposed samples maintained the same levels as

the unexposed sample, while NO_2 exposed samples displayed a decreased ability due to the formation of acid.

When $PM_{2.5}$ was exposed to simulated solar exposure, the EPFR concentration was observed to increase substantially in all samples. Decay from irradiation followed a 2 decay pattern with the shorter, solar decay demonstrating a half-life of 8 hours and the longer decay 9 days. Irradiation also increased the amount of hydroxyl radicals generated from $PM_{2.5}$.

CHAPTER I. INTRODUCTION

The research described herein is from studies on environmentally persistent free radicals (EPFRs) in ambient $PM_{2.5}$. This research is divided into four parts with two overall goals. The first is assessing the EPFR concentration and how they are transformed from common atmospheric reactions. The second is evaluating how these reactions affect the EPFRs' ability to generate biologically damaging hydroxyl radicals.

Previous research already identified EPFRs as an inherent constituent from combustion emissions in addition to ambient $PM_{2.5}$ [1-4]. However, how these EPFRs are affected by common atmospheric reactions, such as with oxygen, nitrogen oxides (NOx), ozone, and solar radiation, are not yet known. For the first study, $PM_{2.5}$ samples were collected from a Louisiana Department of Environmental Quality ambient air monitoring site. This site is near heavy interstate traffic from I-10 in addition to a major industrial corridor of the Mississippi River. Investigations were performed to ascertain the initial EPFR characteristics of $PM_{2.5}$ using electron paramagnetic resonance (EPR) spectroscopy. The $PM_{2.5}$ EPFRs were aged in an ambient environment at two different temperature and humidity settings to elucidate how their behavior changed over time. Additional studies were performed to detect the presence of precursors identified from previous research utilizing GC/MS. Correlations were calculated to identify if any common pollutants or meteorological conditions impact the formation or stability of the EPFRs. Also considering the similarity of EPFRs in $PM_{2.5}$ and cigarettes, a comparison of health effects for EPFRs between $PM_{2.5}$ and cigarettes was calculated.

$PM_{2.5}$ is documented as producing a toxic response from inhalation [5-14]. The exact mechanism is not completely understood, but this research group has identified a catalytic cycle involving EPFRs bound to model PM as a possible source. Confirmation is needed for this cycle in ambient $PM_{2.5}$. Accordingly, the ability of EPFRs in $PM_{2.5}$ to generate hydroxyl radicals was investigated as the second study.

Due to the constant presence of ozone and NO_x in the atmosphere, the interaction of these atmospheric oxidizers with $PM_{2.5}$ bound EPFRs is of interest. Therefore, in the third study, the effects of ozone and NO_x exposure on the EPFR signal and the subsequent generation of hydroxyl radicals were examined.

The sun generates a large amount of UV radiation and corresponds to wavelengths matching normal bond energies [15]. Given this information, the effect of solar radiation may be an important pathway to EPFR formation. Therefore, the effect of simulated solar radiation on the EPFR signal and the resulting generation of hydroxyl radicals were determined in the fourth study.

1.1 Particulate Matter

Particulate matter (PM) is airborne particles resulting from natural and anthropogenic sources. They contain solid particles in addition to liquid droplets and described as a whole by total suspended particles (TSP). This can be further divided into three size categories based on the aerodynamic diameter of the particle, which is the diameter of a sphere with the same terminal velocity as the particle [16]. The largest size is PM_{10}, also known as coarse PM, and defined as PM of 10 to 2.5 μm. $PM_{2.5}$, also known as fine PM, is the intermediate size and represented as PM of 2.5 to 0.1 μm. The smallest is $PM_{0.1}$, also known as ultrafine PM (UFPM), and assigned as PM of 0.1 μm or smaller.

Due to its small size, UFPM mass demonstrates only a few percentage of the TSP mass but constitutes over 90% of the number concentration [17-20]. In $PM_{2.5}$, UFPM composes only 20% of the mass but fulfills 80% of the number concentration [21, 22]. Due to UFPM's small size but large number concentration, this allows a large surface to volume ratio for uptake of toxic pollutants, such as organic compounds, nonvolatile species, and transition metals [19, 23]. Additionally, these properties permit UFPM to remain airborne for extended periods of time and transported over extended distances [24, 25]. For example, studies calculated PM in the US can travel approximately 60 – 600 miles and comparable distances in Asia [26-28].

PM is physically and chemically complex with composition changing between locations, time of the year, and time of the day [29-34]. For example, differences in PM and its oxidative capacity were found between the morning and afternoon [35]. This study cited the reason as PM undergoing atmospheric processes changing the PM composition. This is also applied to differences from a more industrial urban setting to those of a more rural setting [36]. Despite large variations, there is some common components of PM; that is, PM will contain elemental carbon, organic carbon, sulfates, nitrates, natural minerals from alumina/silica, and transition metals, such as iron, manganese, and copper [37-41].

In addition to outdoor PM emissions, PM was identified from indoor activities, such as cigarette smoking, gas stoves, pet dander, and fireplaces [42, 43]. These indoor emissions also include the same kind of composition, though different in concentration, as outdoor sources [44].

1.2 Origin of Combustion Generated EPFRs and PM

$PM_{2.5}$ and its ultrafine component are mainly derived from combustion and thermal processes [37, 45], such as engine exhaust, biomass burning, and industrial processes [30, 31, 46-

52]. Combustion and thermal processes are documented to initiate by radical chain processes and continued due to the intense temperatures dissociating molecules [53-55].

The zone theory of combustion explains this formation in further detail, as displayed in Figure 1.1 [56-58]. This theory branches the combustion process into 4 separate and distinct zones. In zone 1, the fuel is vaporized as well as mixed, and this is noted as the preflame zone. In zone 2, the fuel is introduced into the high temperature flame where the molecular fuel is dissociated into radical products. In zone 3, these radical species proceed by gas phase reactions to condense into nanoparticles or recombine into molecular compounds. In zone 4, the gases are cooled and surface-mediated reactions with transition metals occur. Zone 4 is where the formation of persistent radicals occur from combustion processes [1, 59].

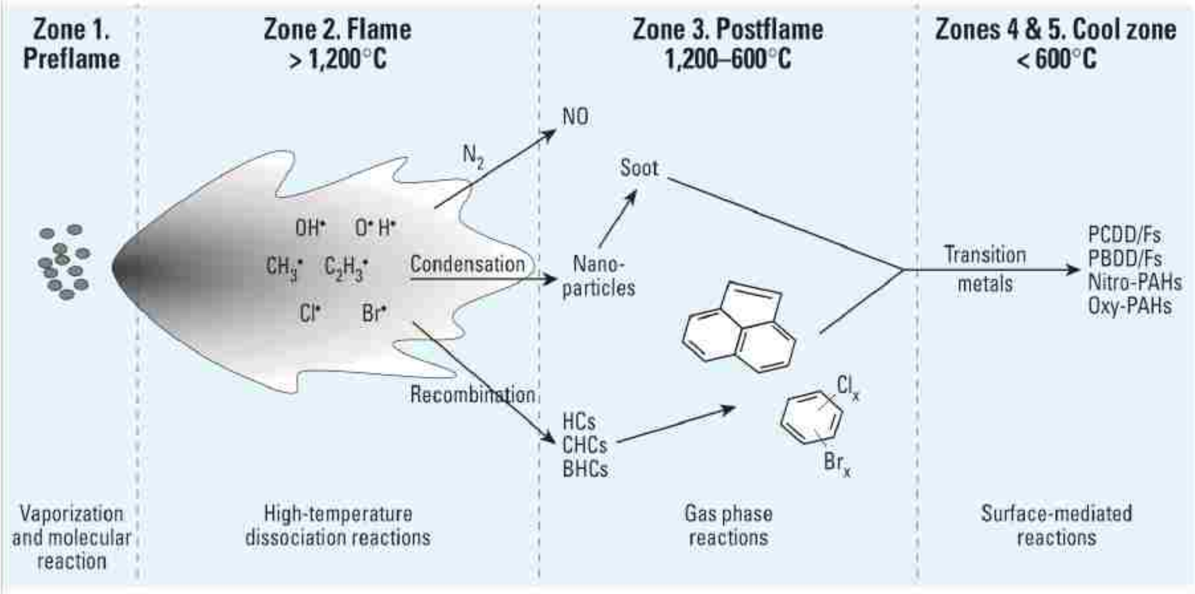

Figure 1.1 Zone theory of combustion in the formation surface-mediated radicals "Reprinted with permission from Reference 58. Copyright 2006 American Chemical Society."

The reactions in zone 4 are what led to the discovery of EPFRs. Previous research revealed the formation of polychlorinated dibenzo-p-dioxins and furans (PCDD/F) resulted from precursors adsorbed onto the surface of metal oxides at temperatures below 600 °C, the same as in zone 4, from the result of surface mediated radical processes [60, 61]. This was a new mechanism for PCDD/F formation due to the established *de novo* pathway needing higher temperatures [62].

Further research established a mechanism for EPFR formation as demonstrated in Figure 1.2. This mechanism is dependent on a catalytically active transition metal, displayed as Cu(II)O and an organic precursor, displayed as hydroquinone. Initially, the organic precursor physisorbs to the surface of the metal oxide. This is followed by chemisorption *via* elimination of water or in chlorinated organics, hydrochloric acid. The metal is subsequently reduced from the chemisorbed organic precursor *via* electron transfer. This step was confirmed from X-ray measurements indicating the metal oxide was indeed reduced from the chemisorbed organic [63]. The overall mechanism results in the formation of a surface-associated organic radical [60].

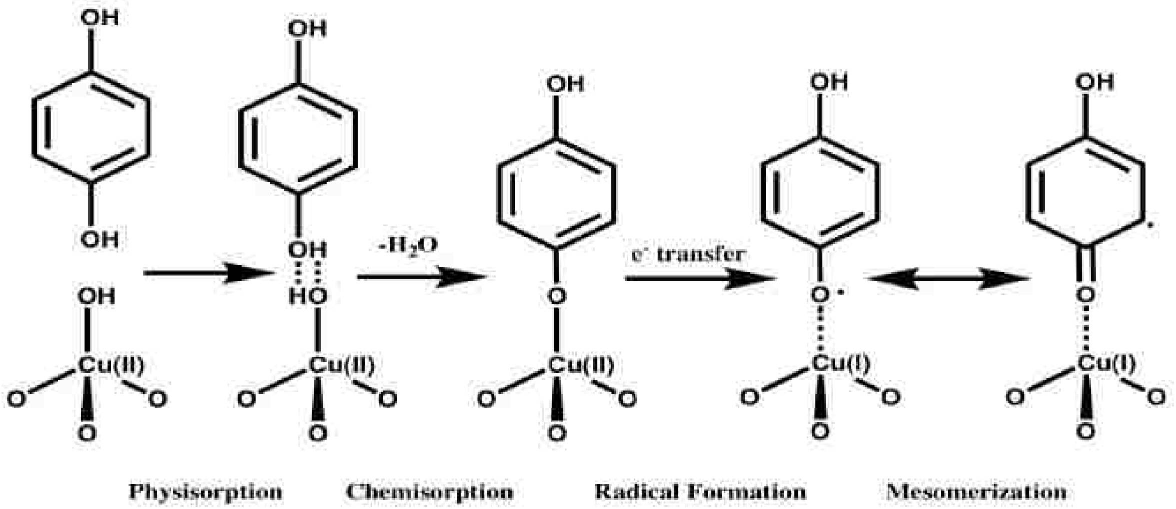

Figure 1.2 Formation of EPFRs from hydroquinone on a Cu(II)O containing particle. "Reprinted with permission from Reference 70. Copyright 2008 American Chemical Society."

Free radicals, unlike EPFRs, have very short half-lives, such as the highly reactive hydroxyl radical exhibiting a half-life of 10^{-9} s [64]. Detection of these free radicals can be quite difficult resulting in the use of low temperature or various spin trapping techniques [65-68]; however, EPFRs associated onto the particle surface imparts additional stabilization to these radicals [59, 69]. This results from the EPFR's dual radical property allowing it to be oxidized enough to be detected by EPR yet reduced enough to allow stability and relatively non-reactivity [60]. Consequently, this allows EPFRs to persist in the environment, hence the name environmentally persistent free radicals (EPFRs) [70].

1.3 EPFRs in Soot

Soot formation has many different formation routes, such as gas phase nucleation, molecular growth, and aggregation of organic species. Previous research demonstrated soot from the combustion of charcoal, coal, diesel, and plastics contain an EPFR signal [69, 71-73]. Due to the broadness of the signal, exact identification was not established and merely noted as a soot radical [73, 74]. Part of this signal was attributed to the radicals entrapped in the bulk of the soot with the unpaired electron delocalized over many conjugated or aromatic bonds [69, 72, 73]. This observation was concluded from stability of the radical signal as well as its apparent unreactive nature to oxygen [69, 72, 73]. These radicals do not migrate to the surface and accordingly cannot undergo oxidation in air allowing them to persist indefinitely.

Soot generated from halogenated hydrocarbons established EPFRs in hazardous waste incinerators with implications for incinerators as a whole [75]. The EPR spectra from this study are given in Figure 1.3. These radicals were mainly carbon centered radicals with two of the soot samples, tetrachloroethylene and bromoform, demonstrating an oxidized carbon or semiquinone-type radical [75]. More recently, studies on radical species formed from the oxidative pyrolysis of 1-methylnaphthalene were performed [76]. Using low temperatures, the gas phase radicals were identified as carbon centered radicals with trace amounts of an oxygen centered radical [76]. The presence of these species was enhanced when $Fe(III)_2O_3$ was added suggesting metal nanoparticles act as a surface mediated mechanism for soot growth by forming and stabilizing PAH radicals [76].

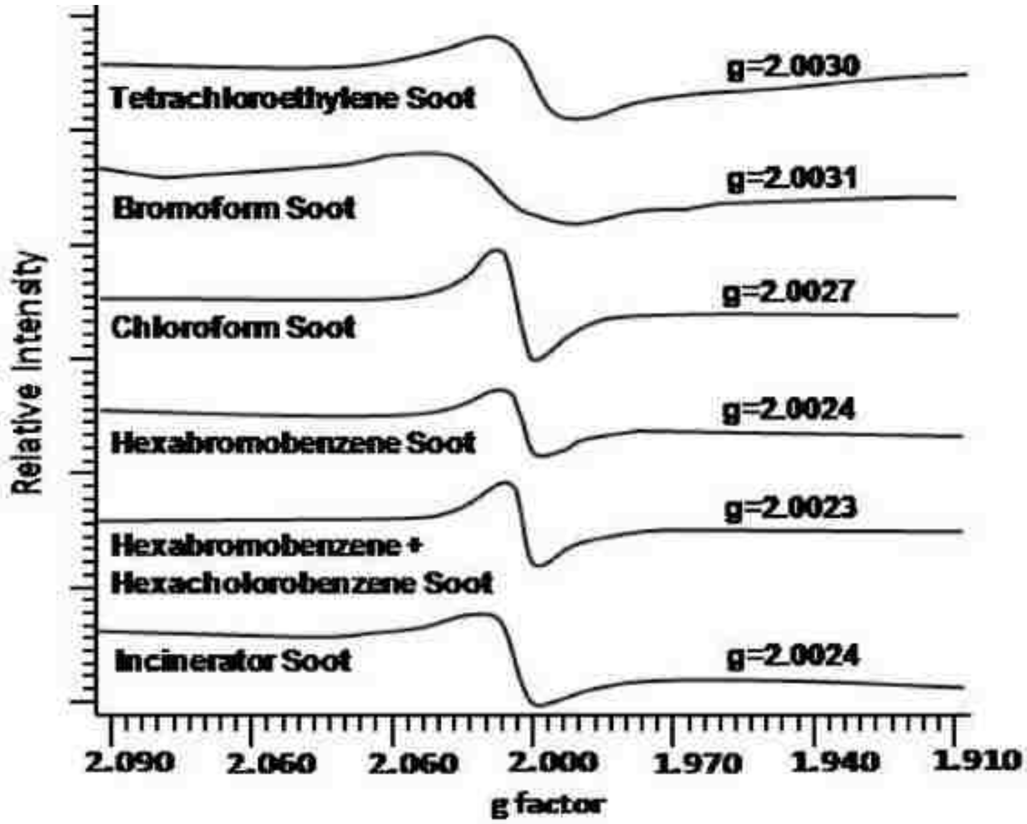

Figure 1.3 EPR spectra of soot from the combustion of toxic halocarbons. "Reprinted with permission from Reference 75. Copyright 2000 American Chemical Society."

1.4 EPFRs in Soils

Demonstrating EPFR formation in combustion, EPFRs were also believed present in soils due to the same redox transition metals present. These transition metals arise from the clay and mineral component of soil. The differences between soils and combustion systems are the reaction times and temperatures [77]. In the combustion systems, the reaction times are in seconds under high temperatures; in soils, the reaction times are over the course of years at ambient temperatures.

In order to understand how soil components, minerals, and organic matter aid in the formation of organic pollutants from contaminated soils, investigations into EPFR formation in soils were performed. From these studies, EPFRs were confirmed present in contaminated soils from superfund sites [77]. Non-contaminated soils outside a superfund site were compared to pentachlorophenol (PCP) contaminated soils inside a superfund site. This finding is displayed in Figure 1.4. The contaminated soil was demonstrated to contain an increase in EPFRs over the

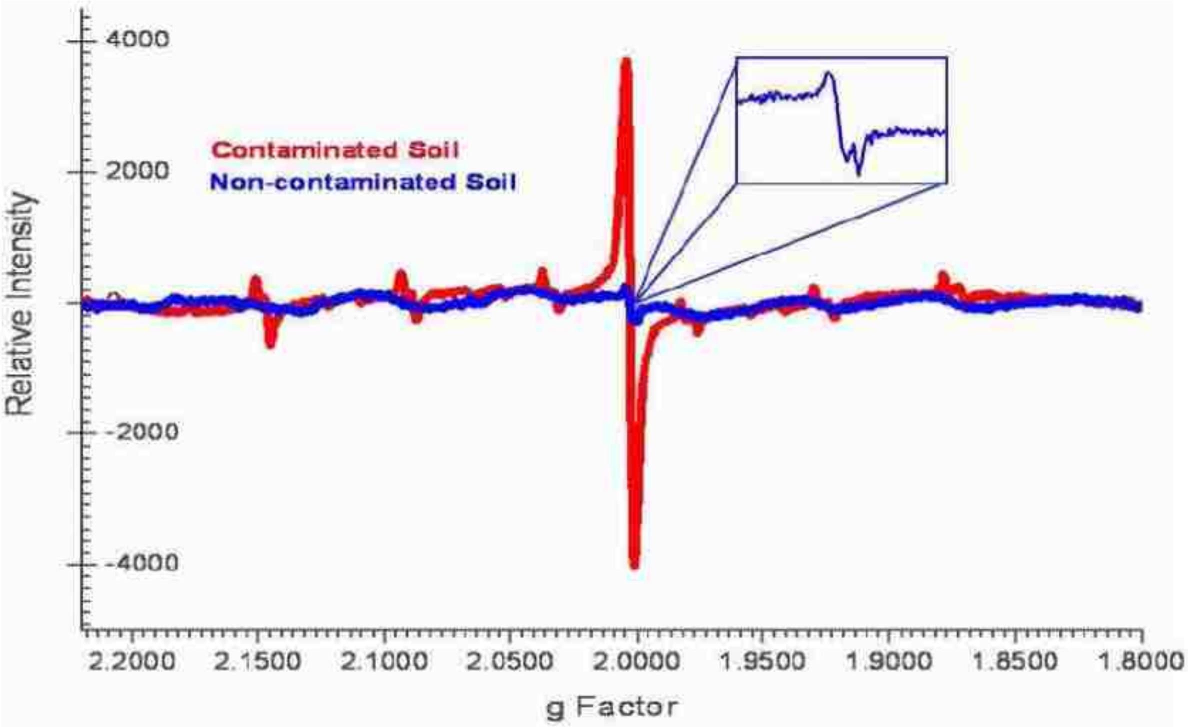

Figure 1.4 EPR spectra of contaminate soils (red) and non-contaminated soils (blue). “Reprinted with permission from Reference 77. Copyright 2011 American Chemical Society.”

non-contaminated site. This increase was attributed to the additional presence of PCP, and this was verified from PCP extracts of the contaminated soils in addition to dosing gas phase PCP onto a clean model soil [77].

Despite remaining outside of the contamination, radicals were still detected in the soil. This stems from humic acid, a major organic component of soil, containing a semiquinone or quinhydrone-type radical [78]. These radicals are generated during formation of humic acid from organic matter through radical polymerization [79-82].

1.5 EPFRs in $PM_{2.5}$

As stated above, combustion processes generate particulate matter ($PM_{2.5}$), and these particles are directly emitted into the atmosphere. $PM_{2.5}$ is also documented as a by-product of metal processing, such as smelting [1, 84-86]. Once the particles are emitted from the aforementioned sources, they undergo atmospheric processes, like photo-oxidation as well as uptake of other gas phase species [87-90]. These gas phase species can include VOCs and other combustion emissions [1, 91, 92]. This suggested ambient $PM_{2.5}$ would likely contain EPFRs. To determine this hypothesis, $PM_{2.5}$ was collected from five US cities and analyzed by EPR [1]. Findings from this study are given in Figure 1.5. Despite the diverse locations for the sample collection, all signals were similar to each other. Perhaps more remarkable was the similarity of the EPR signal from the $PM_{2.5}$ EPFR and the signal from smoking one cigarette.

The radicals observed from $PM_{2.5}$ were suggested as semiquinone radicals [1]. Quinones, including semiquinones, are emitted from combustion processes [93-95], and further investigation revealed quinones were also present in $PM_{2.5}$ [3, 96]. Cigarette smoke is additionally documented to contain semiquinone radicals [97, 98]. Despite both $PM_{2.5}$ and cigarette radical signals attributed to semiquinone radicals, the signals do not exactly match. This was suggested to arise from inhomogeneity of the $PM_{2.5}$ in addition to various degrees of interactions from metals ions [1]. Another implication from this study, although not explicitly stated, is EPFRs will persist for long periods of time from the combustion source, even in the oxidizing and photochemical conditions of the atmosphere.

These processes listed above are not limited to combustion generated PM. They can occur from atmospheric reactions of natural terpenes, such as limonene, pinene, *etc.*, from biogenic emissions [99-102]. These reactions result in aerosol formation and subsequent

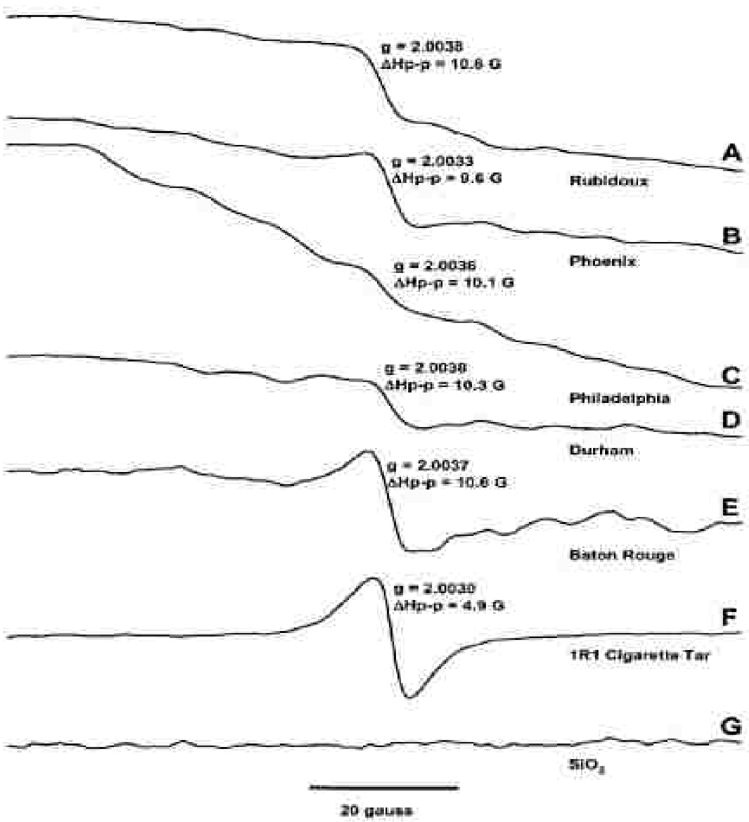

Figure 1.5 EPR spectra of EPFRs in $PM_{2.5}$ from 5 US cities. “Reprinted with permission from Reference 1. Copyright 2001 American Chemical Society.”

agglomeration. After these atmospheric processes occur, these particles are referred to as secondary organic aerosols (SOA).

1.6 Decay of EPFRs

As stated earlier, EPFRs associated onto the particle surface imparts additional stabilization to these radicals and consequently allows them to persist in the environment [59, 69]. This behavior was observed in the long half-lives of radicals from the combustion of charcoal [103], wood, and coal [73]. In the cases of wood and coal, there were two consecutive decays resulting from reaction with oxygen where the relative intensity but not the $\Delta H_{p\text{-}p}$ of the radical signal decreased [73]. Other decay behaviors are also reported. The organic radical decay in peanuts exhibited a fast decay followed by stabilization of the signal, in addition to temperature independent decay behavior [104]. Stabilized organic radical signals were additionally observed in soot from the combustion of plastics [69] as well as the indefinite persistence of semiquinone radicals from cigarette smoke [105]. In addition to natural samples, investigations on radical decay from a model soot system of 1-methylnapthalene and Fe_2O_3 were performed [106]. These studies demonstrated two decays with the presence of Fe_2O_3 generating longer half-lives than just the 1-methylnapthalene soot alone [106].

Previous decays from model EFPR systems demonstrated a range of half-lives in addition to the presence of multiple decays in some cases [70, 107-109]. Organic precursors on CuO displayed one decay with the longest half-life from phenol at 74 min [70]. Decays from Fe_2O_3 also indicated one decay exhibiting an average half-life of 3.1 ± 1.5 days [107]. When the same experiments were performed on Ni, a two decay pattern was observed from the chemisorption of phenol, a faster decay of 0.56 days and a slower decay of 5.2 days [108]. Zn bound EPFRs exhibited two decays from half of the precursors studied [109]. Additionally, Zn bound EPFRs demonstrated the longest decays with phenol displaying half-lives of 10 days for the faster decay and 23 days for the slower decay [109]. The decays from Zn bound EPFRs is given in Figure 1.6. All decay studies implied phenoxyl radicals are the short lived species, while semiquinone radicals are the long lived species [70, 109]. Semiquinone radicals, however, were suggested to decompose into phenoxyl radicals [70, 109].

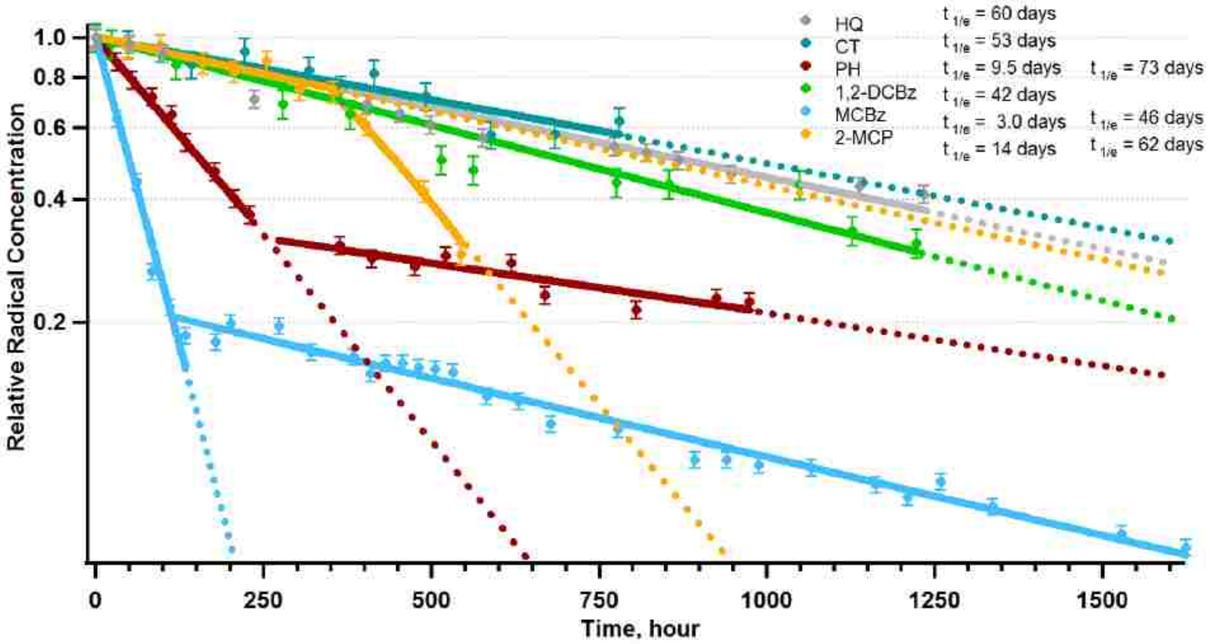

Figure 1.6 Decay of EPFRs on ZnO. HQ is hydroquinone, CT is catechol, PH is phenol, 1,2-DCBz is 1,2-dichlorobenzene, MCBz is monochlorobenzene, and 2-MCP is 2-monochlorophenol. All half-lives given are 1/e half-lives. “Reprinted with permission from Reference 109. Copyright 2011 American Chemical Society.”

1.7 Health Implications from PM and EPFRs

Research in mortality from PM exposure demonstrated higher associations with $PM_{2.5}$ than PM_{10} indicating the smaller size fractions are responsible [110-113]. Additional correlations with $PM_{2.5}$ found any increase in $PM_{2.5}$ levels increase mortality and morbidity [5-14]. These results were verified from a more recent report of association from $PM_{2.5}$ exposure and early death in the United Kingdom [114].

Adverse health effects are implicated from $PM_{2.5}$, including cardiovascular [115-117] and respiratory diseases [118] in addition to lung cancer [12, 119]. These effects are observed to generate the most damage to prone populations, such as the elderly, children, and those already exhibiting cardiovascular and respiratory problems [118, 120, 121]. Even at safe levels, $PM_{2.5}$ is associated with a higher risk of ischemic stroke [122]. A report demonstrated both short and long term exposure to $PM_{2.5}$ leads to increased hospital visits [123]. More ancillary effects suggested a link to faster cognitive decline in older women from an increase in $PM_{2.5}$ levels over a long term, and this is believed to arise from cardiovascular influences [124]. Indoor PM pollution has also been linked to higher incidents of lung cancer for nonsmokers [125].

Other studies investigated the exposure of different PM with common atmospheric oxidizers NO_x and ozone. The oxides of nitrogen are common from combustion of both mobile and stationary sources contributing to the formation of photochemical smog, a known health hazard [126-129]. Reports suggested there were health effects from exposure to NO_2 even below the national air quality standard [130]. When comparing PM alone and with exposure to NO_2, one study observed only minor differences for enhancing acute cardiovascular effects [131]. Others did not notice an effect from exposure of NO_2 with PM suggesting some antagonism between the two [132].

Ozone, a secondary pollutant resulting from reactions of NOx, volatile organic compounds (VOCs), and solar radiation, is documented to induce airway inflammation [133-136]. When exposing ozone and diesel PM, increases in cell epithelial injury or inflammation markers were observed suggesting a cumulative or synergistic effect [137-139]. Other studies distinguished airway hyper-responsiveness when exposed to ozone and carbon black [140]. Even when $PM_{2.5}$ and ozone levels were far below the national standard, decreases in lung function were reported [141]. In addition to exposure studies, correlations between ozone and reactive oxygen species (ROS) generation from PM were observed [142].

Investigators of PM toxicology implicated the importance of particle size in understanding these adverse health effects [143]. PM_{10} contains toxic components but not considered due to filtering by the nose with deposition mainly occurring in the upper respiratory tract [144, 145]. These depositions are eliminated by the mucociliary escalator, where the mucus in the lungs transports foreign objects up the trachea, into the pharynx, and subsequently swallowed [144, 145]. $PM_{2.5}$ has a small aerodynamic radius allowing deeper penetration into the lungs consequently depositing in the alveoli, bronchi, and lower respiratory system [115-117]. Correlations demonstrated $PM_{2.5}$ and its ultrafine component can increase asthma in both adults and children resulting from inflammation of the respiratory tract [113, 146-148]. The smaller component of $PM_{2.5}$, UFPM, even penetrates into the bloodstream and the cell depositing into the mitochondria where structural damage occurs [149]. UFPM also translocates across the blood-brain barrier and ultimately the brain exerting damaging effects [117, 150-153].

Toxicological effects result from oxidative stress triggered when the cell is overwhelmed by ROS generated from the PM [154-158]. ROS includes hydrogen peroxide, superoxide anion, and hydroxyl radical with hydroxyl radical the most biologically damaging of all ROS [159-162]. Superoxide is needed in some normal biological functioning, such as phagocytosis [163], and is naturally created in the body from inefficiencies in the electron transport chain within the mitochondria [164, 165]. Only when the body is overwhelmed with ROS does it become a problem accruing in cellular component damage [149]. When this happens, the body is in a state of oxidative stress resulting in a stress response [144, 166-173]. Maintaining such a state for extended periods of time has been postulated to result in acute and chronic diseases [174, 175] originating from chronic inflammation [176, 177].

However, the exact nature of ROS formation and its source are still debatable. $PM_{2.5}$ is already documented to induce a toxic response from ROS generation whether from wood smoke, other biomass burning, or ambient $PM_{2.5}$, but the specific components responsible are not yet agreed upon [1, 172, 178, 179]. Metals in PM are already established to generate ROS, especially in the presence of hydrogen peroxide due to metal mediated formation of superoxide [156, 180-186]. Specifically, iron was implicated in many of the pro-inflammatory effects because of its ability to generate hydroxyl radicals from hydrogen peroxide [171, 187-195]. Exogenous iron in PM was once thought to be inactive towards the Fenton reaction, because iron exists in its more oxidized form, Fe^{3+}, rather than its reduced form, Fe^{2+}, in addition to immobilization in the particle [196]; however, in the presence of biological reducing agents, iron, as well as other redox active metals, was demonstrated to generate ROS [183, 185, 187, 197]. Furthermore, iron in PM was observed to become partially soluble once introduced into an aqueous solution thereby increasing its bioavailability [2, 4, 171, 195, 198-201].

Along with metals, the adsorbed organic carbon on $PM_{2.5}$ exhibited ROS formation [35, 149, 184, 202-204]. One such organic component was the semiquinone-type radical. The semiquinone radical, capable of redox cycling, produced the superoxide anion by reducing oxygen [97, 98, 168, 172, 173, 205-209]. The superoxide anion underwent dismutation [210] with biological reducing agents producing hydrogen peroxide, and this further reacted with transition metals present in the PM *via* the Fenton reaction. This resulted in hydroxyl radicals causing biological damage, such as DNA strand breaks and scission [168, 207-210]. In addition to dismutating to hydrogen peroxide, superoxide was observed to attack Fe-S clusters in proteins releasing the bound iron and concomitantly allowing availability for the Fenton reaction [211]. A schematic depicting the mechanism of ROS production from a surface-stabilized semiquinone-type radical is given in Figure 1.7.

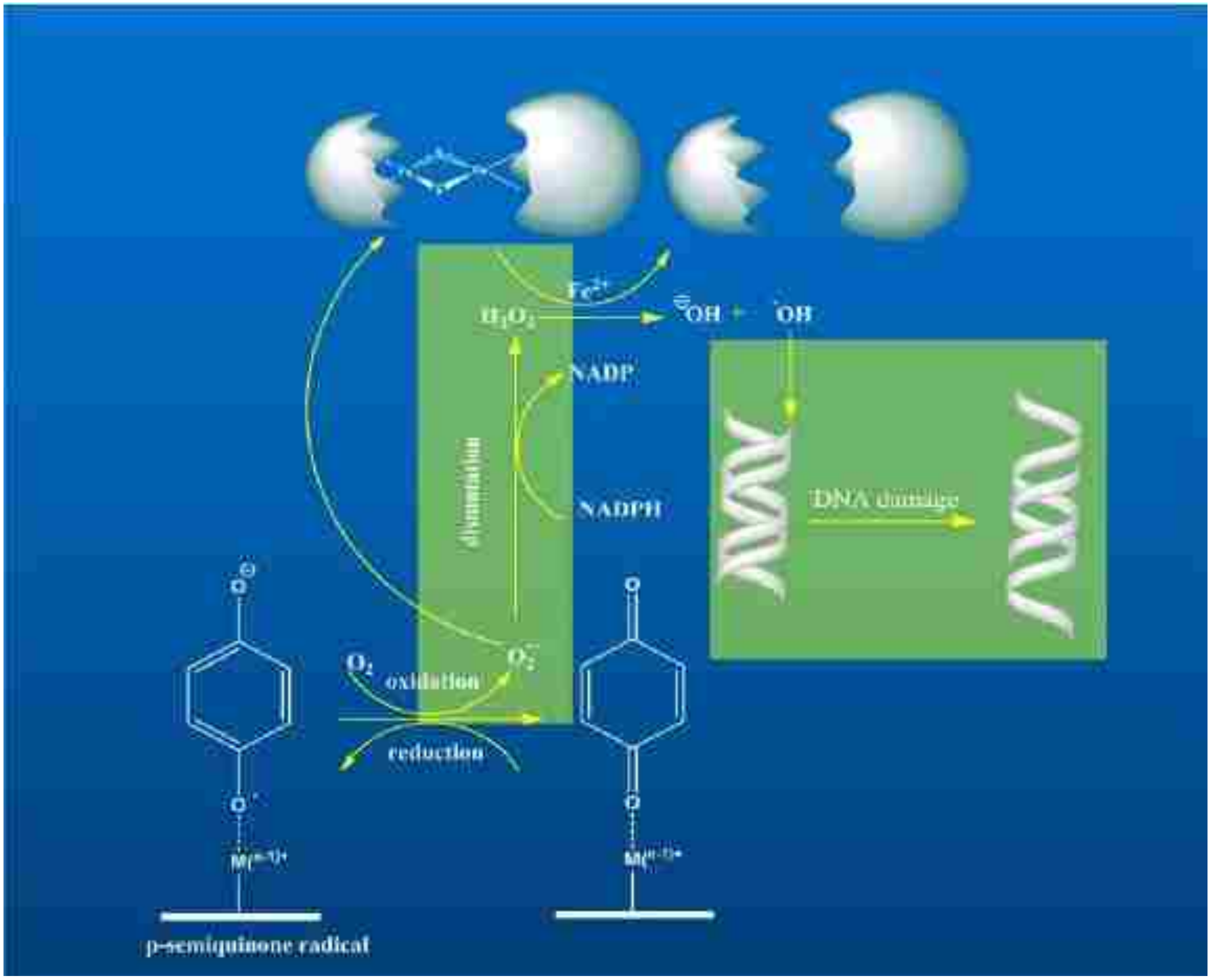

Figure 1.7 Generation of ROS catalyzed by a surface-bound semiquinone radical. "Reprinted with permission from Reference 68. Copyright 2011 American Chemical Society."

Recent evidence demonstrated ROS was generated from the red-ox cycling of a model EPFR system consisting of 4-monochlorophenol bound to CuO demonstrating the importance of both the adsorbed organic and metal [68, 212]. In this study, EPFRs were found to generate significant levels of superoxide anion and hydroxyl radical *in vitro*. Hydroxyl radical production was decreased when catalase, known to eliminate hydrogen peroxide, and superoxide dismutase, known to eliminate the superoxide anion, were added. Furthermore, EPFRs are indicated as biologically active [1, 168, 172]. Studies demonstrated oxidative stress, leading to pulmonary [213-215] and cardiac dysfunction [216-218], resulted from exposure to the model EPFR system.

1.8 Research Objectives

There are four objectives for this research. First is to investigate the concentration of EFPRs in ambient $PM_{2.5}$; observe if the radicals mirror similar decay behavior as the model EPFR system; and determine if any conditions affect the decay. The second is to establish if EPFRs in $PM_{2.5}$ are capable of generating ROS *in vitro* and resolving if the proposed ROS catalytic cycle holds true for ambient PM. The third objective is to expose common atmospheric oxidants to EPFR containing $PM_{2.5}$ and observe any interactions from the exposure and concomitant hydroxyl radical generation. Finally, the fourth objective is to expose the EPFR containing $PM_{2.5}$ to simulated solar radiation and discern any change in the observed EPFR signal in addition to its resulting ability to generate hydroxyl radicals.

The first objective was achieved by collecting $PM_{2.5}$ in an urban environment with heavy interstate traffic and industrial complexes nearby and monitoring their initial concentration and decay over time with electron paramagnetic (EPR) spectroscopy. GC/MS analysis of common organic precursors found in previous model system EPFR research was performed to elucidate and identify, at least partially, the EPFRs in $PM_{2.5}$. Correlations of common meteorological and pollutant conditions collected from the same sampling site were calculated to determine if any of these conditions have any bearing on the initial EPFR properties or decays. In addition to this, calculations comparing the EPFR content of both $PM_{2.5}$ and cigarettes were performed demonstrating the number of equivalent cigarettes one must smoke to gain the same health effects from inhaling $PM_{2.5}$.

The second objective was accomplished by *in vitro* studies of EPFRs in $PM_{2.5}$ to determine if biologically damaging hydroxyl radicals were generated. Due to the short half-life of the hydroxyl radical, spin trapping studies utilizing 5,5-dimethyl-pyrroline-N-oxide (DMPO) as the spin trap were performed. These studies were carried out under different aeration conditions to ascertain how the presence of dissolved oxygen can influence the generation of the hydroxyl radical. Studies also compared freshly collected samples with aged samples to observe if the EPFR concentration alters the generation of hydroxyl radicals. H_2O_2 was also added to confirm the generation of hydroxyl radicals through Fenton reaction.

In the third objective, collected $PM_{2.5}$ was extracted from a filter and used as a powder. This powder was subsequently exposed to NO_x and ozone at different concentrations and reaction times to determine if these oxidants have any effect on the EPFR signal. The exposed samples were compared to unexposed samples to determine if exposure to the oxidant impacted the ability of EPFRs in $PM_{2.5}$. After exposure, the same exposed and unexposed samples' generation of the hydroxyl radical were compared.

The final objective was realized by exposing thin portions of $PM_{2.5}$ powder to a xenon lamp equipped with an AM1.5 filter. The lamp intensity matched insolation levels comparable to the midday intensity for Baton Rouge during the summer. The decay and half-lives resulting from the solar exposure were measured and compared to the previous decay study. The ability to generate altered levels of hydroxyl radicals due to the simulated solar exposure were compared to an unexposed sample.

1.9 References

1. Dellinger, B., et al., *Role of Free Radicals in the Toxicity of Airborne Fine Particulate Matter.* Chemical Research in Toxicology, 2001. **14** (10): p. 1371-1377.

2. Valavanidis, A., et al., *Electron paramagnetic resonance study of the generation of reactive oxygen species catalysed by transition metals and quinoid redox cycling by inhalable ambient particulate matter.* Redox Report, 2005. **10** (1): p. 37-51.

3. Valavanidis, A., et al., *Determination of Selective Quinones and Quinoid Radicals in Airborne Particulate Matter and Vehicular Exhaust Particles.* Environmental Chemistry, 2006. **3** (2): p. 118-123.

4. Valavanidis, A., K. Fiotakis, and T. Vlachogianni, *The Role of Stable Free Radicals, Metals and PAHs of Airborne Particulate Matter in Mechanisms of Oxidative Stress and Carcinogenicity.* , in *Urban Airborne Particulate Matter,* F. Zereini and C.L.S. Wiseman, Editors. 2011, Springer Berlin Heidelberg. p. 411-426.

5. Lave, L.B., E.P. Seskin, and M.J. Chappie, *Air Pollution and Human Health*. 1977: Johns Hopkins University Press. 368 pp.

6. Mendelsohn, R. and G. Orcutt, *An empirical analysis of air pollution dose-response curves.* Journal of Environmental Economics and Management, 1979. **6** (2): p. 85-106.

7. Evans, J.S., T. Tosteson, and P.L. Kinney, *Cross-sectional mortality studies and air pollution risk assessment.* Environment International, 1984. **10** (1): p. 55-83.

8. Lipfert, F.W., *Air pollution and mortality: specification searches using SMSA-based data.* J Environ Econ Manage, 1984. **11** (3): p. 208-43.

9. Özkaynak, H. and G.D. Thurston, *Associations Between 1980 U.S. Mortality Rates and Alternative Measures of Airborne Particle Concentration.* Risk Analysis, 1987. **7** (4): p. 449-461.

10. Archer, V.E., *Air pollution and fatal lung disease in three Utah counties.* Arch Environ Health, 1990. **45** (6): p. 325-34.

11. Bobak, M. and D.A. Leon, *Air pollution and infant mortality in the Czech Republic, 1986-88.* Lancet, 1992. **340** (8826): p. 1010-4.

12. Dockery, D.W., et al., *An Association between Air Pollution and Mortality in Six U.S. Cities.* New England Journal of Medicine, 1993. **329** (24): p. 1753-1759.

13. Pope, C.A., et al., *Cardiovascular Mortality and Long-Term Exposure to Particulate Air Pollution.* Circulation, 2004. **109** (1): p. 71-77.

14. Pope, C.A., 3rd, M. Ezzati, and D.W. Dockery, *Fine-particulate air pollution and life expectancy in the United States.* N Engl J Med, 2009. **360** (4): p. 376-86.

15. Finlayson-Pitts, B.J. and J.N. Pitts, *Chemistry of the Upper and Lower Atmosphere: Theory, Experiments, and Applications*. 1999: Academic. 1040 pp.

16. Hinds, W.C., *Aerosol Technology: Properties, Behavior, and Measurements of Airborne Particles, 2nd Edition*. 1998: Wiley. 464 pp.

17. Seaton, A., et al., *Particulate air pollution and acute health effects.* Lancet, 1995. **345** (8943): p. 176-8.

18. Peters, A., et al., *Respiratory effects are associated with the number of ultrafine particles.* Am J Respir Crit Care Med, 1997. **155** (4): p. 1376-83.

19. Oberdorster, G., *Pulmonary effects of inhaled ultrafine particles.* Int Arch Occup Environ Health, 2001. **74** (1): p. 1-8.

20. Wang, Y.C., et al. *Spatio-temporal variability of ultrafine particle number concentrations in urban atmosphere*. 2010. American Chemical Society.

21. Woo, K.S., et al., *Measurement of Atlanta Aerosol Size Distributions: Observations of Ultrafine Particle Events.* Aerosol Science and Technology, 2001. **34** (1): p. 75-87.

22. Rodriguez, S., et al., *A study on the relationship between mass concentrations, chemistry and number size distribution of urban fine aerosols in Milan, Barcelona and London.* Atmos. Chem. Phys., 2007. **7** (9): p. 2217-2232.

23. Penn, A., et al., *Combustion-derived ultrafine particles transport organic toxicants to target respiratory cells.* Environ Health Perspect, 2005. **113** (8): p. 956-63.

24. D'Alessio, A., et al., *Combustion-generated nanoparticles.* Chim. Ind. (Milan), 1999. **81** (8): p. 1001-1006.

25. Pekkanen, J., et al., *Particulate air pollution and risk of ST-segment depression during repeated submaximal exercise tests among subjects with coronary heart disease: the Exposure and Risk Assessment for Fine and Ultrafine Particles in Ambient Air (ULTRA) study.* Circulation, 2002. **106** (8): p. 933-8.

26. Allen, D.T. and J.R. Turner, *Transport of Atmospheric Fine Particulate Matter: Part 1—Findings from Recent Field Programs on the Extent of Regional Transport within North America.* Journal of the Air & Waste Management Association, 2008. **58** (2): p. 254-264.

27. Wagstrom, K.M. and S.N. Pandis, *Contribution of long range transport to local fine particulate matter concerns.* Atmospheric Environment, 2011. **45** (16): p. 2730-2735.

28. Inomata, Y., et al., *Emission and Atmospheric Transport of Particulate PAHs in Northeast Asia.* Environmental Science & Technology, 2012. **46** (9): p. 4941-4949.

29. Kleeman, M.J., J.J. Schauer, and G.R. Cass, *Size and Composition Distribution of Fine Particulate Matter Emitted from Motor Vehicles.* Environmental Science & Technology, 2000. **34** (7): p. 1132-1142.

30. Linak, W.P., C.A. Miller, and J.O. Wendt, *Comparison of particle size distributions and elemental partitioning from the combustion of pulverized coal and residual fuel oil.* J Air Waste Manag Assoc, 2000. **50** (8): p. 1532-44.

31. Okeson, C.D., et al., *Impact of the composition of combustion generated fine particles on epithelial cell toxicity: influences of metals on metabolism.* Chemosphere, 2003. **51** (10): p. 1121-8.

32. Demerjian, K.L. and V.A. Mohnen, *Synopsis of the temporal variation of particulate matter composition and size.* J. Air Waste Manage. Assoc., 2008. **58** (2): p. 216-233.

33. Perrino, C., et al., *Influence of natural events on the concentration and composition of atmospheric particulate matter.* Atmos. Environ., 2009. **43** (31): p. 4766-4779.

34. Perrone, M.G., et al., *Seasonal variations in chemical composition and in vitro biological effects of fine PM from Milan.* Chemosphere, 2010. **78** (11): p. 1368-1377.

35. Verma, V., et al., *Redox activity of urban quasi-ultrafine particles from primary and secondary sources.* Atmospheric Environment, 2009. **43** (40): p. 6360-6368.

36. Putaud, J.P., et al., *A European aerosol phenomenology - 3: Physical and chemical characteristics of particulate matter from 60 rural, urban, and kerbside sites across Europe.* Atmos. Environ., 2010. **44** (10): p. 1308-1320.

37. Cass, G.R., et al., *The Chemical Composition of Atmospheric Ultrafine Particles.* Philosophical Transactions: Mathematical, Physical and Engineering Sciences, 2000. **358** (1775): p. 2581-2592.

38. Modey, W.K., et al., *Fine particulate (PM2.5) composition in Atlanta, USA: assessment of the particle concentrator-Brigham Young University organic sampling system, PC-BOSS, during the EPA Supersite study.* Atmos. Environ., 2001. **35** (36): p. 6493-6502.

39. Pang, Y., N.L. Eatough, and D.J. Eatough, *PM2.5 semivolatile organic material at Riverside, California: implications for the PM2.5 Federal Reference Method sampler.* Aerosol Sci. Technol., 2002. **36** (3): p. 277-288.

40. Behera, S.N. and M. Sharma, *Reconstructing Primary and Secondary Components of PM2.5 Composition for an Urban Atmosphere.* Aerosol Sci. Technol., 2010. **44** (11): p. 983-992.

41. Lim, S., et al., *Ionic and carbonaceous compositions of PM10, PM2.5 and PM1.0 at Gosan ABC Superstation and their ratios as source signature.* Atmos. Chem. Phys., 2012. **12** (4): p. 2007-2024.

42. See, S.W. and R. Balasubramanian, *Chemical characteristics of fine particles emitted from different gas cooking methods.* Atmospheric Environment, 2008. **42** (39): p. 8852-8862.

43. Majdan, M., et al., *Assessment of the indoor environment and implications for health in Roma villages in Slovakia and Romania.* Cent. Eur. J. Public Health, 2012. **20** (3): p. 199-207.

44. Pekey, B., et al., *Indoor/outdoor concentrations and elemental composition of PM10/PM2.5 in urban/industrial areas of Kocaeli City, Turkey.* Indoor Air, 2010. **20** (2): p. 112-125.

45. Sarofim, A.F., J.S. Lighty, and E.G. Eddings, *Fine particles: Health effects, characterization, mechanisms of formation, and modeling.* Prepr. Symp. - Am. Chem. Soc., Div. Fuel Chem., 2002. **47** (2): p. 618-621.

46. Kleeman, M.J. and G.R. Cass, *Effect of Emissions Control Strategies on the Size and Composition Distribution of Urban Particulate Air Pollution.* Environmental Science & Technology, 1998. **33** (1): p. 177-189.

47. Kleeman, M.J., J.J. Schauer, and G.R. Cass, *Size and Composition Distribution of Fine Particulate Matter Emitted from Wood Burning, Meat Charbroiling, and Cigarettes.* Environmental Science & Technology, 1999. **33** (20): p. 3516-3523.

48. Huffman, G.P., et al., *Characterization of fine particulate matter produced by combustion of residual fuel oil.* J Air Waste Manag Assoc, 2000. **50** (7): p. 1106-14.

49. Chen, Y., et al., *Investigation of the microcharacteristics of PM2.5 in residual oil fly ash by analytical transmission electron microscopy.* Environ Sci Technol, 2004. **38** (24): p. 6553-60.

50. Chen, Y., et al., *Comparison of micron-sized and ultrafine particulate matter from pulverized coal combustion.* Prepr. Symp. - Am. Chem. Soc., Div. Fuel Chem., 2005. **50** (1): p. 241-244.

51. Chen, Y., et al., *Characterization of ultrafine coal fly ash particles by energy-filtered TEM.* J Microsc, 2005. **217** (Pt 3): p. 225-34.

52. Chen, Y., et al., *Transmission electron microscopy investigation of ultrafine coal fly ash particles.* Environ Sci Technol, 2005. **39** (4): p. 1144-51.

53. Cox, R.A., *Atmospheric chemistry of combustion derived pollution.* EPE, Rev. Energ. Primaire, 1984. **18** (4): p. 55-60.

54. Kaneko, T., et al., *Long-lived gas-phase radicals from combustion.* Taiki Osen Gakkaishi, 1989. **24** (2): p. 112-18.

55. Kim, W., M.G. Mungal, and M.A. Cappelli, *Formation and role of cool flames in plasma-assisted premixed combustion.* Appl. Phys. Lett., 2008. **92** (5): p. 051503/1-051503/3.

56. Taylor D, D. and C. Flagan R, *Aerosols from a Laboratory Pulverized Coal Combustor*, in *Atmospheric Aerosol*. 1981, American Chemical Society. p. 157-172.

57. Dellinger, B. and P.H. Taylor, *Chemical aspects of combustion of hazardous wastes.* Cent. Eur. J. Public Health, 1998. **6** (2): p. 79-87.

58. Cormier, S.A., et al., *Origin and health impacts of emissions of toxic by-products and fine particles from combustion and thermal treatment of hazardous wastes and materials.* Environ Health Perspect, 2006. **114** (6): p. 810-7.

59. Dellinger, B., et al., *Formation and stabilization of persistent free radicals.* Proceedings of the Combustion Institute, 2007. **31** (1): p. 521-528.

60. Lomnicki, S. and B. Dellinger, *A Detailed Mechanism of the Surface-Mediated Formation of PCDD/F from the Oxidation of 2-Chlorophenol on a CuO/Silica Surface.* J. Phys. Chem. A, 2003. **107** (22): p. 4387-4395.

61. Nganai, S., S. Lomnicki, and B. Dellinger, *Ferric Oxide Mediated Formation of PCDD/Fs from 2-Monochlorophenol.* Environmental Science & Technology, 2008. **43** (2): p. 368-373.

62. Lustenhouwer, J.W.A., K. Olie, and O. Hutzinger, *Chlorinated dibenzo-p-dioxins and related compounds in incinerator effluents: A review of measurements and mechanisms of formation.* Chemosphere, 1980. **9** (7–8): p. 501-522.

63. Farquar, G.R., et al., *X-ray spectroscopic studies of the high temperature reduction of Cu(II)O by 2-chlorophenol on a simulated fly ash surface.* Environ Sci Technol, 2003. **37** (5): p. 931-5.

64. Sies, H., *Strategies of antioxidant defense.* European Journal of Biochemistry, 1993. **215** (2): p. 213-219.

65. Pryor, W.A., D.G. Prier, and D.F. Church, *Detection of free radicals from low-temperature ozone-olefin reactions by ESR spin trapping: evidence that the radical precursor is a trioxide.* Journal of the American Chemical Society, 1983. **105** (9): p. 2883-2888.

66. Gerlock, J.L., et al., *Fluorescence detection of free radicals by nitroxide scavenging.* Free Radic Res Commun, 1990. **10** (1-2): p. 119-21.

67. Khachatryan, L., et al., *Radicals from the gas-phase pyrolysis of catechol: 1. o-Semiquinone and ipso-catechol radicals.* J Phys Chem A, 2010. **114** (6): p. 2306-2312.

68. Khachatryan, L., et al., *Environmentally Persistent Free Radicals (EPFRs). 1. Generation of Reactive Oxygen Species in Aqueous Solutions.* Environmental Science & Technology, 2011. **45** (19): p. 8559-66.

69. Valavanidis, A., et al., *Persistent free radicals, heavy metals and PAHs generated in particulate soot emissions and residue ash from controlled combustion of common types of plastic.* J. Hazard. Mater., 2008. **156**: p. 277-284.

70. Lomnicki, S., et al., *Copper Oxide-Based Model of Persistent Free Radical Formation on Combustion-Derived Particulate Matter.* Environ. Sci. Technol., 2008. **42**: p. 4982-4988.

71. Ingram, D.J.E., et al., *Paramagnetic resonance in carbonaceous solids.* Nature (London, U. K.), 1954. **174**: p. 797-8.

72. Jankovic, J., et al., *Measurement of short-lived reactive species and long-lived free radicals in air samples from structural fires.* Appl. Occup. Environ. Hyg., 1993. **8**: p. 650-4.

73. Tian, L., et al., *Carbon-Centered Free Radicals in Particulate Matter Emissions from Wood and Coal Combustion.* Energy & Fuels, 2009. **23** (5): p. 2523-2526.

74. Chughtai, A.R., et al., *Adsorption and adsorbate interaction at soot particle surfaces.* Carbon, 1998. **36** (11): p. 1573-1589.

75. Dellinger, B., et al., *The role of combustion-generated radicals in the toxicity of PM2.5.* Proc. Combust. Inst., 2000. **28** (Pt. 2): p. 2675-2681.

76. Herring, P., et al., *Paramagnetic Centers in Soot Formed from the Oxidative Pyrolysis of 1-Methylnaphthalene.* Environmental Science & Technology, 2013. **Submitted**.

77. dela Cruz, A.L., et al., *Detection of environmentally persistent free radicals at a superfund wood treating site.* Environ Sci Technol, 2011. **45** (15): p. 6356-65.

78. Steelink, C. and G. Tollin, *Stable free radicals in soil humic acid.* Biochimica et Biophysica Acta, 1962. **59** (1): p. 25-34.

79. Polewski, K., et al., *The effect of UV and visible light radiation on natural humic acid: EPR spectral and kinetic studies.* Geoderma, 2005. **126** (3–4): p. 291-299.

80. Rosa, A.H., et al., *Multimethod study of the degree of humification of humic substances extracted from different tropical soil profiles in Brazil's Amazonian region.* Geoderma, 2005. **127** (1-2): p. 1-10.

81. Christoforidis, K.C., S. Un, and Y. Deligiannakis, *High-field 285 GHz electron paramagnetic resonance study of indigenous radicals of humic acids.* J Phys Chem A, 2007. **111** (46): p. 11860-6.

82. Jezierski, A., et al., *Electron paramagnetic resonance (EPR) and stable isotope records of paleoenvironmental conditions during peat formation.* Spectrochim Acta A Mol Biomol Spectrosc, 2008. **69** (5): p. 1311-6.

83. Hammel, K.E., et al., *Reactive oxygen species as agents of wood decay by fungi.* Enzyme and Microbial Technology, 2002. **30** (4): p. 445-453.

84. Lee, P.K., et al., *Identification of the major sources contributing to PM2.5 observed in Toronto.* Environ Sci Technol, 2003. **37** (21): p. 4831-40.

85. Gildemeister, A.E., P.K. Hopke, and E. Kim, *Sources of fine urban particulate matter in Detroit, MI.* Chemosphere, 2007. **69** (7): p. 1064-1074.

86. Goix, S., et al., *Influence of source distribution and geochemical composition of aerosols on children exposure in the large polymetallic mining region of the Bolivian Altiplano.* Sci. Total Environ., 2011. **412-413**: p. 170-184.

87. Pooley, F.D. and M. Mille. *Composition of air pollution particles*. 1999. Academic.

88. Venkatachari, P., et al., *Characterization of Wintertime Reactive Oxygen Species Concentrations in Flushing, New York.* Aerosol Science and Technology, 2007. **41** (2): p. 97-111.

89. Heringa, M.F., et al., *Investigations of primary and secondary particulate matter of different wood combustion appliances with a high-resolution time-of-flight aerosol mass spectrometer.* Atmos. Chem. Phys., 2011. **11** (12): p. 5945-5957.

90. Zeng, T. and Y. Wang, *Nationwide summer peaks of OC/EC ratios in the contiguous United States.* Atmos. Environ., 2011. **45** (3): p. 578-586.

91. Kleindienst, T.E., et al., *Determination of Secondary Organic Aerosol Products from the Photooxidation of Toluene and their Implications in Ambient PM2.5.* Journal of Atmospheric Chemistry, 2004. **47** (1): p. 79-100.

92. Wang, G., et al., *Water-soluble organic compounds in PM2.5 and size-segregated aerosols over Mount Tai in North China Plain.* Journal of Geophysical Research: Atmospheres, 2009. **114** (D19).

93. Ramdahl, T. and G. Becher, *Characterization of polynuclear aromatic hydrocarbon derivatives in emissions from wood and cereal straw combustion.* Analytica Chimica Acta, 1982. **144** (0): p. 83-91.

94. Trenholm, A., *Identification of PICs in hazardous waste combustion emissions.* Waste Manage. (Oxford), 1999. **18** (6-8): p. 485-492.

95. Donaldson, K., et al., *Combustion-derived nanoparticles: A review of their toxicology following inhalation exposure.* Part. Fibre Toxicol., 2005. **2**.

96. Fraser, M.P., et al., *Air Quality Model Evaluation Data for Organics. 5. C6-C22 Nonpolar and Semipolar Aromatic Compounds.* Environ. Sci. Technol., 1998. **32** (12): p. 1760-1770.

97. Pryor, W.A., D.G. Prier, and D.F. Church, *Electron-Spin Resonance Study of Mainstream and Sidestream Cigarette Smoke: Nature of the Free Radicals in Gas-Phase Smoke and in Cigarette Tar*. Environmental Health Perspectives, 1983. **47**: p. 345-355.

98. Pryor, W.A., *Cigarette smoke radicals and the role of free radicals in chemical carcinogenicity*. Environ Health Perspect, 1997. **105 Suppl 4**: p. 875-82.

99. Koch, S., et al., *Formation of new particles in the gas-phase ozonolysis of monoterpenes.* Atmos. Environ., 2000. **34** (23): p. 4031-4042.

100. Venkatachari, P., et al., *Measurement of Particle-Bound Reactive Oxygen Species in Rubidoux Aerosols.* Journal of Atmospheric Chemistry, 2005. **50** (1): p. 49-58.

101. Bones, D.L., et al., *Appearance of strong absorbers and fluorophores in limonene-O3 secondary organic aerosol due to NH4+-mediated chemical aging over long time scales.* J. Geophys. Res., [Atmos.], 2010. **115**(D5): p. D05203/1-D05203/14.

102. Chen, X., P.K. Hopke, and W.P.L. Carter, *Secondary Organic Aerosol from Ozonolysis of Biogenic Volatile Organic Compounds: Chamber Studies of Particle and Reactive Oxygen Species Formation.* Environmental Science & Technology, 2010. **45** (1): p. 276-282.

103. Yordanov, N.D. *Introduction to the theory of electron paramagnetic resonance and its application to the study of aerosols*. 1999. Lewis.

104. Yordanov, N.D. and R. Mladenova, *EPR study of thermally generated free radicals in nuts.* Int. J. Food Sci. Technol., 2007. **42**: p. 1384-1389.

105. Pryor, W.A., *Biological effects of cigarette smoke, wood smoke, and the smoke from plastics: the use of electron spin resonance.* Free Radic Biol Med, 1992. **13** (6): p. 659-76.

106. Herring, P., et al., *Fe2O3 nanoparticle mediated molecular growth and soot inception from the oxidative pyrolysis of 1-methylnaphthalene.* Proceedings of the Combustion Institute, (2012).

107. Vejerano, E., S. Lomnicki, and B. Dellinger, *Formation and Stabilization of Combustion-Generated Environmentally Persistent Free Radicals on an Fe(III)2O3/Silica Surface.* Environ. Sci. Technol., 2011. **45**: p. 589-594.

108. Vejerano, E., S.M. Lomnicki, and B. Dellinger, *Formation and Stabilization of Combustion-Generated, Environmentally Persistent Radicals on Ni(II)O Supported on a Silica Surface.* Environ. Sci. Technol., 2012. **46**: p. 9406-9411.

109. Vejerano, E., S. Lomnicki, and B. Dellinger, *Lifetime of combustion-generated environmentally persistent free radicals on Zn(II)O and other transition metal oxides.* J. Environ. Monit., 2012. **14**: p. 2803-2806.

110. Pope, C.A., 3rd, et al., *Heart rate variability associated with particulate air pollution.* Am Heart J, 1999. **138** (5 Pt 1): p. 890-9.

111. Ostro, B., et al., *Air pollution and mortality: results from a study of Santiago, Chile.* J Expo Anal Environ Epidemiol, 1996. **6** (1): p. 97-114.

112. Burnett, R.T., et al., *Association between particulate- and gas-phase components of urban air pollution and daily mortality in eight Canadian cities.* Inhal Toxicol, 2000. **12 Suppl 4**: p. 15-39.

113. Ackermann-Liebrich, U., et al., *Lung function and long term exposure to air pollutants in Switzerland. Study on Air Pollution and Lung Diseases in Adults (SAPALDIA) Team.* Am J Respir Crit Care Med, 1997. **155** (1): p. 122-9.

114. Yim, S.H.L. and S.R.H. Barrett, *Public Health Impacts of Combustion Emissions in the United Kingdom.* Environmental Science & Technology, 2012. **46** (8): p. 4291-4296.

115. Calderon-Garciduenas, L., et al., *Canines as sentinel species for assessing chronic exposures to air pollutants: part 1. Respiratory pathology.* Toxicol Sci, 2001. **61** (2): p. 342-55.

116. Calderon-Garciduenas, L., et al., *Canines as sentinel species for assessing chronic exposures to air pollutants: part 2. Cardiac pathology.* Toxicol Sci, 2001. **61** (2): p. 356-67.

117. Nemmar, A., et al., *Passage of inhaled particles into the blood circulation in humans.* Circulation, 2002. **105** (4): p. 411-414.

118. Boezen, M., et al., *Peak expiratory flow variability, bronchial responsiveness, and susceptibility to ambient air pollution in adults.* Am J Respir Crit Care Med, 1998. **158** (6): p. 1848-54.

119. Pope, C.A., 3rd, et al., *Lung cancer, cardiopulmonary mortality, and long-term exposure to fine particulate air pollution.* JAMA, 2002. **287** (9): p. 1132-41.

120. Carter, J.D., et al., *Cytokine production by human airway epithelial cells after exposure to an air pollution particle is metal-dependent.* Toxicol Appl Pharmacol, 1997. **146** (2): p. 180-8.

121. Schwartz, J., *What are people dying of on high air pollution days?* Environ Res, 1994. **64** (1): p. 26-35.

122. Wellenius Ga, B.M.R.C.B.A. and et al., *AMbient air pollution and the risk of acute ischemic stroke.* Archives of Internal Medicine. **172** (3): p. 229-234.

123. Kloog, I., et al., *Acute and Chronic Effects of Particles on Hospital Admissions in New-England.* PLoS ONE. **7** (4): p. e34664.

124. Weuve J, et al., *EXposure to particulate air pollution and cognitive decline in older women.* Archives of Internal Medicine. **172** (3): p. 219-227.

125. Mu, L., et al., *Indoor air pollution and risk of lung cancer among Chinese female non-smokers.* Cancer Causes Control, 2013.

126. Magee, P.N., *Nitrogen as health hazard.* Ambio, 1977. **6** (2-3): p. 123-5.

127. Graham, J.A., D.E. Gardner, and D.B. Menzel, *Health effects issues of nitrogen oxides (NOx) emissions*, 1979, EPA. p. 2/1-2/46.

128. Goldstein, B.D., R.J.W. Melia, and C.D.V. Florey, *Indoor nitrogen oxides.* Bull. N. Y. Acad. Med., 1981. **57** (10): p. 873-82.

129. Kagawa, J., *Evaluation of biological significance of nitrogen oxides exposure.* Tokai J. Exp. Clin. Med., 1985. **10** (4): p. 349-53.

130. Latza, U., S. Gerdes, and X. Baur, *Effects of nitrogen dioxide on human health: Systematic review of experimental and epidemiological studies conducted between 2002 and 2006.* International Journal of Hygiene and Environmental Health, 2009. **212** (3): p. 271-287.

131. Huang, Y.C., et al., *Synergistic effects of exposure to concentrated ambient fine pollution particles and nitrogen dioxide in humans.* Inhal Toxicol, 2012. **24** (12): p. 790-7.

132. Gong, H., Jr., et al., *Respiratory responses to exposures with fine particulates and nitrogen dioxide in the elderly with and without COPD.* Inhalation Toxicol., 2005. **17**: p. 123-132.

133. Holtzman, M.J., et al., *Importance of airway inflammation for hyperresponsiveness induced by ozone.* Am. Rev. Respir. Dis., 1983. **127** (6): p. 686-90.

134. Seltzer, J., et al., *Ozone-induced change in bronchial reactivity to methacholine and airway inflammation in humans.* J. Appl. Physiol., 1986. **60** (4): p. 1321-6.

135. Koren, H.S., et al., *Ozone-induced inflammation in the lower airways of human subjects.* Am. Rev. Respir. Dis., 1989. **139** (2): p. 407-15.

136. Kriebel, D. and T.J. Smith, *A nonlinear pharmacologic model of the acute effects of ozone on the human lungs.* Environ. Res., 1990. **51** (2): p. 120-46.

137. Adamson, I.Y.R., R. Vincent, and S.G. Bjarnason, *Cell injury and interstitial inflammation in rat lung after inhalation of ozone and urban particulates.* Am. J. Respir. Cell Mol. Biol., 1999. **20**: p. 1067-1072.

138. Bosson, J., et al., *Diesel exhaust exposure enhances the ozone-induced airway inflammation in healthy humans.* Eur Respir J, 2008. **31** (6): p. 1234-40.

139. Farraj, A.K., et al., *Increased lung resistance after diesel particulate and ozone co-exposure not associated with enhanced lung inflammation in allergic mice.* Inhal Toxicol, 2010. **22** (1): p. 33-41.

140. Jakab, G.J. and D.R. Hemenway, *Concomitant exposure to carbon black particulates enhances ozone-induced lung inflammation and suppression of alveolar macrophage phagocytes.* J. Toxicol. Environ. Health, 1994. **41**: p. 221-31.

141. Thaller, E.I., et al., *Moderate increases in ambient PM2.5 and ozone are associated with lung function decreases in beach lifeguards.* J. Occup. Environ. Med., 2008. **50**: p. 202-211.

142. Hung, H.-F. and C.-S. Wang, *Experimental determination of reactive oxygen species in Taipei aerosols.* Journal of Aerosol Science, 2001. **32** (10): p. 1201-1211.

143. Warheit, D.B., et al., *Comparative Pulmonary Toxicity Inhalation and Instillation Studies with Different TiO2 Particle Formulations: Impact of Surface Treatments on Particle Toxicity.* Toxicological Sciences, 2005. **88** (2): p. 514-524.

144. Oberdorster, G., et al., *Association of particulate air pollution and acute mortality: involvement of ultrafine particles?* Inhal Toxicol, 1995. **7** (1): p. 111-24.

145. Oberdoerster, G., *Effects and fate of inhaled ultrafine particles.* ACS Symp. Ser., 2005. **890** (Nanotechnology and the Environment): p. 37-59.

146. Chestnut, L.G., et al., *Pulmonary function and ambient particulate matter: epidemiological evidence from NHANES I.* Arch Environ Health, 1991. **46** (3): p. 135-44.

147. Tashkin, D.P., et al., *The UCLA population studies of chronic obstructive respiratory disease: XI. Impact of air pollution and smoking on annual change in forced expiratory volume in one second.* Am J Respir Crit Care Med, 1994. **149** (5): p. 1209-17.

148. Wang, B., et al., *Particulate matter, sulfur dioxide, and pulmonary function in never-smoking adults in Chongqing, China.* Int J Occup Environ Health, 1999. **5** (1): p. 14-9.

149. Li, N., et al., *Ultrafine particulate pollutants induce oxidative stress and mitochondrial damage.* Environ Health Perspect, 2003. **111** (4): p. 455-60.

150. Frampton, M.W., *Systemic and cardiovascular effects of airway injury and inflammation: ultrafine particle exposure in humans.* Environ Health Perspect, 2001. **109 Suppl 4**: p. 529-32.

151. Oberdorster, G., *Significance of particle parameters in the evaluation of exposure-dose-response relationships of inhaled particles.* Inhal Toxicol, 1996. **8 Suppl**: p. 73-89.

152. Utell, M.J. and M.W. Frampton, *Acute health effects of ambient air pollution: the ultrafine particle hypothesis.* J Aerosol Med, 2000. **13** (4): p. 355-59.

153. Oberdorster, G., et al., *Translocation of inhaled ultrafine particles to the brain.* Inhal Toxicol, 2004. **16** (6-7): p. 437-45.

154. Prahalad, A.K., et al., *Ambient air particles: effects on cellular oxidant radical generation in relation to particulate elemental chemistry.* Toxicol Appl Pharmacol, 1999. **158** (2): p. 81-91.

155. Han, J.Y., K. Takeshita, and H. Utsumi, *Noninvasive detection of hydroxyl radical generation in lung by diesel exhaust particles.* Free Radic Biol Med, 2001. **30** (5): p. 516-25.

156. Knaapen, A.M., et al., *Soluble metals as well as the insoluble particle fraction are involved in cellular DNA damage induced by particulate matter.* Mol Cell Biochem, 2002. **234-235** (1-2): p. 317-26.

157. Prahalad, A.K., et al., *Air pollution particles mediated oxidative DNA base damage in a cell free system and in human airway epithelial cells in relation to particulate metal content and bioreactivity.* Chem Res Toxicol, 2001. **14** (7): p. 879-87.

158. Ayres, J.G., et al., *Evaluating the toxicity of airborne particulate matter and nanoparticles by measuring oxidative stress potential--a workshop report and consensus statement.* Inhal Toxicol, 2008. **20** (1): p. 75-99.

159. Girotti, A.W., *Mechanisms of lipid peroxidation.* J Free Radic Biol Med, 1985. **1** (2): p. 87-95.

160. Gardner, H.W., *Oxygen radical chemistry of polyunsaturated fatty acids.* Free Radic Biol Med, 1989. **7** (1): p. 65-86.

161. Breen, A.P. and J.A. Murphy, *Reactions of oxyl radicals with DNA.* Free Radic Biol Med, 1995. **18** (6): p. 1033-77.

162. Cohen, G., S. Yakushin, and D. Dembiec-Cohen, *Protein L-dopa as an index of hydroxyl radical attack on protein tyrosine.* Anal Biochem, 1998. **263** (2): p. 232-9.

163. Curnutte, J.T., *Superoxide production by phagocytic leukocytes: the scientific legacy of Bernard Babior.* J Clin Invest, 2004. **114** (8): p. 1054-7.

164. Liu, Y., G. Fiskum, and D. Schubert, *Generation of reactive oxygen species by the mitochondrial electron transport chain.* J Neurochem, 2002. **80** (5): p. 780-7.

165. Turrens, J.F., *Mitochondrial formation of reactive oxygen species.* The Journal of Physiology, 2003. **552** (2): p. 335-344.

166. Oberdorster, G., et al., *Thermal degradation events as health hazards: particle vs gas phase effects, mechanistic studies with particles.* Acta Astronaut, 1992. **27**: p. 251-6.

167. Oberdörster, G., et al., *Increased Pulmonary Toxicity of Inhaled Ultrafine Particles: Due to Lung Overload Alone?* Annals of Occupational Hygiene, 1994. **38** (inhaled particles VII): p. 295-302.

168. Pryor, W.A., et al., *Fractionation of aqueous cigarette tar extracts: fractions that contain the tar radical cause DNA damage.* Chem Res Toxicol, 1998. **11** (5): p. 441-8.

169. Peters, A., et al., *Increased Particulate Air Pollution and the Triggering of Myocardial Infarction.* Circulation, 2001. **103** (23): p. 2810-2815.

170. Gurgueira, S.A., et al., *Rapid increases in the steady-state concentration of reactive oxygen species in the lungs and heart after particulate air pollution inhalation.* Environ Health Perspect, 2002. **110** (8): p. 749-55.

171. Valavanidis, A., A. Salika, and A. Theodoropoulou, *Generation of hydroxyl radicals by urban suspended particulate air matter. The role of iron ions.* Atmospheric Environment, 2000. **34** (15): p. 2379-2386.

172. Squadrito, G.L., et al., *Quinoid redox cycling as a mechanism for sustained free radical generation by inhaled airborne particulate matter.* Free Radical Biology and Medicine, 2001. **31** (9): p. 1132-1138.

173. Hirakawa, K., et al., *Catechol and Hydroquinone Have Different Redox Properties Responsible for Their Differential DNA-damaging Ability.* Chem. Res. Toxicol., 2002. **15** (1): p. 76-82.

174. Hamade, A.K., R. Rabold, and C.G. Tankersley, *Adverse cardiovascular effects with acute particulate matter and ozone exposures: interstrain variation in mice.* Environ Health Perspect, 2008. **116** (8): p. 1033-9.

175. Li, N., T. Xia, and A.E. Nel, *The role of oxidative stress in ambient particulate matter-induced lung diseases and its implications in the toxicity of engineered nanoparticles.* Free Radic Biol Med, 2008. **44** (9): p. 1689-99.

176. Hakim, J., *[Reactive oxygen species and inflammation].* C R Seances Soc Biol Fil, 1993. **187** (3): p. 286-95.

177. Bartsch, H. and J. Nair, *Chronic inflammation and oxidative stress in the genesis and perpetuation of cancer: role of lipid peroxidation, DNA damage, and repair.* Langenbecks Arch Surg, 2006. **391** (5): p. 499-510.

178. De Kok, T., et al., *Toxicological assessment of ambient and traffic-related particulate matter: A review of recent studies.* Mutation Research-Reviews in Mutation Research, 2006. **613** (2-3): p. 103-122.

179. Danielsen, P.H., et al., *Oxidative Stress, DNA Damage, and Inflammation Induced by Ambient Air and Wood Smoke Particulate Matter in Human A549 and THP-1 Cell Lines.* Chemical Research in Toxicology, 2011. **24** (2): p. 168-184.

180. Kitajima, N., S. Fukuzumi, and Y. Ono, *Formation of superoxide ion during the decomposition of hydrogen peroxide on supported metal oxides.* The Journal of Physical Chemistry, 1978. **82** (13): p. 1505-1509.

181. Shi, T., et al., *Hydroxyl radical generation by electron paramagnetic resonance as a new method to monitor ambient particulate matter composition.* J Environ Monit, 2003. **5** (4): p. 550-6.

182. Shi, T., et al., *Temporal variation of hydroxyl radical generation and 8-hydroxy-2'-deoxyguanosine formation by coarse and fine particulate matter.* Occup Environ Med, 2003. **60** (5): p. 315-21.

183. Briede, J.J., et al., *Development and application of an electron spin resonance spectrometry method for the determination of oxygen free radical formation by particulate matter.* Environ Sci Technol, 2005. **39** (21): p. 8420-6.

184. Ntziachristos, L., et al., *Relationship between redox activity and chemical speciation of size-fractionated particulate matter.* Part Fibre Toxicol, 2007. **4**: p. 5.

185. Vidrio, E., H. Jung, and C. Anastasio, *Generation of hydroxyl radicals from dissolved transition metals in surrogate lung fluid solutions.* Atmospheric Environment, 2008. **42** (18): p. 4369-4379.

186. Shen, H. and C. Anastasio, *Formation of hydroxyl radical from San Joaquin Valley particles extracted in a cell-free surrogate lung fluid.* Atmos Chem Phys, 2011. **11** (18): p. 9671-9682.

187. Kumagai, Y., et al., *Generation of reactive oxygen species during interaction of diesel exhaust particle components with NADPH-cytochrome P450 reductase and involvement of the bioactivation in the DNA damage.* Free Radic Biol Med, 1997. **22** (3): p. 479-87.

188. Nel, A.E., D. Diaz-Sanchez, and N. Li, *The role of particulate pollutants in pulmonary inflammation and asthma: evidence for the involvement of organic chemicals and oxidative stress.* Curr Opin Pulm Med, 2001. **7** (1): p. 20-6.

189. Saldiva, P.H., et al., *Lung inflammation induced by concentrated ambient air particles is related to particle composition.* Am J Respir Crit Care Med, 2002. **165** (12): p. 1610-7.

190. Baulig, A., et al., *Physicochemical characteristics and biological activities of seasonal atmospheric particulate matter sampling in two locations of Paris.* Environ Sci Technol, 2004. **38** (22): p. 5985-92.

191. Kunzli, N., et al., *Comparison of oxidative properties, light absorbance, total and elemental mass concentration of ambient PM2.5 collected at 20 European sites.* Environ Health Perspect, 2006. **114** (5): p. 684-90.

192. Vidrio, E., et al., *Generation of Hydroxyl Radicals from Ambient Fine Particles in a Surrogate Lung Fluid Solution.* Environmental Science & Technology, 2009. **43** (3): p. 922-927.

193. Wang, Y., et al., *Probing the source of hydrogen peroxide associated with coarse mode aerosol particles in southern California.* Environ Sci Technol, 2010. **44** (11): p. 4070-5.

194. Shafer, M.M., et al., *Reactive oxygen species activity and chemical speciation of size-fractionated atmospheric particulate matter from Lahore, Pakistan: an important role for transition metals.* J Environ Monit, 2010. **12** (3): p. 704-15.

195. Verma, V., et al., *Contribution of transition metals in the reactive oxygen species activity of PM emissions from retrofitted heavy-duty vehicles.* Atmospheric Environment, 2010. **44** (39): p. 5165-5173.

196. Kukier, U., et al., *Composition and element solubility of magnetic and non-magnetic fly ash fractions.* Environmental Pollution, 2003. **123** (2): p. 255-266.

197. Pan, C.J., et al., *Inherent redox properties of diesel exhaust particles: catalysis of the generation of reactive oxygen species by biological reductants.* Toxicol Sci, 2004. **81** (1): p. 225-32.

198. Antonini, J.M., et al., *Metal composition and solubility determine lung toxicity induced by residual oil fly ash collected from different sites within a power plant.* Mol Cell Biochem, 2004. **255** (1-2): p. 257-65.

199. See, S.W., Y.H. Wang, and R. Balasubramanian, *Contrasting reactive oxygen species and transition metal concentrations in combustion aerosols.* Environmental Research, 2007. **103** (3): p. 317-324.

200. DiStefano, E., et al., *Determination of metal-based hydroxyl radical generating capacity of ambient and diesel exhaust particles.* Inhal Toxicol, 2009. **21** (9): p. 731-8.

201. Cheung, K.L., et al., *Emissions of Particulate Trace Elements, Metals and Organic Species from Gasoline, Diesel, and Biodiesel Passenger Vehicles and Their Relation to Oxidative Potential.* Aerosol Science and Technology, 2010. **44** (7): p. 500-513.

202. Cho, A.K., et al., *Redox activity of airborne particulate matter at different sites in the Los Angeles Basin.* Environ Res, 2005. **99** (1): p. 40-7.

203. Jeng, H.A., *Chemical composition of ambient particulate matter and redox activity.* Environ Monit Assess, 2010. **169** (1-4): p. 597-606.

204. Verma, V., et al., *Physicochemical and oxidative characteristics of semi-volatile components of quasi-ultrafine particles in an urban atmosphere.* Atmospheric Environment, 2011. **45** (4): p. 1025-1033.

205. Borish, E.T., et al., *Cigarette tar causes single-strand breaks in DNA.* Biochem Biophys Res Commun, 1985. **133** (2): p. 780-6.

206. Church, D.F. and W.A. Pryor, *Free-radical chemistry of cigarette smoke and its toxicological implications.* Environ Health Perspect, 1985. **64**: p. 111-26.

207. Li, Y. and M.A. Trush, *Reactive oxygen-dependent DNA damage resulting from the oxidation of phenolic compounds by a copper-redox cycle mechanism.* Cancer Res, 1994. **54** (7 Suppl): p. 1895s-1898s.

208. Stone, K., et al., *The ESR properties, DNA nicking, and DNA association of aged solutions of catechol versus aqueous extracts of tar from cigarette smoke.* Arch Biochem Biophys, 1995. **319** (1): p. 196-203.

209. Schweigert, N., et al., *DNA degradation by the mixture of copper and catechol is caused by DNA-copper-hydroperoxo complexes, probably DNA-Cu(I)OOH.* Environ Mol Mutagen, 2000. **36** (1): p. 5-12.

210. Pryor, W.A., *Oxy-radicals and related species: their formation, lifetimes, and reactions.* Annu Rev Physiol, 1986. **48**: p. 657-67.

211. Kohanski, M.A., et al., *A common mechanism of cellular death induced by bactericidal antibiotics.* Cell, 2007. **130** (5): p. 797-810.

212. Khachatryan, L. and B. Dellinger, *Environmentally Persistent Free Radicals (EPFRs)-2. Are Free Hydroxyl Radicals Generated in Aqueous Solutions?* Environmental Science & Technology, 2011. **45** (21): p. 9232-9239.

213. Balakrishna, S., et al., *Environmentally persistent free radicals amplify ultrafine particle mediated cellular oxidative stress and cytotoxicity.* Part Fibre Toxicol, 2009. **6**: p. 11.

214. Fahmy, B., et al., *In vitro and in vivo assessment of pulmonary risk associated with exposure to combustion generated fine particles.* Environ Toxicol Pharmacol, 2010. **29** (2): p. 173-82.

215. Thevenot, P.T., et al., *Radical-Containing PM0.2 Initiates Epithelial-to-Mesenchymal Transitions in Airway Epithelial Cells.* Am J Respir Cell Mol Biol, 2012.

216. Lord, K., et al., *Environmentally persistent free radicals decrease cardiac function before and after ischemia/reperfusion injury in vivo.* J. Recept. Signal Transduction, 2011. **31** (2): p. 157-167.

217. Mahne, S., et al., *Environmentally persistent free radicals decrease cardiac function and increase pulmonary artery pressure.* Am. J. Physiol., 2012. **303** (5, Pt. 2): p. H1135-H1142.

218. Varner, K.J., et al. *Environmentally Persistent Free Radicals Decrease Cardiac Function In Vivo*. 2012. 68th Southwest Regional Meeting of the American Chemical Society. American Chemical Society.

CHAPTER II. EXPERIMENTAL

2.1 $PM_{2.5}$ Sampling Site Description

$PM_{2.5}$ samples were acquired from a Louisiana Department of Environmental Quality (LDEQ) ambient air monitoring station situated 30 ft away from roadside and 10 ft off the ground. This site is located on the north side of the LSU campus in Baton Rouge, LA near heavy traffic from Interstate 10 and a major industrial corridor of the Mississippi River. An aerial view of the location is displayed in Figure 2.1.

Figure 2.1 Aerial view of the $PM_{2.5}$ sampling site. The arrow shows the exact location of the $PM_{2.5}$ samplers.

2.2 $PM_{2.5}$ Sampling

Samples were collected using a Thermo Scientific Partisol-Plus Model 2025 equipped with a $PM_{2.5}$ fractionator. The flow rate was 16.7 L/min, and samples were collected on a Whatman 2 μm polytetrafluoroethylene (PTFE) 46.2 mm diameter filter with a polypropylene supported ring for 24 hours.

In addition to the Thermo sampler, samples were collected using a Tisch Environmental TE-6070V with a $PM_{2.5}$ size selective inlet. Each sample was allowed to collect 24 hours at a flow rate of 1100 L/min on a glass fiber filter (Whatman GF/A 8 x 10 in).

2.3 Extraction of $PM_{2.5}$ from Various Filters

2.3.1 Extraction from PTFE Filters

The extraction procedure closely followed extraction procedures in the literature [1]. After collection, filters had the support ring removed, analyzed for an initial radical concentration and transferred into 0.01 M PBS solution prepared in ultra-pure double distilled H_2O (UP H_2O) to maintain the pH at 7.4. The solution with filters were shaken for 15 min on a Daigger Vortex Genie 2, sonicated 5 min (Fisher Scientific FS20) at 40 W, and shaken again for 15 min. The filter was removed from suspension, dried, and the difference in weight determined how much $PM_{2.5}$ was removed [1, 2].

2.3.2 Extraction of $PM_{2.5}$ from Binder Free Glass Fiber Filters

This extraction procedure closely followed extraction procedures found in the literature [3]. After collection, the PM loaded filter was cut into several small pieces and placed in a flask with 50 mL of ultrapure double distilled H_2O (UP H_2O). The flask was manually shaken until the filter had mostly broken down in solution forming a thick suspension. After which, the suspension was sonicated for 20 min (Fischer Scientific FS10 at 40 W) to facilitate additional removal of PM from the filter. The filter pieces were removed from the PM solution and centrifuged to remove any remaining filter fibers. This was decanted and dried in a crucible at 102 °C for 5 hours. The resulting powder was removed from the crucible and measured by EPR spectroscopy.

2.4 $PM_{2.5}$ Analysis

2.4.1 $PM_{2.5}$ Metal Analysis

The metal content of $PM_{2.5}$ samples was quantified by utilizing Inductively Coupled Plasma – Atomic Emission Spectroscopy (ICP-AES). The whole filter, in the case of the PTFE filter, or part of the whole filter, in the case of the GF/A filter, was placed in a beaker. The sample was digested in 10 mL ICP grade HNO_3 solution for 48 h in a preheated block at an approximate temperature of 50 °C. This was subsequently diluted with 10 mL of 3% HNO_3 solution. A 1 mL aliquot was taken and diluted to 100 mL with 3% HNO_3 solution. The samples were analyzed for all the metal content, including: Al, As, Ba, Cd, Co, Cr, Cu, Fe, Mn, Ni, Pb, Si, and Zn.

2.4.2 GC/MS Analysis of Substituted Phenols

An Agilent 6890 Gas Chromatograph (GC) coupled with a 5973 Mass Selective Detector (MS) in the manual injection mode was utilized with the following parameters: column type 50 J&W DB5 MS 60 m x 0.25 mm i.d. x 0.25 μm, preceded by 5 m of 0.25 mm deactivated retention gap; injection type and temperature - splitless / 250 °C; column temperature program - initial 60 °C hold for 6 minutes, ramp 10 °C/min to 180 °C, 15 °C/min to 300 °C, hold for 2 minutes; total run time was 28.0 minutes; carrier gas - Helium; transfer line temperature – 280 °C; injection volume - 1 µL; column flow - 1 µL/min (constant flow); solvent Delay - 14 minutes; MS source temperature – 230 °C; MS quadrupole temperature – 150 °C; MS mode - SIM; ion dwell time – 100 ms. The mass-spectral library (NIST 98 version 1.6d) was used to identify the extraction products.

2.4.2.1 Sample Preparation

The filter was placed in a 50 mL conical flask containing 10 mL of tert-butyl methyl ether (TBME) and 0.16 mg of o-chlorophenol as the internal standard. The mixture was shaken for 20 min, and 250 µL of the sample extract was transferred to an amber vial with an additional 500 µL of TBME as well as 250 µL of N,O-bis(trimethylsilyl)trifluoroacetamide (BSTFA) for a total volume of 1000 µL. The vial was capped using Teflon/Silicone 11 mm crimp caps and mixed. The contents of the vial were heated in a preheated heating block for 30 min at 76 °C (± 5 °C).

Table 2.1 Standard calibration concentrations for GC/MS

Calibration Standard	Volume (mL) of Stock Solution	Final Volume (mL)
1	0.10	50
2	0.25	50
3	0.50	50
4	1.00	50
5	1.50	50
6	2.50	50
7	3.50	50

2.4.2.2 Standard Calibration Preparation

A standard stock solution was prepared by adding 40 mg phenol, 10 mg o-cresol, 10 mg m-cresol, 10 mg p-cresol, 100 mg catechol, 10 mg resorcinol, 80 mg of hydroquinone, 16 mg o-chlorophenol to TBME in a 100 mL amber volumetric flask. From this stock solution, aliquots, as presented in Table 2.1, were taken and diluted to 50 mL with TBME in a 50 mL volumetric flask. The concentrations of each standard are shown in Table 2.2.

Table 2.2 Substituted phenol standard calibration concentrations

Compound	Concentration (μg/mL)						
	Standard 1	Standard 2	Standard 3	Standard 4	Standard 5	Standard 6	Standard 7
Phenol	0.8	2.0	4.0	8.0	12.0	20.0	28.0
o-Cresol	0.2	0.5	1.0	2.0	3.0	5.0	7.0
m-Cresol	0.2	0.5	1.0	2.0	3.0	5.0	7.0
p-Cresol	0.2	0.5	1.0	2.0	3.0	5.0	7.0
Catechol	2.0	5.0	10.0	20.0	30.0	50.0	70.0
Resorcinol	0.2	0.5	1.0	2.0	3.0	5.0	7.0
Hydroquinone	1.6	4.0	8.0	16.0	24.0	40.0	56.0

2.4.2.3 Analysis and Calculation

The substituted phenol concentrations were calculated using equation 1 by calculating the peak area ratio of the sample analyte to o-chlorophenol. This was compared to the standards from the 7 point calibration curve and divided by the sample weight to obtain the concentration of the analyte from the sample in ppm (μg/g).

$$C = \frac{R*S*V}{m}$$ **equation 1**

where C (ug/g) is the concentration of the substituted phenol in the sample; m is the mass of the sample; V (mL) is the dilution factor of the sample; R is the peak area ratio of the analyte to o-chlorophenol; and S is the estimated concentration of the sample derived from the linear equation of the calibration curve.

2.4.3 EPR Analysis

$PM_{2.5}$ loaded filters or $PM_{2.5}$ powder were positioned in high purity quartz EPR tubes and analyzed at room temperature with a Bruker EMX -- 10/2.7 EPR Spectrometer. Samples were measured in a dual cavity with modulation and microwave frequencies of 100 kHz and 9.76 GHz, respectively. The parameters used to measure the radical concentration signal were: 2.05 mWatt power; modulation amplitude of 4.0 G; scan range of 100 G; time constant of 40.96 msec corresponding to a conversion of 163.84 msec; sweep time of 167.77 seconds; receiver gain 3.56×10^4; and three scans using 1024 points. Before any sample measurement, a vacuum sealed DPPH standard was measured at the same parameters listed above. This was performed to ensure proper working operation of the EPR. The DPPH standard, in vacuum, was not observed to decay and maintained a stable signal within ±11%.

2.4.3.1 Analysis and Calculation

All ΔH_{p-p} and g-factors were measured and calculated with the Bruker WINEPR data processing software. The radical concentrations were calculated by using the formula found in equation 2. Overall, this was calculated by comparing the area of the 1st derivative signal peak, as calculated by the ΔH_{p-p}^2 * relative intensity, to a DPPH standard 4-point calibration curve [4].

$$C = \frac{A * RG_{DPPH}}{A_{DPPH} * RG * m}$$ **equation 2**

where: C_2 is the radical concentration of the sample in spins/g; A is the area count of the sample; RG_{DPPH} is the receiver gain used to acquire the DPPH signal; A_{DPPH} is the area count of DPPH; RG is the receiver gain used to acquire the sample; and m is the mass of the sample analyzed.

2.4.3.2 Calibration Curve

A calibration curve was prepared to determine the quantitative radical concentration of samples measured by EPR. 5.4 mg of DPPH was weighed using a microbalance with 1 μg readability. This was dissolved in 100mL of benzene to make a stock solution of 54 μg/mL. From this, a 1 mL aliquot was removed and subsequently diluted to 10 mL with benzene. The concentration of the diluted standard was analyzed using a UV-Vis-NIR spectrophotometer (Shimadzu, model UV-3101PC, double beam) with the following parameters: λ_{max} at 520 nm and a molar extinction coefficient (ε) of 12,800 $M^{-1}cm^{-1}$ [5, 6]. This verified the concentration of the original stock solution, after accounting for dilution, as 1.37×10^{-4} M. Using the original DPPH standard solution, four different aliquots of the DPPH solution were taken (20 μL, 60 μL, 80 μL, and 100 μL) and placed in a high purity quartz EPR tube. This range was used to correspond to the normal concentration range of all radicals measured. The samples were dried by flowing nitrogen. Additional nitrogen was slowly flowed in the tube to keep the dry DPPH under an inert environment until EPR analysis. The area counts were determined by $\Delta H_{p\text{-}p}^2$ * relative intensity of the DPPH 1st derivative signal [4]. The area count was plotted against the amount of DPPH used to generate the calibration curve. The calibration curve was found to have an R value of 0.98, and the calibration curve generated was used for the quantitative calculation of all samples in these studies.

2.5 Determination of Half-Lives of EPFRs in $PM_{2.5}$

After obtaining a final weight, the filter was removed from the polypropylene supported ring and analyzed by EPR to ascertain its initial spin concentration. The sample was placed in a controlled temperature and humidity incubator to age in order to determine the persistency of the bound radicals. Two separate temperature and humidity settings were employed for this investigation. One setting at room temperature and humidity while the other at a temperature of 30 °C and a relative humidity of 50 (± 5%). The incubator was maintained under ambient air circulation with the aim of reproducing previous decay experiments. Subsequent analyses were performed intermittently, normalized to the initial spin concentration, and plotted against time from the initial analysis. An exponential regression was performed on the plotted data in order to calculate the decay rate and 1/e half-lives of the radicals.

2.5.1 Calculation of 1/e Half-Life

A pseudo-first order decay where oxygen is the reactant in excess was applied to all samples, because molecular oxygen is documented as the principle pathway for organic radical removal by peroxide radical formation or radical decomposition [7-10]. This can be written as:

$$R + O_2 \rightarrow S$$

where R is the radical and S is the product. The rate decay for this reaction is written as:

$$\frac{d[R]}{dt} = K[O_2][R] \qquad \textbf{equation 3}$$

As stated above, the oxygen is in excess, therefore its contribution is negligible. In other words, there is a steady state of oxygen, or

$$\frac{d[O_2]}{dt} = 0$$

With that, equation 3 then integrates to

$$dln[R] = kdt \quad \text{where } k=K\,[O_2]$$

$$\int_{R_0}^{R_f} dln[R] = -\int_0^t k\,dt$$

$$lnR_f - lnR_0 = -kt$$

$$ln\frac{R_f}{R_0} = -kt \qquad \textbf{equation 4}$$

$$\frac{R_f}{R_0} = e^{-kt} \qquad \textbf{equation 5}$$

resulting in the normalized radical concentration as a function of the decay rate and time. The 1/e half-life is the time it takes for the initial radical concentration to decay to 1/e, that is,

$$R_f = 1/e * R_0$$

Substituting this into equation 5 gives,

$$\frac{1}{e}R_0 = R_0e^{-kt}$$

$$t_{\frac{1}{e}} = \frac{1}{k} \qquad \textbf{equation 6}$$

For a first order reaction, the 1/e half-life results in the reciprocal of the rate constant. As shown, using a 1/e half-life allows for easier conversions from the reaction rate and used instead of a normal half-life.

2.6 Meteorological Data

All meteorological data was retrieved from the LDEQ ambient monitoring station as sample collection, except for solar and ultraviolet (UV) radiation measurements which were obtained from the capitol monitoring site less than a mile away.

2.7 Calculation of Pearson's Correlation Coefficient

In order to observe a direct (linear) dependence between two factors, the Pearson's correlation coefficient was calculated using the formula in equation 7

$$p = \frac{n(\sum xy)-(\sum x)(\sum y)}{\sqrt{[\sum x^2-(\sum x)^2][n\sum y^2-(\sum y)^2]}} \qquad \textbf{equation 7}$$

where p is the correlation coefficient, n is the number of samples correlated, x is the first item, and y is the second item. Calculating the correlation between the two items resulted in a correlation coefficient between -1.0 and 1.0, where 1.0 indicated a perfect direct relationship (linear) between the two items and -1.0 indicated a complete anticorrelation. In the case of an anticorrelation, this implied the two items are inversely related to each other. If the correlation coefficient was 0, then there was no correlation or an insignificant correlation. Correlations were considered significant when $p > 0.05$ or when $p < -0.05$.

2.8 Calculation for Equivalent Cigarettes Smoked from Inhaling $PM_{2.5}$

The number of equivalent cigarettes smoked from inhaling $PM_{2.5}$ was calculated first by converting the $PM_{2.5}$ radical concentration to radicals inhaled daily using equation 8:

$$RI_{PM} = RC_{PM} * F * PC_{PM} * V \qquad \textbf{equation 8}$$

where RI_{PM} is the radicals inhaled from $PM_{2.5}$ (radicals/day); RC_{PM} is the averaged radical concentration in $PM_{2.5}$ (radicals/g); F is the conversion from g to µg; PC_{PM} is the particle concentration of $PM_{2.5}$ (µg/m^3); and V is the volume of air breathed daily for an adult male (20 m^3/day)[11]. This was then compared to the number of radicals inhaled from smoking a cigarette using equation 9:

$$EQ = \frac{RI_{PM}}{(RC_{cig} * C_{tar})} \qquad \textbf{equation 9}$$

where EQ is the number of equivalent cigarettes smoked; RC_{cig} is the radical concentration in cigarette tar (radicals/g tar)[12-16]; and C_{tar} is the amount of tar per cigarette (g tar/cigarette).

2.9 Spin Trapping of Hydroxyl Radical

2.9.1 Materials

2,2-diphenyl-1-picrylhydrazyl (DPPH), deferoxamine mesylate (DFO, assay 92.5%, TLS), and 0.01 M phosphate-buffered saline pH 7.4 (PBS, NaCl 0.138 M, KCl 0.0027 M) were all purchased from Sigma-Aldrich. High purity 5,5-dimethyl-1-pyroline-N-oxide (DMPO, 99%+, GLC) was obtained from Enzo Life Sciences and used without additional purification. Hydrogen peroxide (Assay, 30%) and diethylenetriaminepentaacetic acid (DETAPAC, 99%) were purchased from Fluka Analytical. In the few experiments using DFO and DETAPAC, the solutions were made to a final concentration of 0.1mM DFO or DETAPAC in sample solution. A 0.03% H_2O_2 solution was made by diluting 100 µL of H_2O_2 in 100 mL ultrapure H_2O. The concentration was verified by UV-VIS absorption to be 0.0104 M. This was further diluted with sample to give a final concentration of approximately 2 mM H_2O_2.

Compressed air was utilized to prepare aerobic samples and compressed UHP N_2 for anaerobic samples. Unless otherwise stated, aeration or N_2 purging times were 10 min.

2.9.2 Chelex Treatment of H_2O

1.3 g of Chelex resin was added to 10 mL PBS solution and mixed rigorously for 1 hour. The PBS solutions with resin were left overnight before use and filtered from solution using a Fisherbrand P5 filter paper.

2.9.3 *In Vitro* Studies

A 0.01 M PBS solution was prepared in H_2O to maintain the pH at 7.4 and aerated for 10 min using compressed air. PM suspensions were made for each sample and subsequently diluted with additional PBS to a volume of 190 μL containing a final concentration of approximately 400-500 μg/mL. DMPO (10 μL from a freshly prepared solution of 3 M) was added to the dilutions and vigorously shaken for 30 s at a final volume of 200 μL. This concentration of DMPO (150 mM) was found to prevent secondary reactions, such as dimerization [17] and decomposition reactions with molecular oxygen. 20 μL of the suspension was transferred to an EPR capillary tube (i.d. ~1 mm, o.d. 1.55 mm) and sealed at one end with sealant (Fisher brand). The capillary was inserted in a 4 mm EPR tube and placed in the EPR resonator. The EPR spectra of DMPO-OH adducts were taken at specified times from initial DMPO addition using the following parameters: scan range of 100 G; time constant of 40.96 msec corresponding to a conversion of 163.84 msec; sweep time of 167.77 seconds; receiver gain 3.56×10^4; modulation amplitude of 0.80 G, a power of 10.25 mW, and two scans. The resulting 4-line peak areas for DMPO-OH adducts, as calculated by $\Delta H_{p\text{-}p}^2$ * relative intensity for each peak and reported in arbitrary units, were summed together for each time interval collected. The calculated area was then plotted against the time from the initial DMPO addition. This resulted in a DMPO-OH curve for each sample.

2.10 Effects of NO_x and O_3 on EPFRs in $PM_{2.5}$

2.10.1 Materials

2,2-diphenyl-1-picrylhydrazyl (DPPH), copper turnings, phosphate buffered saline pH 7.4 (PBS, NaCl 0.138 M, KCl 0.0027 M), and potassium iodide (Reagent Plus, 99%) were all purchased from Sigma-Aldrich. Concentrated nitric acid and boric acid were purchased from Fischer Scientific, and high purity 5,5-dimethyl-1-pyroline-N-oxide (DMPO) came from Enzo Life Sciences and used without any additional purification.

All nitrogen and air used was ultra-high purity (UHP) grade. All water employed was double distilled milli-Q water.

2.10.2 O_3 Exposure

An Enmet Corporation model 04052-011 ozone generator was operated so a minimal air flow was maintained (100 mL/min), as a Teflon tube was inserted within 2 - 3 mm of the PM powder inside an EPR tube (inner diameter 9.07 mm, length 178 mm). The slow flow prevented any PM from being blown out of the tube while still exposing to adequate amounts of ozone. The exit went to a gas washing bottle where an ozone indicator solution was maintained. The ozone indicator solution was prepared using the KI method [18] of detection by mixing 3.1 g H_3BO_3 with 5.0 g KI in 500 mL of H_2O. Total ozone exposure was found to be 2 ppm which converts to 2.760×10^{-6} torr.

2.10.3 NO Exposure

Approximately 5 g of Cu turnings was added into a stoppered flask connected to a gas line and collection flask. N_2 was purged through the collection system for 1 hr to remove any

O_2. Nitric acid was added to the flask by a globe funnel to start the reaction. The line was flushed with freshly formed NO for an additional 30 min, allowing time to react with any trace O_2 still present before condensing the NO in a flask using liquid N_2. The gas was purified by gas distillation using a vacuum system before use. Samples were placed in a vacuum line and evacuated down to less than 10^{-2} torr before exposure to NO. The tube containing the NO and sample was sealed and allowed to react over the specified time with the radical concentration monitored periodically. After exposure, unreacted NO was removed by vacuum for 30 min and the radical concentration was inspected again.

2.10.4 NO/NO_2 Exposure

NO_2 was produced by further oxidation of NO by air. The collection flask was opened to ambient air to form NO_2 and confirmed by the presence of orange fumes in the system. The NO/NO_2 was condensed back in the collection tube using liquid N_2. The entire system was evacuated out again and purified from traces of oxygen by gas distillation. The exact ratio of NO/NO_2 was not determined. The procedure for sample exposure was the same as NO.

2.10.5 Spin Trapping of Hydroxyl Radical After Exposure

Spin trapping of hydroxyl radicals generated from a reference and sample exposed to the oxidant of interest are described in Section 2.9 on page 46.

2.11 Simulated Solar Exposure of EPFRs in $PM_{2.5}$

2.11.1 Irradiation of Sample.

5 - 8 mg of sample was loaded in a high purity quartz EPR tissue flat cell. An initial radical concentration of the sample was measured. The loaded flat cell was placed in a Model

3940 Series Forma Environmental Chamber and irradiated by an Oriel Universal Xenon Arc Lamp at 150 W equipped with an Air Mass (AM) 1.5 filter. Using a LP02 pyranometer, insolation of the sample at 950 W/m^2 was verified. This value corresponded with the Baton Rouge June/July midday maximum insolation as recorded by a Louisiana Department of Environmental Quality ambient air monitoring station. After exposure, the sample radical signal was measured. The procedure was repeated for 15 min, 30 min, 60 min, and 90 min exposure time resulting in a total of 195 min insolation.

2.11.2 Spin Trapping of Hydroxyl Radical After Exposure

Spin trapping of hydroxyl radicals generated from a reference and sample exposed to the simulated solar radiation are described in Section 2.9 on page 46.

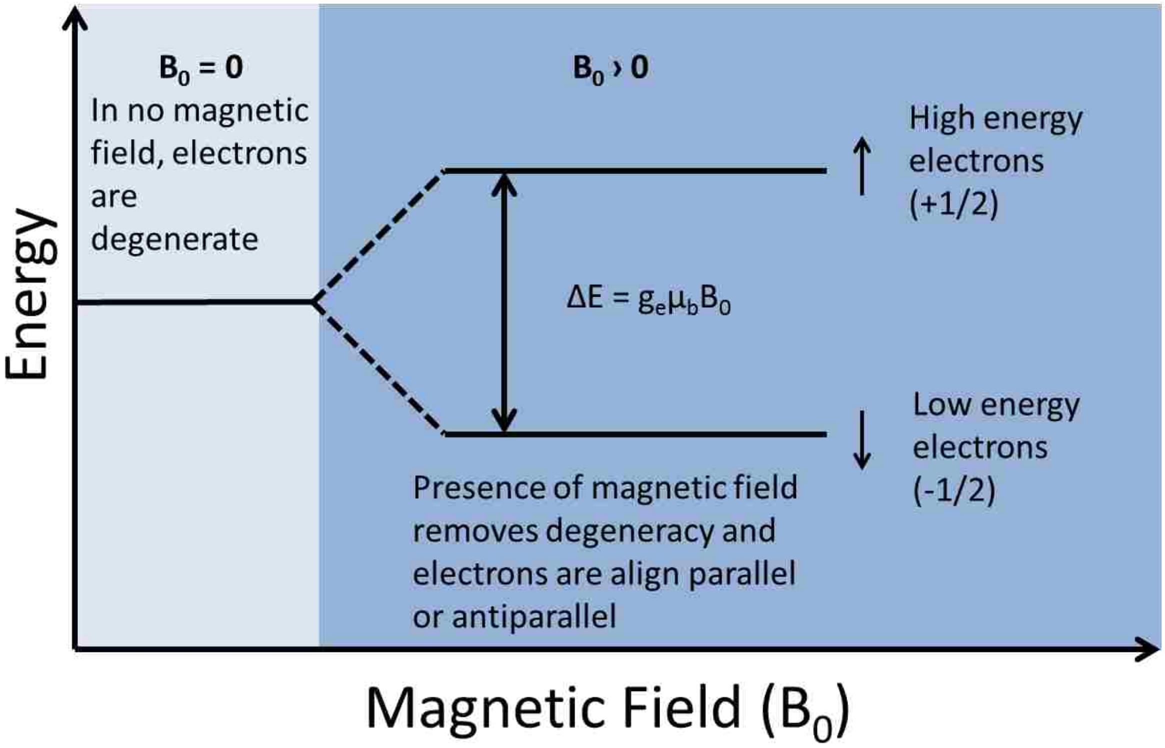

Figure 2.2 The Zeeman Effect

2.12 Basics of EPR Spectroscopy

EPR spectroscopy is used to detect species with one or more unpaired electrons by the Zeeman effect. In the absence of a magnetic field (B_0), the two electron states, α (+1/2, the high energy electron) and β (-1/2, the low energy electron), are degenerate, and the electrons are oriented randomly. When an external magnetic field is applied, the unpaired electrons align either parallel or antiparallel to the external magnetic field. This results in the α and β states having different energies. This is called the Zeeman effect (cf. Figure 2.2).

Due to the electrons favoring the lower energy state, the Boltzman population in the β

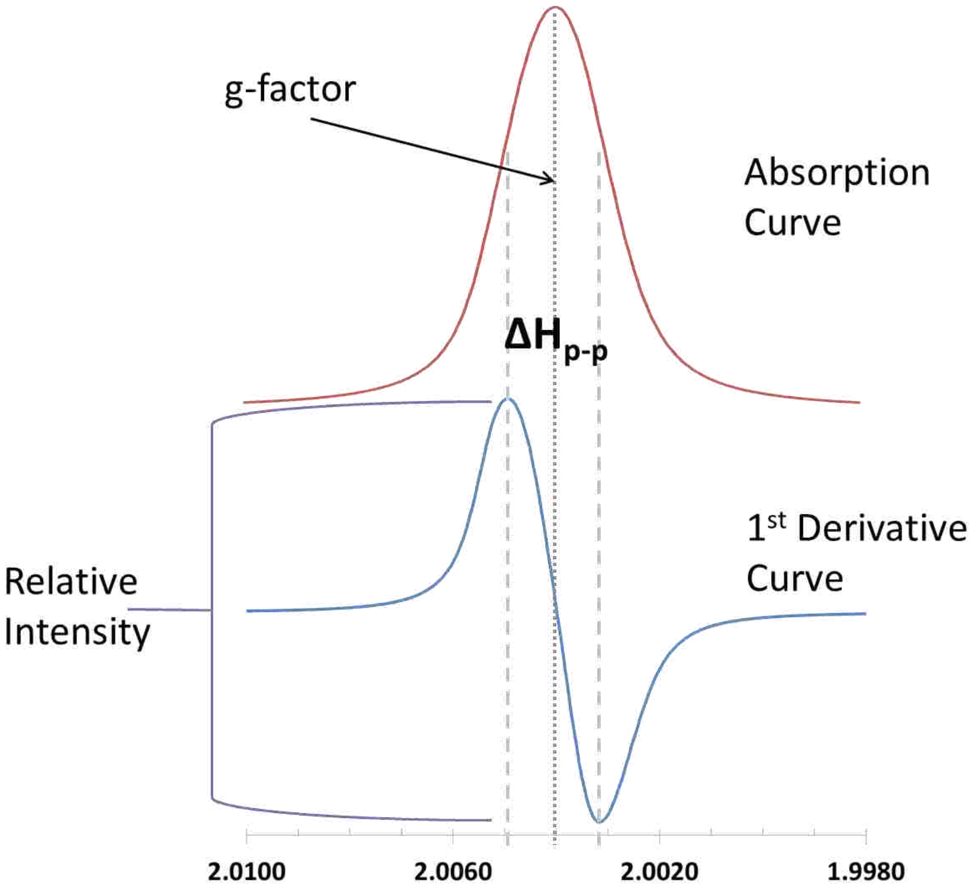

Figure 2.3 Example of an absorption and first derivative EPR spectrum

state is more than α state. Keeping the microwave radiation frequency constant, the magnetic field is scanned until the energy splitting of the two states is matched by the incident radiation.

When these conditions are met, a field of resonance is achieved, and given by equation 10:

$$h\nu = g\mu_0 B$$ **equation 10**

where: h is Plank's constant ($h = 6.63\text{x}10^{-24}$ Js); ν (in Hz) is the frequency of the incident microwave radiation; μ_0 is the Bohr magneton ($\mu_0 = 9.27\text{x}10^{-24}$ JT^{-1}); and B (in Tesla or Gauss) is the magnetic field. An example of an absorption and a first-derivative EPR spectra are given in Figure 2.3.

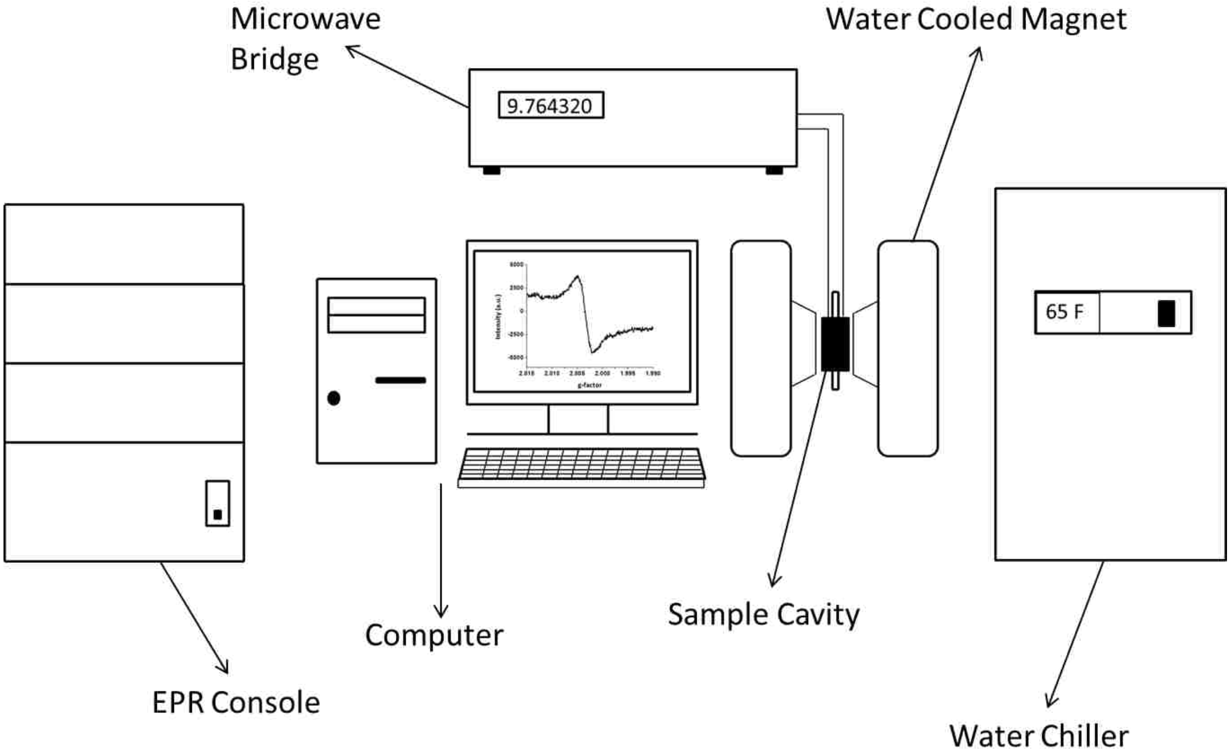

Figure 2.4 Schematic representation of EPR instrumentation

2.13 EPR Instrumentation

The Bruker EMX EPR utilized for all experiments is depicted in Figure 2.4. Samples were loaded into the sample cavity with a continuous nitrogen flow to maintain a water free environment. This is important as water, with a high dielectric constant, will absorb part of the microwave radiation resulting in false measurements. The sample cavity is located between 2 water cooled (65 °F) magnets, and the microwave radiation enters into the sample cavity by the microwave bridge. All EPR component control is operated through the EPR console with a user interface observed on a computer. All data acquisition and processing are also performed through the computer.

2.14 References

1. Shi, T.M., et al., *Hydroxyl radical generation by electron paramagnetic resonance as a new method to monitor ambient particulate matter composition.* Journal of Environmental Monitoring, 2003. **5** (4): p. 550-556.

2. Valavanidis, A., K. Fiotakis, and T. Vlachogianni, *The Role of Stable Free Radicals, Metals and PAHs of Airborne Particulate Matter in Mechanisms of Oxidative Stress and Carcinogenicity.* , in *Urban Airborne Particulate Matter*, F. Zereini and C.L.S. Wiseman, Editors. 2011, Springer Berlin Heidelberg. p. 411-426.

3. Valavanidis, A., et al., *Electron paramagnetic resonance study of the generation of reactive oxygen species catalysed by transition metals and quinoid redox cycling by inhalable ambient particulate matter.* Redox Report, 2005. **10** (1): p. 37-51.

4. Chesnut, D.B., *On the use of AW2 method for integrated line intensities from first-derivative presentations.* J. Magn. Reson., 1977. **25**: p. 373-4.

5. Yordanov, N.D. and A. Christova, *DPPH as a primary standard for quantitative EPR spectrometry*. Applied Magnetic Resonance, 1994. **6** (1-2): p. 341-345.

6. Weil, J.A. and J.R. Bolton, *Basic Principles of Paramagnetic Resonance*, in *Electron Paramagnetic Resonance*. 2006, John Wiley & Sons, Inc.

7. Barckholtz, C., M.J. Fadden, and C.M. Hadad, *Computational Study of the Mechanisms for the Reaction of O2(3Σg) with Aromatic Radicals.* The Journal of Physical Chemistry A, 1999. **103** (40): p. 8108-8117.

8. Korkmaz, M. and M. Polat, *Free radical kinetics of irradiated durum wheat.* Radiation Physics and Chemistry, 2000. **58** (2): p. 169-179.

9. Tonokura, K., et al., *Cavity Ring-down Study of the Visible Absorption Spectrum of the Phenyl Radical and Kinetics of Its Reactions with Cl, Br, Cl2, and O2.* The Journal of Physical Chemistry A, 2002. **106** (24): p. 5908-5917.

10. Dellinger, B., et al., *Formation and stabilization of persistent free radicals.* Proceedings of the Combustion Institute, 2007. **31** (1): p. 521-528.

11. *Recommendations for and documentation of biological values for use in risk assessment*, Environmental Protection Agency, Editor 1988: Washington, DC.

12. Pryor, W.A., D.G. Prier, and D.F. Church, *Electron-Spin Resonance Study of Mainstream and Sidestream Cigarette Smoke: Nature of the Free Radicals in Gas-Phase Smoke and in Cigarette Tar.* Environmental Health Perspectives, 1983. **47**: p. 345-355.

13. Pryor, W., et al., *The radicals in cigarette tar: their nature and suggested physiological implications.* Science, 1983. **220** (4595): p. 425-427.

14. Blakley, R.L., D.D. Henry, and C.J. Smith, *Lack of correlation between cigarette mainstream smoke particulate phase radicals and hydroquinone yield.* Food and Chemical Toxicology, 2001. **39** (4): p. 401-406.

15. Valavanidis, A. and E. Haralambous, *A comparative study by electron paramagnetic resonance of free radical species in the mainstream and sidestream smoke of cigarettes with conventional acetate filters and bio-filters.* Redox Report, 2001. **6** (3): p. 161-171.

16. Baum, S.L., et al., *Electron spin resonance and spin trap investigation of free radicals in cigarette smoke: development of a quantification procedure.* Analytica Chimica Acta, 2003. **481** (1): p. 1-13.

17. Janzen, E.G., et al., *Detection of alkyl, alkoxyl, and alkyperoxyl radicals from the thermolysis of azobis(isobutyronitrile) by ESR/spin trapping. Evidence for double spin adducts from liquid-phase chromatography and mass spectroscopy.* J. Am. Chem. Soc., 1990. **112**: p. 8279-84.

18. Shechter, H., *Spectrophotometric method for determination of ozone in aqueous solutions.* Water Research, 1973. **7** (5): p. 729-739.

CHAPTER III. EPFRS AND THEIR HALF-LIVES IN PM$_{2.5}$

3.1 Detection of EPFRs in PM$_{2.5}$

The first objective was to investigate if EPFRs decayed in ambient air similar to the previous reports of the model EPFR system, and this was performed by an expansive study of collected PM$_{2.5}$. The samples decayed in two temperature settings, one at ambient conditions and another at 30 °C and 50% relative humidity. Correlations with the metal content of the sample as well as the conditions during collection were calculated to explain the radical content and decay behavior.

3.1.1 Initial Radical Concentrations

All collected PM$_{2.5}$ samples initially displayed a single, unstructured organic peak exhibiting an average $\Delta H_{p\text{-}p}$ of 5 - 8 Gauss. The relatively wide peak in addition to a lack of hyperfine splitting implied multiple organic species of the same radical family present or signal broadening by organic-metal interactions [1-4]. These signals displayed initial g-factors of 2.0035 ± 0.0004 suggesting semiquinone-type radicals in a complex matrix [1-3, 5-10]

In addition to an organic peak, the presence of paramagnetic metals was detected. These metal peaks were persistent throughout the decay and not observed to degrade. The most common peak was Fe^{3+} at an approximate g-factor of 2.1 attributed to Fe^{3+} distributed in clusters [11, 12]. The presence of Mn(I=5/2) was also noticed in two samples collected on April 30th and May 1st of 2010, and this is believed to result from the *in situ* oil burn in the Gulf of Mexico. Aside from the noticeable smell of these fumes in Baton Rouge, the NOAA HYSPLIT model calculated air trajectory during this time shows air from the burns passing over our sampler (data not shown).

The average initial radical concentration along with the number of samples for each decay category (*vide infra*) are displayed in Table 3.1. The displayed concentrations resulted from an average weight of 512 ± 300 μg collected per day. The overall radical concentration is comparable to the same concentration range from cigarette smoke [1], corresponding to 69 ppm as a semiquinone radical. A complete list of samples' initial radical concentration, decay rate, and 1/e half-lives are given in APPENDIX 1 on page 120.

Table 3.1 Range of initial radical concentration and the number of samples for each decay category

Decay Category	Range of Initial Radical Concentration (radicals/g)	# Samples
Fast Decay /Slow Decay	$2.32\text{x}10^{16}$ - $3.48\text{x}10^{18}$	54
Slow Decay	$2.02\text{x}10^{16}$ - $1.34\text{x}10^{18}$	27
No Decay	$2.65\text{x}10^{16}$ - $1.17\text{x}10^{18}$	21
Fast Decay /No Decay	$5.92\text{x}10^{16}$ - $1.99\text{x}10^{18}$	12
Overall	$2.02\text{x}10^{16}$ – $3.48\text{x}10^{18}$	94

3.2 Decay of Radical Signal

Decay of a well behaved radical signal is presented in Figure 3.1. All decays resulted from a diminishing relative intensity. There was no consistent broadening or narrowing of the signal during decay with the $\Delta H_{p\text{-}p}$ maintaining an average 6.49 ± 1.69 Gauss for all samples. The g-factor slightly increased throughout the decay by an average of 0.0002, and this is attributed to sample oxidation, therefore consistent with the elimination of organic radicals by reaction with oxygen [2, 13-15]. Although, there is also the possibility of losing more of the carbon centered radicals thereby shifting the g-factor higher.

There was no difference in decay behavior between the two temperature-humidity settings chosen. With $PM_{2.5}$ constituents changing daily, any differences in decay rate from temperature are not apparent; however, only 30 samples were analyzed using the lower parameters, so analyzing more samples at the lower conditions might identify an observable trend.

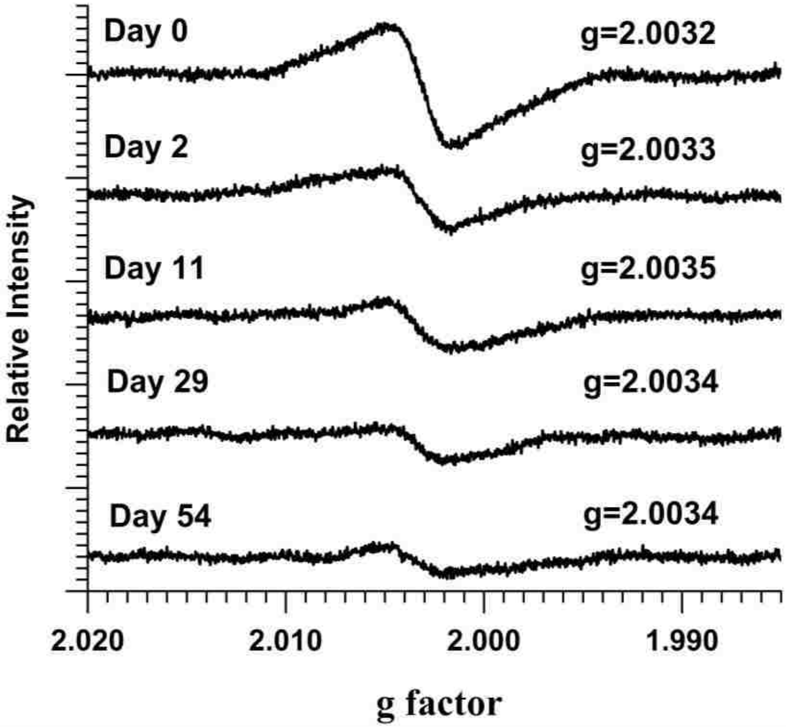

Figure 3.1 Decay of organic radical signal over 2 months as observed by EPR spectra. The g-factors are included to indicate oxidation of the radicals as the signal decays.

3.3 Categories of Decay

As displayed in Figure 3.2, four categories of decay were observed. The majority (47%) exhibited two consecutive decays with a relatively fast decay followed by a slower decay, Figure 3.2A. The fast decay rate was 0.05 – 0.002 hr^{-1} corresponding to a 1/e half-life of 1 – 21 days, and the slow decay rate was 0.002 – $8x10^{-6}$ hr^{-1} equivalent to a 1/e half-life of 21 – 5028 days.

The large range for the slow decay results from seven samples decaying extremely slowly yet consistently with 1/e half-lives of 1000 – 5000 days. When these samples were removed, the slow 1/e half-life was 21 – 417 days.

A single slow decay was observed from approximately a quarter (24%) of the samples, Figure 3.2B. The decay rate was 0.01 – 2×10^{-5} hr^{-1} indicating a 1/e half-life of 4 – 2083 days. Comparable to the previous category, there were two samples shifting the range. When these

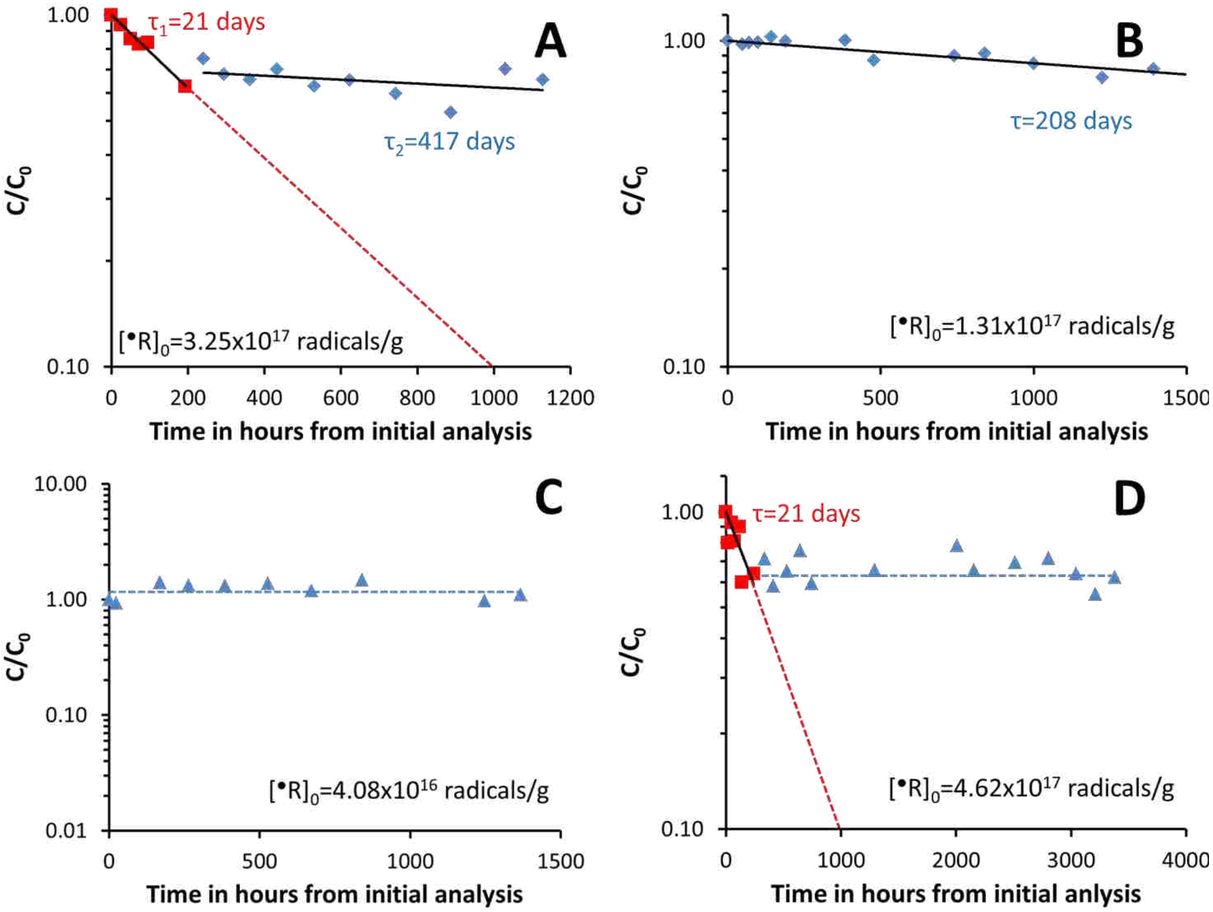

Figure 3.2 Representation of the 4 categories of decay observed. All represented decays occurred at 30 C and 50% RH. All displayed half-lives are 1/e half-lives. **A.** Representation of samples exhibiting two consecutive decays, a relatively fast decay followed by a slower decay (47% of samples). **B.** Representation of samples exhibiting one slow decay (23%). **C.** Representation of samples exhibiting no decay (18%). **D.** Representation of samples exhibiting a relatively fast decay followed by no decay (11%).

were removed, the 1/e half-life was 4 – 595 days. This range is similar to the previous category suggesting these samples may also exhibit a fast decay; however, due to a long atmospheric residence time, they decayed before an initial measurement.

The last two decay types were no decay (18%), Figure 3.2C, and a relatively fast decay followed by no decay (11%), Figure 3.2D. Similar to the first category, fast decay rate was 0.159 – 0.002 hr^{-1} analogous to a 1/e half-life of 0.25 – 21 days. Due to the unknown range of residence times in the atmosphere, decay 2C may just be after the fast decay in 2D was completed.

In all cases, we attribute the faster decay (displayed as τ~21 days) to decomposition of a phenoxyl-type radical [3, 16]. This is further supported from correlations of phenol with the initial radical concentration in addition to the fast decay rate (*vide infra*). The slow decay is attributed to decomposition of a semiquinone-type radical (displayed as τ~208 and 417 days) [17]. The no decay pattern is explained by radicals entrapped in the bulk of $PM_{2.5}$ or restricted in a solid matrix (*i.e.* internal radicals) where the unpaired electron is delocalized over many conjugated or aromatic bonds [3, 10, 18-21]. These radicals remain internal and cannot undergo oxidation in air and therefore persist indefinitely.

3.4 Substituted Phenol Analysis

Of all the substituted phenols measured, only phenol was above the detection limit of the instrumentation. The phenol concentration was correlated to the initial $\Delta H_{p\text{-}p}$, initial radical concentration, initial g-factor, and the fast/slow decay rate. As observed in Figure 3.3A, the phenol data exhibited a strong correlation with the initial $\Delta H_{p\text{-}p}$ where the presence of more phenol increased the initial $\Delta H_{p\text{-}p}$. This suggested agreement with the concept of concentration broadening [22, 23], where an increase in the same specific radical constituent will increase the ΔH_{p-p}.

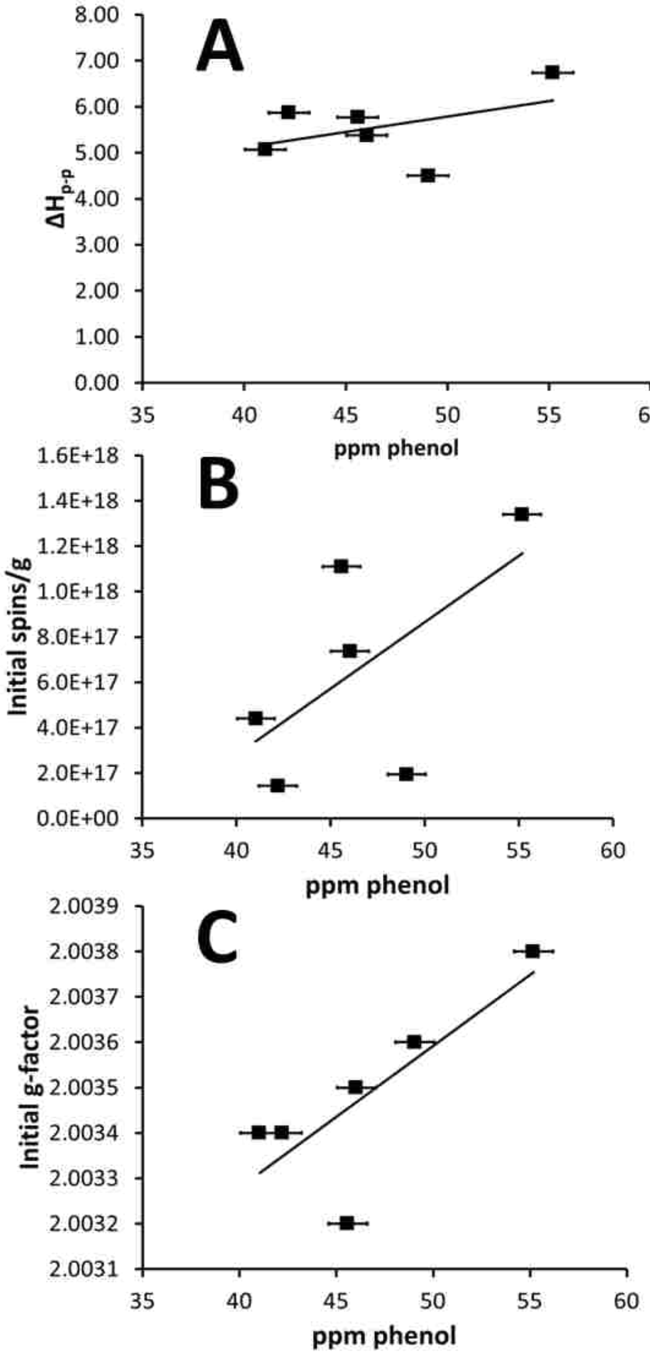

Figure 3.3 Plots of phenol correlations. **A.** Initial ΔH_{p-p} vs. phenol concentration with a correlation value of p=0.95. **B.** Initial spins/g vs. phenol concentration with a correlation value of p=0.61. **C.** Initial g-factor vs. phenol concentration with a correlation value of p=0.97

There was a strong association from the initial radical concentration where an increase in phenol resulted in an increased radical concentration, Figure 3.3B. This does not suggest only phenoxyl radicals are present in $PM_{2.5}$. This is supported from the g-factor correlation, Figure 3.3C. A shift in g-factor occurs when there is a change in radical species. For example, existence of a semiquinone-type radical, one of the persistent radicals, was considered present in tobacco tar [24] and PM [2, 3], and more recently, semiquinone redox cycling was demonstrated in the oxidative capacity of $PM_{2.5}$ [25]. The increased presence of a semiquinone-type radical, more oxygen centered in nature when compared to the phenoxyl radical [26], will increase the g-factor. This is corroborated by the radical signal, because the organic radical signal is a single, broad, unstructured peak in all the samples studied; therefore, multiple superimposed radical signals may be present [3, 10, 21].

Correlations of phenol with the fast decay conveyed a very significant correlation of $p=0.60$ ($n=7$). In contrast to this, the slow decay exhibited a weak, negative correlation of $p=-0.20$ ($n=3$). These associations further implicate the fast decay to occur from phenoxyl radical decomposition.

3.5 Metals Analysis and Correlation

There was a wide variety and concentration of metals found in $PM_{2.5}$. Although, there were weakly significant or no correlations observed with metals. The complete list of metal data for all samples studied in addition to their correlations with the initial radical concentration and decay rates are presented in APPENDIX 1 on page 120.

3.6 Meteorological and Atmospheric Pollutant Correlations

In general, meteorological correlations were not strong. The highest positive association for initial radical concentration resulted from ozone (p=0.28) implying the importance of photochemical processes for EPFR formation. This is supported by positive relationships with both solar (p=0.14) and UV radiation (p=0.12). Correlations for the fast decay indicated the presence of ozone (p=-0.10) as well as solar (p=-0.45) and UV radiation (p=-0.42) decrease the fast decay rate. Previous sets of relationships demonstrate the ability of all three to increase the radical concentration; so consequently, their presence will slow down the fast decay rate due to new radical formation. Correlations for the slow decay were the weakest overall and less clear. Detailed data for meteorological conditions and atmospheric pollutants used in addition to their respective associations are presented in APPENDIX 1 on page 120.

3.7 Comparison of Radicals Inhaled in $PM_{2.5}$ to Cigarettes

Our research demonstrated EPFRs induce various types of heart and respiratory dysfunction in rats and mice similar to those observed from smoking cigarettes [27-29]. While direct comparison of EPFR effects in $PM_{2.5}$ and cigarette smoke were not performed, the data suggests common EPFRs in cigarette tar and $PM_{2.5}$ result in very similar human diseases.

In order to assess the potentially negative health consequences of $PM_{2.5}$, the overall average concentration of radicals from $PM_{2.5}$ in Baton Rouge was compared to the average concentration of radicals in cigarette smoke [24, 30-33]. The outcome is expressed as the equivalent number of cigarettes a person smokes in a day from exposure to the same number of EPFRs inhaled from polluted air, Table 3.2. An example calculation using the US 24-hour $PM_{2.5}$ concentration average is given below.

Table 3.2 Number of equivalent cigarettes smoked from inhaling PM$_{2.5}$ with 95% Confidence Interval. All PM$_{2.5}$ data is for 2007-2009 designation values from reference 34.

Average Concentrations and Regulatory Standards		**Concentration of PM$_{2.5}$ (µg/m^3)**	**# of equivalent cigarettes**
US 24 hour average		26.9	0.3±0.1 per day
US yearly average		10.6	47±16 per year
EPA 24 hour standard (2011)		35	0.4±0.1 per day
EPA yearly standard (2011)		15	67±23 per year
24 Hour PM$_{2.5}$ Non-Attainment Locations			
Region	**State**	**PM$_{2.5}$ 24-hour Design Value (µg/m^3) †**	**# of equivalent cigarettes**
Chico	CA	59	0.7±0.2
Cleveland-Akron-Lorain	OH	36	0.4±0.1
Fairbanks	AK	57	0.7±0.2
Klamath Falls	OR	47	0.6±0.2
Liberty-Clairton	PA	50	0.6±0.2
Logan	UT-ID	40	0.5±0.2
Los Angeles-South Coast Air Basin	CA	49	0.6±0.2
Milwaukee-Racine	WI	37	0.5±0.2
Oakridge	OR	41	0.5±0.2
Pittsburgh-Beaver Valley	PA	37	0.5±0.2
Provo	UT	50	0.6±0.2
Sacramento	CA	51	0.6±0.2
Salt Lake City	UT	48	0.6±0.2
San Francisco Bay Area	CA	36	0.4±0.1
San Joaquin Valley	CA	70	0.9±0.3
Seattle-Tacoma	WA	46	0.6±0.2
Steubenville-Weirton	OH-WV	37	0.5±0.2
Yuba City-Marysville	CA	42	0.5±0.2

†Design Values are computed from PM$_{2.5}$ monitoring data reported to the EPA's Air Quality System from the local agencies. Exceptional events (wildfires, construction, volcanic eruption) are not included in the calculation.

$$RI_{PM} = RC_{PM} * F * PC_{PM} * V$$

$$3.84x10^{17}\frac{radicals}{g} * 1x10^{-6}\frac{g}{\mu g} * 26.9\frac{\mu g}{m^3} * 20\frac{m^3}{day}$$

$$RI_{PM} = 2.07x10^{14}\frac{radicals}{day}$$

$$EQ = \frac{RI_{PM}}{\left(RC_{cig} * C_{tar}\right)}$$

$$\frac{2.07x10^{14}\frac{radicals}{day}}{\left(4.75x10^{16}\frac{radicals}{g\ tar} * 0.013\ \frac{g\ tar}{cigarette}\right)}$$

$$EQ = 0.3\ cigarettes$$

Based on the initial radical concentration and the US 24-hour air quality data, each person in the US smokes the equivalent of 0.3 cigarettes per day from $PM_{2.5}$ inhalation. The same calculation using the US yearly average results in 47 cigarettes per year. In the more polluted areas (based on air quality exceedances), such as San Joaquin Valley, each person smokes nearly a full cigarette per day and as high as 101 cigarettes per year.

3.8 References

1. Squadrito, G.L., et al., *Quinoid redox cycling as a mechanism for sustained free radical generation by inhaled airborne particulate matter.* Free Radical Biology and Medicine, 2001. **31** (9): p. 1132-1138.

2. Dellinger, B., et al., *Formation and stabilization of persistent free radicals.* Proceedings of the Combustion Institute, 2007. **31** (1): p. 521-528.

3. Lomnicki, S., et al., *Copper Oxide-Based Model of Persistent Free Radical Formation on Combustion-Derived Particulate Matter.* Environ. Sci. Technol., 2008. **42**: p. 4982-4988.

4. Valavanidis, A., K. Fiotakis, and T. Vlachogianni, *The Role of Stable Free Radicals, Metals and PAHs of Airborne Particulate Matter in Mechanisms of Oxidative Stress and Carcinogenicity.* , in *Urban Airborne Particulate Matter*, F. Zereini and C.L.S. Wiseman, Editors. 2011, Springer Berlin Heidelberg. p. 411-426.

5. Lachocki, T.M., D.F. Church, and W.A. Pryor, *Persistent free radicals in woodsmoke: An ESR spin trapping study.* Free Radical Biology and Medicine, 1989. **7** (1): p. 17-21.

6. Pryor, W.A., *Cigarette smoke radicals and the role of free radicals in chemical carcinogenicity.* Environ Health Perspect, 1997. **105 Suppl 4**: p. 875-82.

7. Valavanidis, A., A. Salika, and A. Theodoropoulou, *Generation of hydroxyl radicals by urban suspended particulate air matter. The role of iron ions.* Atmospheric Environment, 2000. **34** (15): p. 2379-2386.

8. Valavanidis, A., et al., *Electron paramagnetic resonance study of the generation of reactive oxygen species catalysed by transition metals and quinoid redox cycling by inhalable ambient particulate matter.* Redox Report, 2005. **10** (1): p. 37-51.

9. Valavanidis, A., et al., *Determination of Selective Quinones and Quinoid Radicals in Airborne Particulate Matter and Vehicular Exhaust Particles.* Environmental Chemistry, 2006. **3** (2): p. 118-123.

10. Valavanidis, A., et al., *Persistent free radicals, heavy metals and PAHs generated in particulate soot emissions and residue ash from controlled combustion of common types of plastic.* J. Hazard. Mater., 2008. **156**: p. 277-284.

11. Kumar, B., C. Chen, and S. Lin, *Effects of melting atmosphere on properties of a glass in the calcia-phosphorus pentoxide-iron sesquioxide system.* Phys. Chem. Glasses, 1992. **33** (5): p. 204-6.

12. Ardelean, I., et al., *EPR and magnetic susceptibility studies of iron ions in 70TeO2·25B2O3·5PbO glass matrix.* Solid State Communications, 1997. **102** (4): p. 341-346.

13. Barckholtz, C., M.J. Fadden, and C.M. Hadad, *Computational Study of the Mechanisms for the Reaction of O2(3Σg) with Aromatic Radicals.* The Journal of Physical Chemistry A, 1999. **103** (40): p. 8108-8117.

14. Korkmaz, M. and M. Polat, *Free radical kinetics of irradiated durum wheat.* Radiation Physics and Chemistry, 2000. **58** (2): p. 169-179.

15. Tonokura, K., et al., *Cavity Ring-down Study of the Visible Absorption Spectrum of the Phenyl Radical and Kinetics of Its Reactions with Cl, Br, Cl2, and O2.* The Journal of Physical Chemistry A, 2002. **106** (24): p. 5908-5917.

16. Vejerano, E., S. Lomnicki, and B. Dellinger, *Lifetime of combustion-generated environmentally persistent free radicals on Zn(II)O and other transition metal oxides.* J. Environ. Monit., 2012. **14**: p. 2803-2806.

17. Vejerano, E., S. Lomnicki, and B. Dellinger, *Formation and Stabilization of Combustion-Generated Environmentally Persistent Free Radicals on an Fe(III)2O3/Silica Surface.* Environ. Sci. Technol., 2011. **45**: p. 589-594.

18. Borg, D.C. *Oxygen free radicals and tissue injury: a reference outline*. 1993. Birkhaeuser.

19. Jankovic, J., et al., *Measurement of short-lived reactive species and long-lived free radicals in air samples from structural fires.* Appl. Occup. Environ. Hyg., 1993. **8**: p. 650-4.

20. Yordanov, N.D. and R. Mladenova, *EPR study of thermally generated free radicals in nuts.* Int. J. Food Sci. Technol., 2007. **42**: p. 1384-1389.

21. Tian, L., et al., *Carbon-Centered Free Radicals in Particulate Matter Emissions from Wood and Coal Combustion.* Energy & Fuels, 2009. **23** (5): p. 2523-2526.

22. Eaton, S.S. and G.R. Eaton, *Interaction of spin labels with transition metals.* Coordination Chemistry Reviews, 1978. **26** (3): p. 207-262.

23. Filippov, A.I., *Nature of the concentration contributions to the EPR line widths of solutions of copper(II) diethyldithiocarbamate.* Theoretical and Experimental Chemistry, 1984. **20** (1): p. 101-104.

24. Pryor, W., et al., *The radicals in cigarette tar: their nature and suggested physiological implications.* Science, 1983. **220** (4595): p. 425-427.

25. Gehling, W., L. Khachatryan, and B. Dellinger, *Hydroxyl Radical Generation from Environmentall Persistent Free Radicals (EPFRs) in PM2.5.* Environ Sci Technol, 2013. **Submitted**.

26. McFerrin, C.A., R.W. Hall, and B. Dellinger, *Ab initio study of the formation and degradation reactions of semiquinone and phenoxyl radicals.* Journal of Molecular Structure: THEOCHEM, 2008. **848** (1–3): p. 16-23.

27. Lord, K., et al., *Environmentally persistent free radicals decrease cardiac function before and after ischemia/reperfusion injury in vivo.* J Recept Signal Transduct Res, 2011. **31** (2): p. 157-67.

28. Fahmy, B., et al., *In vitro and in vivo assessment of pulmonary risk associated with exposure to combustion generated fine particles.* Environ Toxicol Pharmacol, 2010. **29** (2): p. 173-82.

29. Balakrishna, S., et al., *Environmentally persistent free radicals amplify ultrafine particle mediated cellular oxidative stress and cytotoxicity.* Part Fibre Toxicol, 2009. **6**: p. 11.

30. Pryor, W.A., D.G. Prier, and D.F. Church, *Electron-Spin Resonance Study of Mainstream and Sidestream Cigarette Smoke: Nature of the Free Radicals in Gas-Phase Smoke and in Cigarette Tar.* Environmental Health Perspectives, 1983. **47**: p. 345-355.

31. Blakley, R.L., D.D. Henry, and C.J. Smith, *Lack of correlation between cigarette mainstream smoke particulate phase radicals and hydroquinone yield.* Food and Chemical Toxicology, 2001. **39** (4): p. 401-406.

32. Valavanidis, A. and E. Haralambous, *A comparative study by electron paramagnetic resonance of free radical species in the mainstream and sidestream smoke of cigarettes with conventional acetate filters and ‘bio-filters&#8217.* Redox Report, 2001. **6** (3): p. 161-171.

33. Baum, S.L., et al., *Electron spin resonance and spin trap investigation of free radicals in cigarette smoke: development of a quantification procedure.* Analytica Chimica Acta, 2003. **481** (1): p. 1-13.

34. 2007-2009 $PM_{2.5}$ Design Value Report. http://www.epa.gov/airtrends/values.html (accessed 1/31/11).

CHAPTER IV. HYDROXYL RADICAL GENERATION FROM EPFRs IN $PM_{2.5}$

4.1 Detection of Hydroxyl Radicals Utilizing Spin Traps

The second objective was to investigate whether a previously proposed catalytic cycle for a model system remained true for $PM_{2.5}$. Previous work demonstrated model EPFRs to generate •OH by utilizing 5,5-dimethyl-N-oxide (DMPO) as a spin trapping agent. Spin trapping with nitrones and nitroso compounds allow the detection of short-lived radical species [1, 2] by reacting the spin trap molecule and a radical to produce a stable aminoxyl or nitroxide species, respectively. This resulting formation is referred to as a spin adduct. The spin trap gives a unique EPR spectrum depending on the radical trapped, and this allows the radical to be identified. This can sometimes be difficult for more complicated species, but relatively simple for the hydroxyl radical.

4.1.1 Proposed Mechanism for Hydroxyl Radical Generation

The proposed red-ox cycle for EPFRs associated with metals in $PM_{2.5}$ [3-9] is displayed in Figure 4.1. In this cycle, the EPFR is formed as the transition metal is reduced. The surface bound EPFR is deprotonated in water and reduces oxygen to the superoxide anion. The superoxide anion undergoes a dismutation reaction to form H_2O_2 followed by the Fenton reaction using the surface bound metal to generate •OH and an oxidized metal. If biological reducing agents were present, a reduction of the metal occurs, allowing electron transfer, and regeneration of the original EPFR-metal system.

Detecting the red-ox reactions of EPFRs associated in a matrix with other metals and organics is challenging. Many types of spin traps are used for spin trapping experiments, e.g. DMPO, DEPMPO (5-diethoxyphosphoryl-5-methyl-1-pyroline-N-oxide), and fluorescent reagents, e.g. dichlorofluorescein, dithiothreitol. All these assays are sensitive to different types of organics and metals found in PM [11]. Furthermore, there are many types of PM used in these experiments, e.g. wood smoke, diesel exhaust, coarse (PM_{10}), fine ($PM_{2.5}$), and ultrafine ($PM_{0.1}$) particles [5, 6, 12-17]. This can make comparison between studies difficult and therefore only the general trends are discussed.

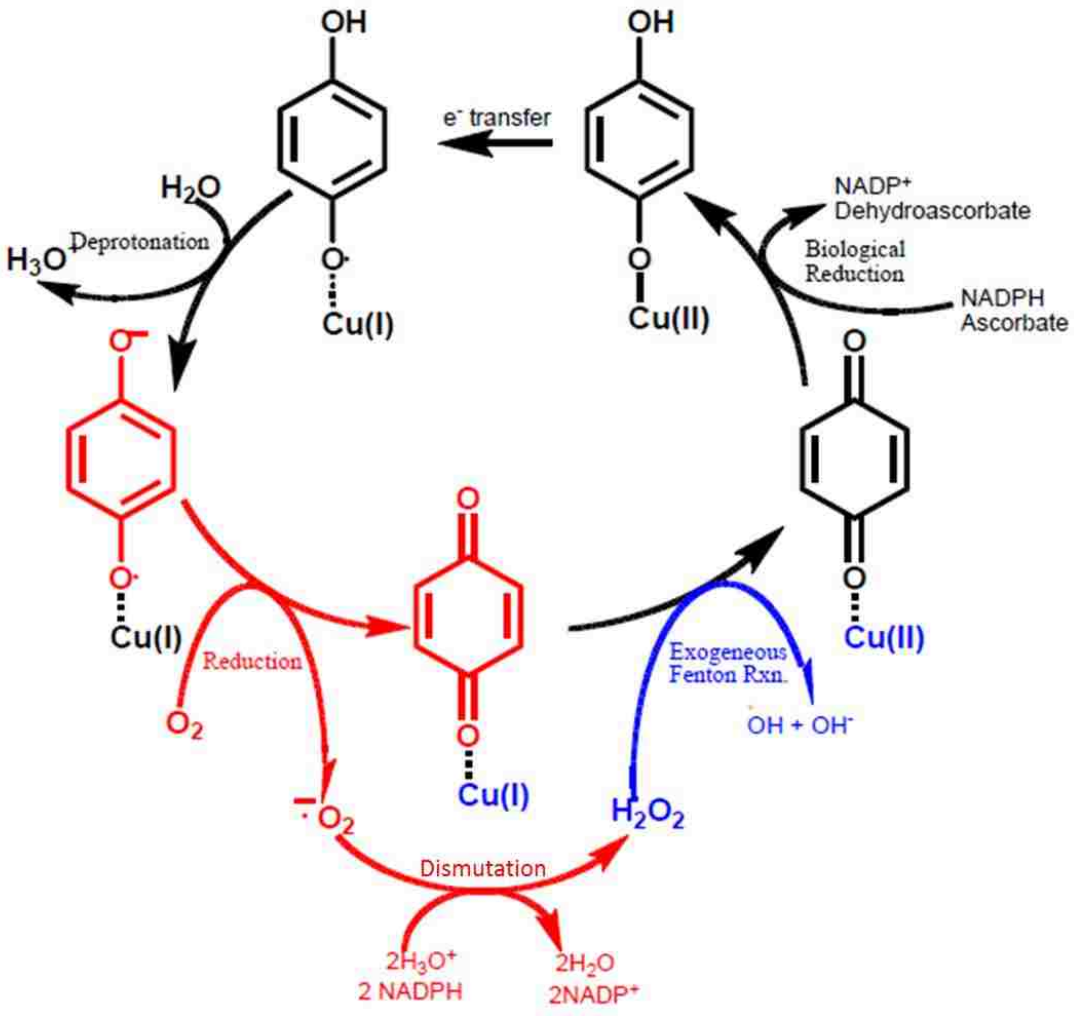

Figure 4.1 Proposed mechanism for ROS generation by a semiquinone EPFR-CuO particle system. The reactions in red denote proposed reactions for the reduction of O_2 to $O_2^{\bullet -}$ by a surface bound semiquinone. This is followed by a dismutation to H_2O_2 which undergoes a Fenton reaction (in this example Cu^{1+} instead of the usual Fe^{2+}), indicated by the blue line, to form •OH and an oxidized Cu. The remaining reactions marked in black complete the cycle by regenerating the reduced metal followed by an electron transfer to produce the original semiquinone-CuO system [2, 10]. "Reprinted with Permission from Reference 9. Copyright 2011 Bentham Science Publishers."

4.2 EPR Spectra

The EPR examination of all $PM_{2.5}$ samples exhibited a single, unstructured peak with a $\Delta H_{p\text{-}p}$ between 5-8 Gauss, indicating multiple organic species of the same radical family present or broadening by organic-metal interaction [4, 18-20]. All sample g-factors were in the range of 2.0030-2.0043, indicating a group of semiquinone-type or other oxygenated radicals [4, 5, 18, 19, 21-25] (cf. Figure 4.2). The concentrations were in the range of $\sim 10^{16}$-10^{17} radicals/g of $PM_{2.5}$, which is comparable to the concentration range in cigarette smoke [4]. This corresponds to 1.8 - 18 ppm as a semiquinone radical.

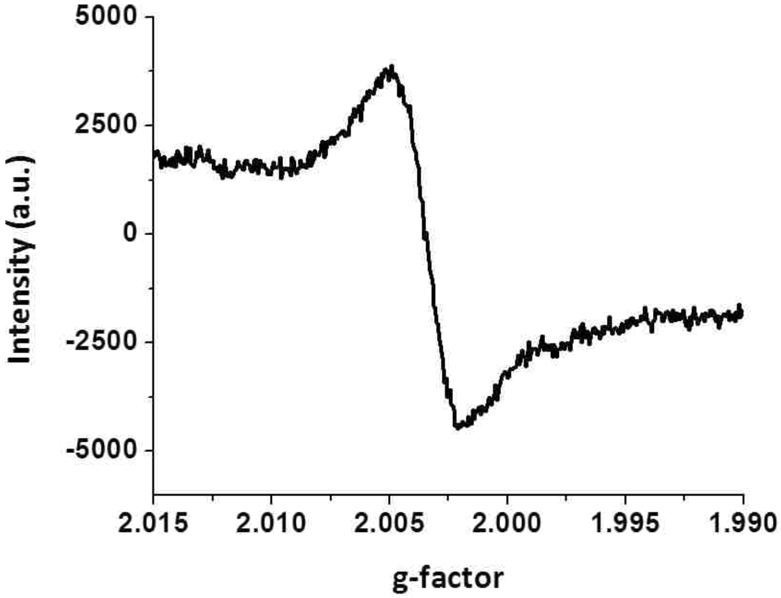

Figure 4.2 EPR spectrum of EPFR in $PM_{2.5}$. The radical concentration was 5.57×10^{17} radicals/g ($\Delta H_{p\text{-}p}$ =5.28 G, g = 2.0035). The drift in the spectrum is from Fe^{3+} signal.

Transition metal concentrations in representative $PM_{2.5}$ samples are presented in Table 4.1.; however, the data is for total metals, while there is only interest in surface-associated metals. Because the metal concentrations varied significantly from sample to sample, the variation in hydroxyl radical generation could not be tested between samples. Instead, the

Table 4.1 Transition metals found in representative $PM_{2.5}$ samples (ppm).

Sample Name	Al	As	Cd	Co	Cr	Cu	Fe	Mn	Ni	Pb	Si	Zn
102N	32.94	0.212	0.062	0.031	0.21	5.04	41.08	1.09	0.43	1.37	77.62	9.57
108	21.76	0.059	0.033	0.022	0.09	3.19	27.30	0.71	0.20	0.56	52.63	8.92
112	19.60	0.097	0.044	0.024	0.08	2.91	25.09	0.66	0.22	0.75	52.47	9.00
141	42.38	0.212	0.027	0.027	0.11	2.62	36.08	1.28	0.20	0.68	90.80	9.85
147	36.84	0.050	0.025	0.032	0.17	3.00	34.46	1.26	0.34	0.62	86.24	5.62
36188	331.71	1.648	0.295	0.368	0.93	59.48	253.97	11.23	4.36	4.23	486.89	46.459
36191	101.01	0.000	0.094	0.078	0.38	7.32	84.09	3.99	1.27	1.73	181.59	17.389

suspended $PM_{2.5}$ was allowed to decay over time, and the difference in the hydroxyl radical generation in the original and decayed radical samples were compared.

4.3 Fresh vs. aged $PM_{2.5}$ samples

The PM samples were aged at room temperature in PBS solution. Typical 1:2:2:1 spectra, indicative of the DMPO-OH spin adduct [24, 25] were observed in PBS solutions containing $PM_{2.5}$ and DMPO. The comparisons of hydroxyl radical generation in two samples are depicted in Figure 4.3. When the $PM_{2.5}$ was left in a suspended solution for 2 days, a reduction of 35% in the DMPO-OH intensity was seen in one sample, Figure 4.3A, and when suspended in solution for 1 day, an 11% reduction in a second sample, Figure 4.3B . A reduction in $^{\bullet}OH$ generation after aging was also observed by others when H_2O_2 was added [23]. Likewise, a reduction in integrated fluorescence activity or oxidative capacity after aging was observed [14, 26-28]. Unfortunately, due to small extraction weights from the filter (on the order of 200-300 μg) and subsequent measurements using the same small sample volume, an exact radical concentration could not be established after the aging occurred. Previous experiments have shown polar solvents can extract EPFRs from the particles but are eliminated after extraction either through hydrogen abstraction, radical dimerization, or radical-radical recombination [29].

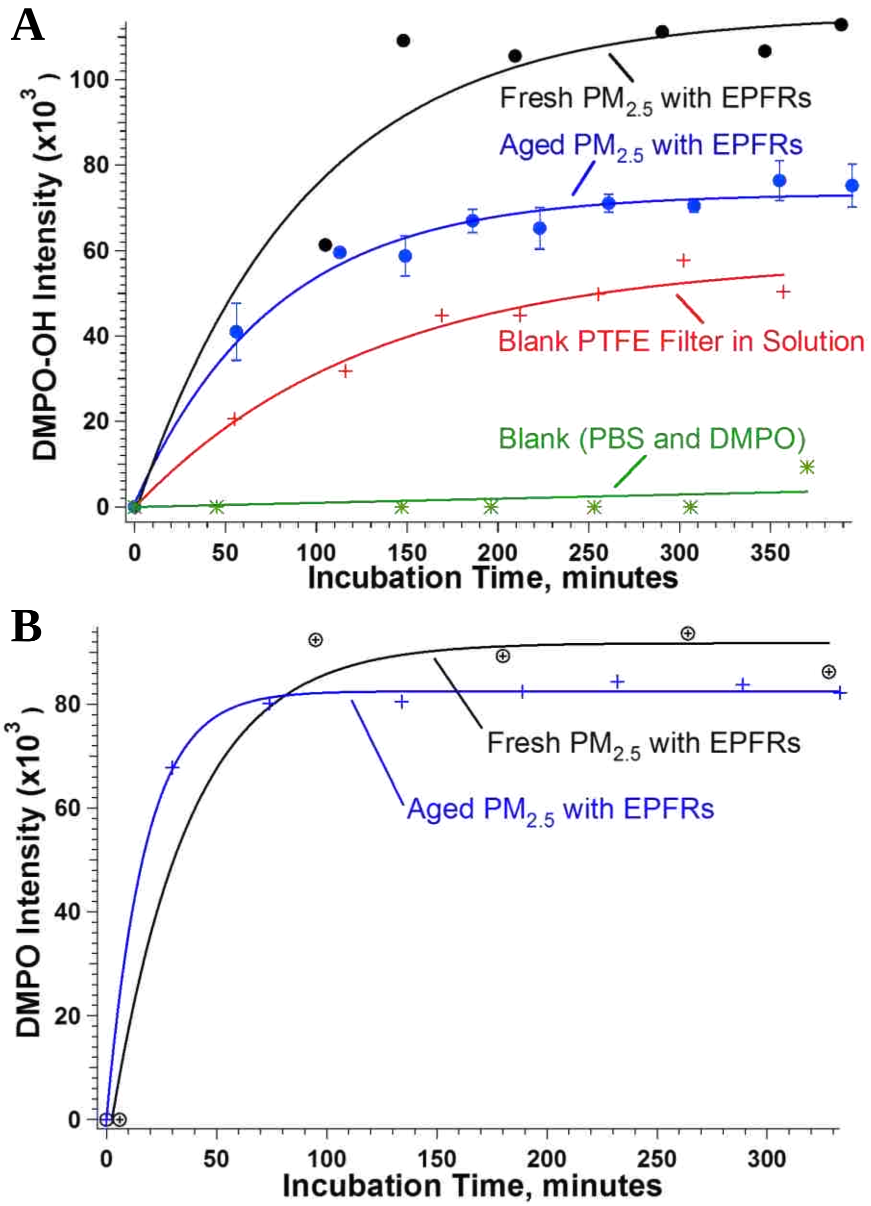

Figure 4.3 Generation of the DMPO-OH adduct signal over time. **A.** Generation of DMPO-OH adduct from blank solution of PBS + DMPO (green), a blank PTFE filter (red), freshly extracted $PM_{2.5}$ (black), and $PM_{2.5}$ extract suspension aged in the dark for 2 days. This was from sample 141, where the initial radical concentration was 3.37×10^{17} radicals/g. **B.** Demonstration of another sample (#36191 with a radical concentration of 6.94×10^{16} radicals/g) to depress DMPO-OH adduct formation after aged in the dark for 1 day.

The blank solution (PBS + DMPO) did not have any significant contribution to the formation of $^\bullet$OH; however, the extracted blank PTFE filter was found to consistently generate DMPO-OH, Figure 4.3A. This was expected as a result of the sonication readily removing any loosely bound metals in the filter. Additionally, DMPO is well documented to be easily hydrolyzed, in the presence of metals, into DMPO-OH as an experimental artifact [7, 8]. The ability of the PTFE filter to generate low levels of the DMPO-OH adduct was also reported elsewhere [30]. However, all sample signals in this report were at least 2x greater than the blank filter.

4.4 Effect of Particle Concentration

The effectiveness of red-ox cycling (Figure 4.1) may be observed in dependence of the DMPO-OH adduct concentration generated vs. incubation time at two different particle concentrations, Figure 4.4**.** The larger particle concentration exhibited a larger DMPO-OH adduct intensity. Similar behavior has been reported for PM samples with the addition of H_2O_2 and other ROS detection methods [6, 31].

4.5 Addition of H_2O_2

Addition of H_2O_2 into the $PM_{2.5}$ suspension resulted in an average doubling of the DMPO-OH formation (data not shown). With the blank filter, there was a 60% increase of DMPO-OH production, further suggesting the leeching of metals from the PTFE filter during extraction. Data generated from H_2O_2 addition is consistent with literature data demonstrating metals in $PM_{2.5}$, or other analogous systems, can catalyze $^\bullet$OH formation in the presence of H_2O_2 [6-8, 16, 32-35]. Addition of H_2O_2 to the system facilitates ROS formation *via* the exogenous Fenton reactions (Figure 4.1). However, in these experiments, external addition of H_2O_2 was not needed to generate $^\bullet$OH. What was observed in this study was a combination of EPFRs and surface metals working *in tandem* towards ROS formation.

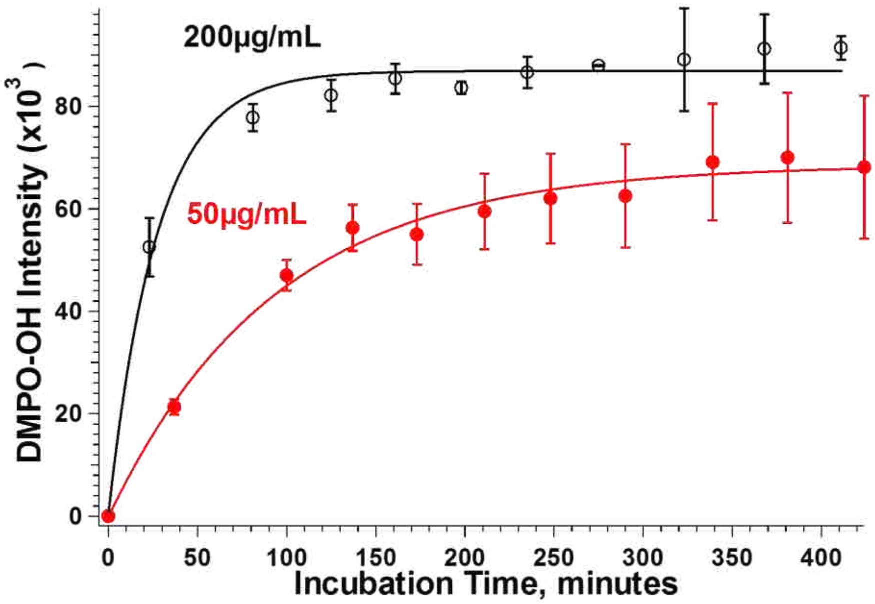

Figure 4.4 Impact of particle concentration on DMPO-OH adduct generation. This is from sample 36191.

4.6 Air Rich vs. N_2 Purged $PM_{2.5}$ Suspensions

To determine the effect of dissolved oxygen on ROS production, a suspension was purged with pure N_2 to remove dissolved O_2. Without O_2, the suspension, while containing EPFRs, cannot generate hydroxyl radicals due to blocking the superoxide and H_2O_2 formation channel (cf. Figure 4.1). The non-purged samples generated 13% greater quantity of $^\bullet$OH than the purged sample, Figure 4.5A. This is similar to the literature, where formation of $^\bullet$OH was eliminated by N_2 purging, unless H_2O_2 was added [6]. This was consistent with previous work where the largest differences between the control (CuO on amorphous Si) and the EPFR model system were observed when the suspensions were aerated resulting in the EPFR model system having the larger DMPO-OH adduct formation [8].

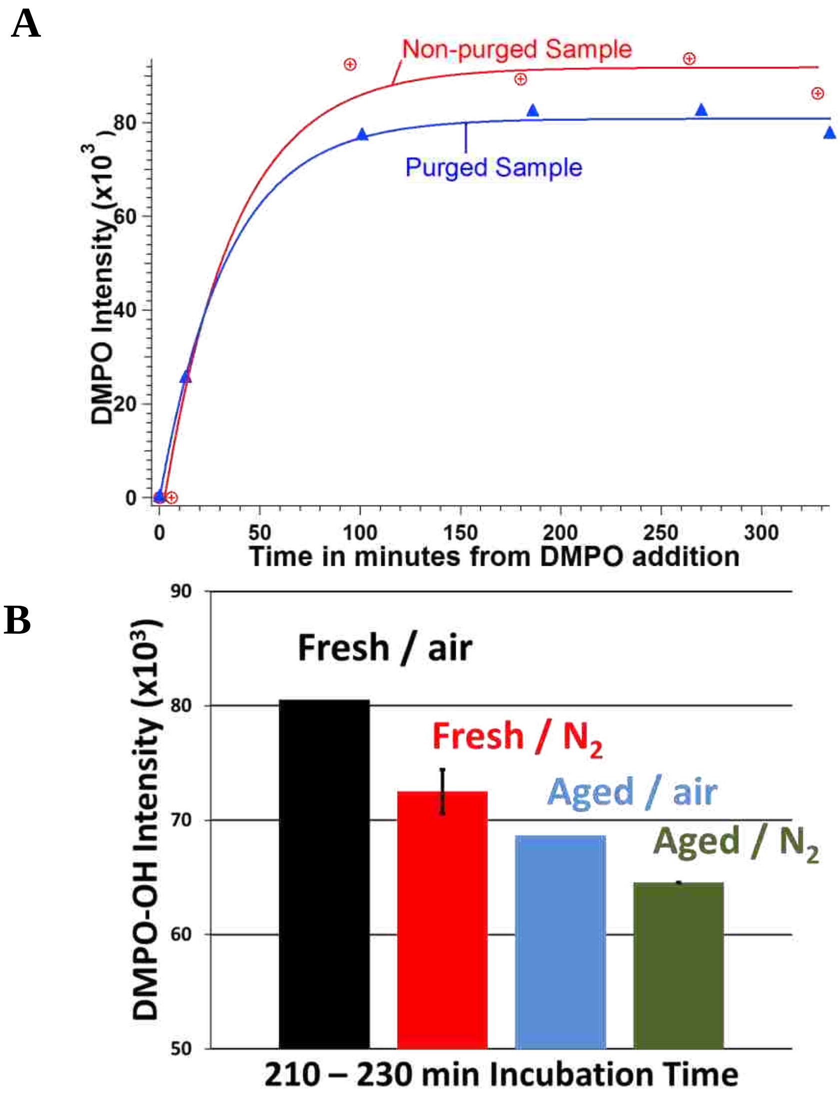

Figure 4.5 DMPO-OH adducts accumulation vs. time at different conditions for sample # 36191: **A**. 10 min aeration (labeled as Non-purged Sample) and 10 min N_2 purging (labeled as Purged Sample) of freshly extracted PM. **B**. Fresh and aged (19 days) samples aerated or purged by N_2.

Following the 19 day decay in solution, the non-purged sample decreased by 18% from when it was fresh, while only a 10% diminution was observed between the fresh and aged non-purged sample (Figure 4.5B**).** A 5% decrease in DMPO-OH intensity was observed between the aged non-purged and purged sample. The lesser effect in the aged sample is simply thought due to a reduced presence of the organic radical. Overall, there was a 21% decrease from the fresh non-purged sample to the decayed purged sample. This decrease demonstrates the impact

EPFRs have on ROS formation as it was already documented the oxidation state of Fe^{2+}, the main contributor to the Fenton reaction in $PM_{2.5}$, changes little over the course of 40 days [15].

4.7 "Passive" vs. "Active" $PM_{2.5}$

There were a few samples not altering in hydroxyl radical formation under different conditions (cf. 4.6A), which is referred to as passive, *versus* the samples developing differences

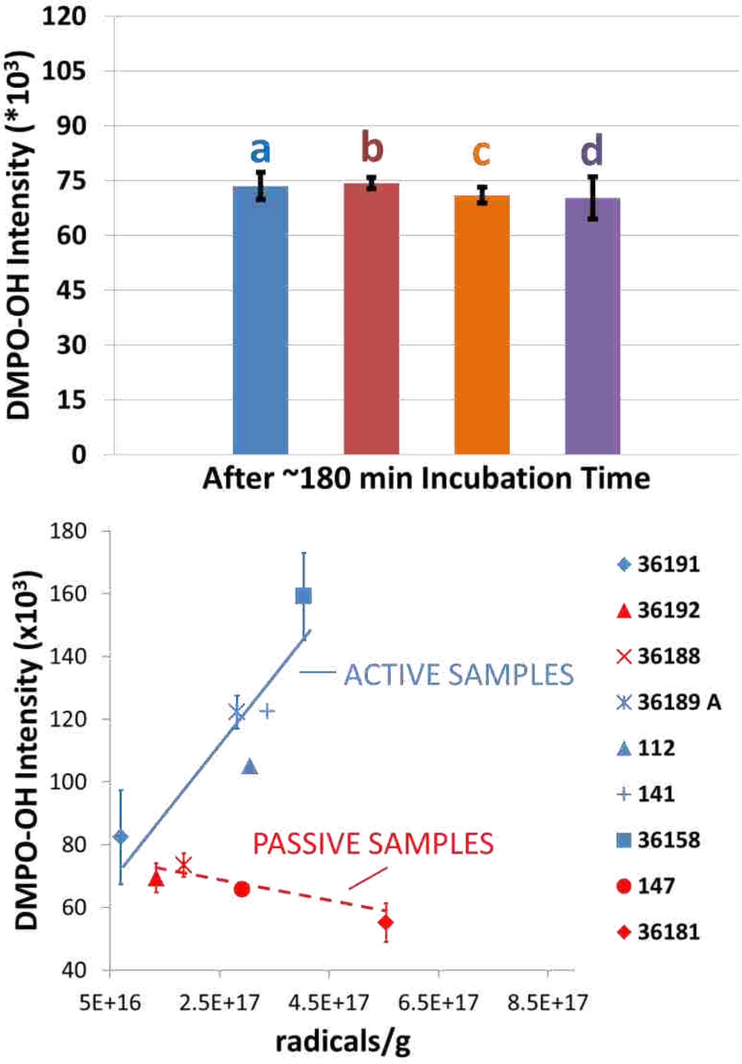

Figure 4.6 Demonstration of a passive sample and comparison of active and passive samples. **A**. Demonstration of a passive sample # 36188 with no impact from aeration. The initial radical conentration was 1.84×10^{17} radical/g. (a) - aeration for 10 min, (b) - aeration for 1 hr, (c) - aeration for 2 hr, and (d) - purged with N_2 for 2 hr. **B**. DMPO-OH adducts concentration vs. radical concentration for active (solid line) and passive (dashed line) samples.

in hydroxyl radical generation, referred to as active (cf. 4.6B). The active set produced fewer hydroxyl radicals from a lack of oxygen or longer aging and corresponded to a reduction in DMPO-OH intensity. The active set of samples exhibited an average increase of the DMPO-OH signal when the samples increased in radical concentration, Figure 4.6B. Conversely, the passive samples exhibited no dependence on aging time or aeration and were relatively independent of the radical concentration.

The active radicals are probably external (or sterically available) enabling reaction on the exposed surface. The passive radicals are probably internal where no species can react with them. Other researchers reference the presence of internal radicals and no change in the EPR signal of combusted plastics after 6 months [25]. DEP samples generate little $^{\bullet}$OH and may also be internal radicals [6].

4.8 References

1. Janzen, E.G. and B.J. Blackburn, *Detection and identification of short-lived free radicals by an electron spin resonance trapping technique.* Journal of the American Chemical Society, 1968. **90** (21): p. 5909-5910.

2. Forshult, S., C. Lagercrantz, and K. Torssell, *Use of nitroso compounds as scavengers for the study of short-lived free radicals in organic reactions.* Acta Chem. Scand., 1969. **23** (2): p. 522-30.

3. Dellinger, B., et al., *Role of Free Radicals in the Toxicity of Airborne Fine Particulate Matter.* Chemical Research in Toxicology, 2001. **14** (10): p. 1371-1377.

4. Squadrito, G.L., et al., *Quinoid redox cycling as a mechanism for sustained free radical generation by inhaled airborne particulate matter.* Free Radical Biology and Medicine, 2001. **31** (9): p. 1132-1138.

5. Valavanidis, A., et al., *Electron paramagnetic resonance study of the generation of reactive oxygen species catalysed by transition metals and quinoid redox cycling by inhalable ambient particulate matter.* Redox Report, 2005. **10** (1): p. 37-51.

6. Alaghmand, M. and N.V. Blough, *Source-Dependent Variation in Hydroxyl Radical Production by Airborne Particulate Matter.* Environmental Science & Technology, 2007. **41** (7): p. 2364-2370.

7. Khachatryan, L., et al., *Environmentally Persistent Free Radicals (EPFRs). 1. Generation of Reactive Oxygen Species in Aqueous Solutions.* Environmental Science & Technology, 2011. **45** (19): p. 8559-66.

8. Khachatryan, L. and B. Dellinger, *Environmentally Persistent Free Radicals (EPFRs)-2. Are Free Hydroxyl Radicals Generated in Aqueous Solutions?* Environmental Science & Technology, 2011. **45** (21): p. 9232-9239.

9. Pan, C.J., et al., *Inherent redox properties of diesel exhaust particles: catalysis of the generation of reactive oxygen species by biological reductants.* Toxicol Sci, 2004. **81** (1): p. 225-32.

10. Dellinger, B., et al., *Free radicals in tobacco smoke.* Mini-Rev. Org. Chem., 2011. **8**: p. 427-433.

11. Ayres, J.G., et al., *Evaluating the toxicity of airborne particulate matter and nanoparticles by measuring oxidative stress potential--a workshop report and consensus statement.* Inhal Toxicol, 2008. **20** (1): p. 75-99.

12. Donaldson, K., et al., *Free radical activity of PM10: iron-mediated generation of hydroxyl radicals.* Environ Health Perspect, 1997. **105 Suppl 5**: p. 1285-9.

13. Li, N., et al., *Ultrafine particulate pollutants induce oxidative stress and mitochondrial damage.* Environmental Health Perspectives, 2003. **111** (4): p. 455-460.

14. Beck-Speier, I., et al., *Oxidative stress and lipid mediators induced in alveolar macrophages by ultrafine particles.* Free Radic Biol Med, 2005. **38** (8): p. 1080-92.

15. Majestic, B.J., J.J. Schauer, and M.M. Shafer, *Application of synchrotron radiation for measurement of iron red-ox speciation in atmospherically processed aerosols.* Atmos. Chem. Phys., 2007. **7**: p. 2475-2487.

16. Nawrot, T.S., et al., *Oxidative properties of ambient PM2.5 and elemental composition: Heterogeneous associations in 19 European cities.* Atmospheric Environment, 2009. **43** (30): p. 4595-4602.

17. Verma, V., et al., *Redox activity of urban quasi-ultrafine particles from primary and secondary sources.* Atmospheric Environment, 2009. **43** (40): p. 6360-6368.

18. Dellinger, B., et al., *Formation and stabilization of persistent free radicals.* Proceedings of the Combustion Institute, 2007. **31** (1): p. 521-528.

19. Lomnicki, S., et al., *Copper Oxide-Based Model of Persistent Free Radical Formation on Combustion-Derived Particulate Matter.* Environmental Science & Technology, 2008. **42** (13): p. 4982-4988.

20. Valavanidis, A., K. Fiotakis, and T. Vlachogianni, *The Role of Stable Free Radicals, Metals and PAHs of Airborne Particulate Matter in Mechanisms of Oxidative Stress and Carcinogenicity*, in *Urban Airborne Particulate Matter*, F. Zereini and C.L.S. Wiseman, Editors. 2011, Springer Berlin Heidelberg. p. 411-426.

21. Lachocki, T.M., D.F. Church, and W.A. Pryor, *Persistent free radicals in woodsmoke: An ESR spin trapping study.* Free Radical Biology and Medicine, 1989. **7** (1): p. 17-21.

22. Pryor, W.A., *Cigarette smoke radicals and the role of free radicals in chemical carcinogenicity.* Environ Health Perspect, 1997. **105 Suppl 4**: p. 875-82.

23. Valavanidis, A., A. Salika, and A. Theodoropoulou, *Generation of hydroxyl radicals by urban suspended particulate air matter. The role of iron ions.* Atmospheric Environment, 2000. **34** (15): p. 2379-2386.

24. Valavanidis, A., et al., *Determination of Selective Quinones and Quinoid Radicals in Airborne Particulate Matter and Vehicular Exhaust Particles.* Environmental Chemistry, 2006. **3** (2): p. 118-123.

25. Valavanidis, A., et al., *Persistent free radicals, heavy metals and PAHs generated in particulate soot emissions and residue ash from controlled combustion of common types of plastic.* J. Hazard. Mater., 2008. **156**: p. 277-284.

26. Hung, H.-F. and C.-S. Wang, *Experimental determination of reactive oxygen species in Taipei aerosols.* Journal of Aerosol Science, 2001. **32** (10): p. 1201-1211.

27. Venkatachari, P., et al., *Measurement of Particle-Bound Reactive Oxygen Species in Rubidoux Aerosols.* Journal of Atmospheric Chemistry, 2005. **50** (1): p. 49-58.

28. Wang, Y., et al., *Probing the source of hydrogen peroxide associated with coarse mode aerosol particles in southern California.* Environ Sci Technol, 2010. **44** (11): p. 4070-5.

29. Truong, H., S. Lomnicki, and B. Dellinger, *Potential for Misidentification of Environmentally Persistent Free Radicals as Molecular Pollutants in Particulate Matter.* Environmental Science & Technology, 2010. **44** (6): p. 1933-1939.

30. Shi, T., et al., *Temporal variation of hydroxyl radical generation and 8-hydroxy-2'-deoxyguanosine formation by coarse and fine particulate matter.* Occup. Environ. Med., 2003. **60**: p. 315-321.

31. Briede, J.J., et al., *Development and application of an electron spin resonance spectrometry method for the determination of oxygen free radical formation by particulate matter.* Environmental Science & Technology, 2005. **39** (21): p. 8420-8426.

32. Kitajima, N., S. Fukuzumi, and Y. Ono, *Formation of superoxide ion during the decomposition of hydrogen peroxide on supported metal oxides.* The Journal of Physical Chemistry, 1978. **82** (13): p. 1505-1509.

33. Antonini, J.M., et al., *Metal composition and solubility determine lung toxicity induced by residual oil fly ash collected from different sites within a power plant.* Mol. Cell. Biochem., 2004. **255**: p. 257-265.

34. Jung, H., et al., *Quantitative measurements of the generation of hydroxyl radicals by soot particles in a surrogatelung fluid.* Atmospheric Environment, 2006. **40** (6): p. 1043-1052.

35. Vidrio, E., H. Jung, and C. Anastasio, *Generation of hydroxyl radicals from dissolved transition metals in surrogate lung fluid solutions.* Atmospheric Environment, 2008. **42** (18): p. 4369-4379.

36. Li, B., N.V. Blough, and P.L. Gutierrez, *Trace detection of hydroxyl radicals during the redox cycling of low concentrations of diaziquone: a new approach.* Free Radical Biol. Med., 2000. **29**: p. 548-556.

37. DiStefano, E., et al., *Determination of metal-based hydroxyl radical generating capacity of ambient and diesel exhaust particles.* Inhalation Toxicology, 2009. **21** (8-11): p. 731-738.

38. Shen, H. and C. Anastasio, *A comparison of hydroxyl radical and hydrogen peroxide generation in ambient particle extracts and laboratory metal solutions.* Atmospheric Environment, 2012. **46** (0): p. 665-668.

39. Shafer, M.M., et al., *Reactive oxygen species activity and chemical speciation of size-fractionated atmospheric particulate matter from Lahore, Pakistan: an important role for transition metals.* Journal of Environmental Monitoring, 2010. **12** (3): p. 704-715.

40. Verma, V., et al., *Contribution of transition metals in the reactive oxygen species activity of PM emissions from retrofitted heavy-duty vehicles.* Atmospheric Environment, 2010. **44** (39): p. 5165-5173.

41. Shen, H. and C. Anastasio, *Formation of hydroxyl radical from San Joaquin Valley particles extracted in a cell-free surrogate lung fluid.* Atmos. Chem. Phys., 2011. **11** (18): p. 9671-9682.

42. Eiguren-Fernandez, A., et al., *Redox and electrophilic properties of vapor- and particle-phase components of ambient aerosols.* Environmental Research, 2010. **110** (3): p. 207-212.

43. Frikke-Schmidt, H., et al., *Effect of vitamin C and iron chelation on diesel exhaust particle and carbon black induced oxidative damage and cell adhesion molecule expression in human endothelial cells.* Toxicol Lett, 2011. **203** (3): p. 181-9.

44. Zhu, B.-Z., et al., *Metal-independent production of hydroxyl radicals by halogenated quinones and hydrogen peroxide: an ESR spin trapping study.* Free Radical Biology and Medicine, 2002. **32** (5): p. 465-473.

45. Burkitt, M.J., *Esr Spin Trapping Studies Into of Nature of the Oxidizing Species Formed in the Fenton Reaction: Pitfalls Associated With of Use Of 5,5-Dimethyl-1-Pyrroline-n-Oxide in the Detection of the Hydroxyl Radical.* Free Radical Research, 1993. **18** (1): p. 43-57.

46. Ntziachristos, L., et al., *Relationship between redox activity and chemical speciation of size-fractionated particulate matter.* Particle and fibre toxicology, 2007. **4**: p. 5.

47. Baulig, A., et al., *Physicochemical characteristics and biological activities of seasonal atmospheric particulate matter sampling in two locations of Paris.* Environ Sci Technol, 2004. **38** (22): p. 5985-92.

48. Kunzli, N., et al., *Comparison of oxidative properties, light absorbance, total and elemental mass concentration of ambient PM2.5 collected at 20 European sites.* Environ Health Perspect, 2006. **114** (5): p. 684-90.

49. Vidrio, E., et al., *Generation of Hydroxyl Radicals from Ambient Fine Particles in a Surrogate Lung Fluid Solution.* Environmental Science & Technology, 2009. **43** (3): p. 922-927.

50. Shi, T.M., et al., *Hydroxyl radical generation by electron paramagnetic resonance as a new method to monitor ambient particulate matter composition.* Journal of Environmental Monitoring, 2003. **5** (4): p. 550-556.

51. Jeng, H.A., *Chemical composition of ambient particulate matter and redox activity.* Environmental Monitoring and Assessment, 2010. **169** (1-4): p. 597-606.

52. Park, S., et al., *The role of iron in reactive oxygen species generation from diesel exhaust particles.* Toxicology in Vitro, 2006. **20** (6): p. 851-857.

53. See, S.W., Y.H. Wang, and R. Balasubramanian, *Contrasting reactive oxygen species and transition metal concentrations in combustion aerosols.* Environmental Research, 2007. **103** (3): p. 317-324.

54. Cheung, K.L., et al., *Emissions of Particulate Trace Elements, Metals and Organic Species from Gasoline, Diesel, and Biodiesel Passenger Vehicles and Their Relation to Oxidative Potential.* Aerosol Science and Technology, 2010. **44** (7): p. 500-513.

55. Daher, N., et al., *Comparison of the Chemical and Oxidative Characteristics of Particulate Matter (PM) Collected by Different Methods: Filters, Impactors, and BioSamplers.* Aerosol Science and Technology, 2011. **45** (11): p. 1294-1304.

CHAPTER V. EFFECTS OF NO_X AND OZONE ON EPFRs IN $PM_{2.5}$ AND THEIR ABILITY TO GENERATE HYDROXYL RADICALS

The previous chapters indicated oxygen reduces the EPFR concentration in $PM_{2.5}$ as well as reducing hydroxyl radical formation. Thus, the third objective was to determine how the presence of other oxidizing species, NO_X and ozone, affect the EPFRs in $PM_{2.5}$. Subsequently, understanding how exposure of these oxidizing agents altered hydroxyl radical generation was of interest.

5.1 Initial EPR Measurements of $PM_{2.5}$ and Extraction

The initial EPR examination of all $PM_{2.5}$ samples displayed a single, unstructured organic radical peak [1]. The average $\Delta H_{p\text{-}p}$ was 6-7 Gauss, and this implied multiple organic species of the same radical family present or broadening by organic-metal interactions [2-5]. All initial g-factors were in the range of 2.0038 – 2.0043, characteristic for a group of semiquinone radicals or more oxygenated radicals in a complex matrix [2-4, 6-11]. All $PM_{2.5}$ samples immediately before exposure exhibited an average initial radical concentration of $2.08\text{x}10^{17} \pm 0.66\text{x}10^{17}$

Table 5.1 Radical concentration of $PM_{2.5}$ after extraction from filter *.

Date of collection	Number of collection Days	Radical Concentration After Extraction (radicals/g)
1/30/2012	7	$5.38\text{x}10^{16}$
2/6/2012	19	$2.43\text{x}10^{17}$
2/24/2012	7	$2.78\text{x}10^{17}$
3/2/2012	13	$8.05\text{x}10^{16}$
3/14/2012	6	$1.66\text{x}10^{17}$
3/20/2012	8	$1.43\text{x}10^{17}$

* Due to difficulties to measure the radical concentration on the glass fiber filter, only the radical concentration following extraction is given as accurate data.

radicals/g, Table 5.1. This radical concentration is comparable to the same concentration range from cigarette smoke [2], corresponding to 37 ppm as a semiquinone radical.

The effect of extraction from the binder free glass fiber filter on the $PM_{2.5}$ radical signal is displayed in Figure 5.1. Inspection of the wide magnetic range indicated the presence of Fe^{3+} at g-factors of 4.2950, from a strong rhombic distorted tetrahedral or octahedral position [12-16], and 2.1343, from Fe^{3+} distributed in clusters [16, 17], (black spectrum in Figure 5.1). As observed in Figure 5.1, the Fe^{3+} peaks are significantly diminished after extraction (red spectrum), and this arises from surface associated Fe^{3+} dissolving into solution.

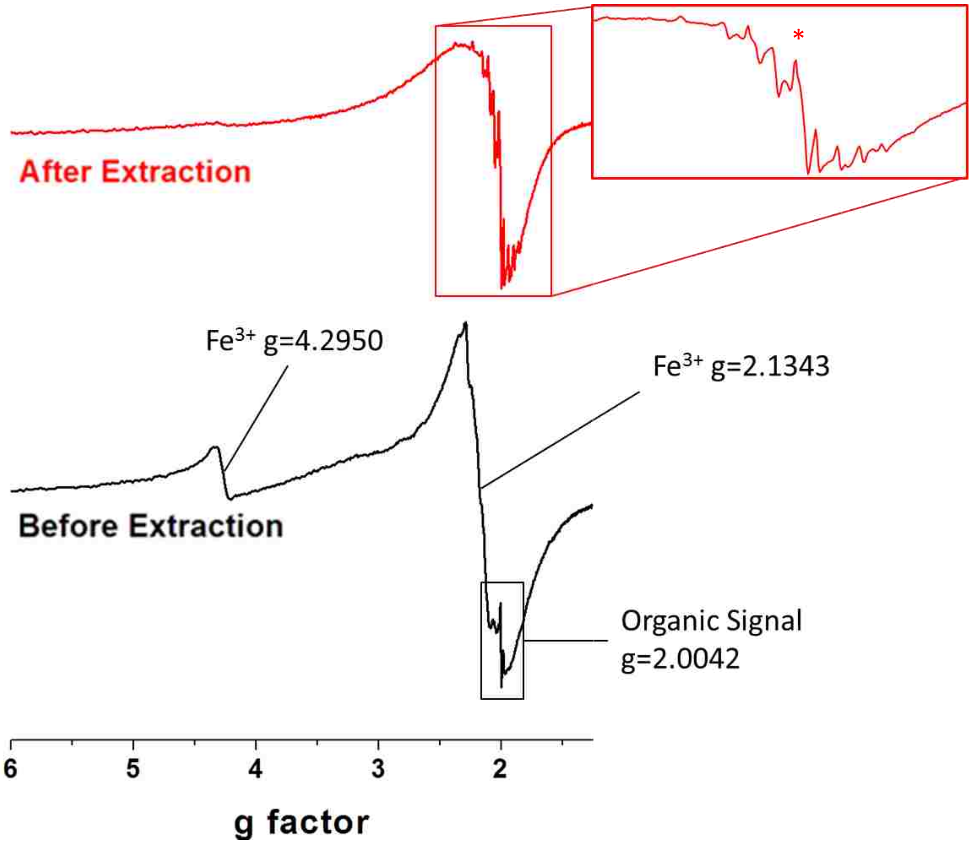

Figure 5.1 Effect of extraction on the $PM_{2.5}$ powder spectrum collected from 3/14/12 (1150 G - 5500 G range). Inset is a close up of the organic radical signal (singlet) overlaid on Mn signal (6 equidistant lines) in the range 3200 – 3600 G.

At the same time, the extra signals (the red inset of Figure 5.1) resulting from extraction are attributed to a strong Mn^{2+} (I=5/2) presence. The singlet line among the spectrum of Mn^{2+} at g = 2.0042 (highlighted by the red asterisk) is the organic radical. After extraction, the organic radical concentration was indicated to decrease [18]. Overall, this data indicates care must be taken in the identification of radicals when the soluble fraction dissolves in solution thus drastically changing the EPFR environment, Figure 5.1.

5.2 Effect of Ozone on $PM_{2.5}$

The outcome of ozone exposure to the radical signal is displayed in Figure 5.2 A and B. In regards to the organic radical, the g_{app} remained the same at 2.0039, Figure 5.2B, and there

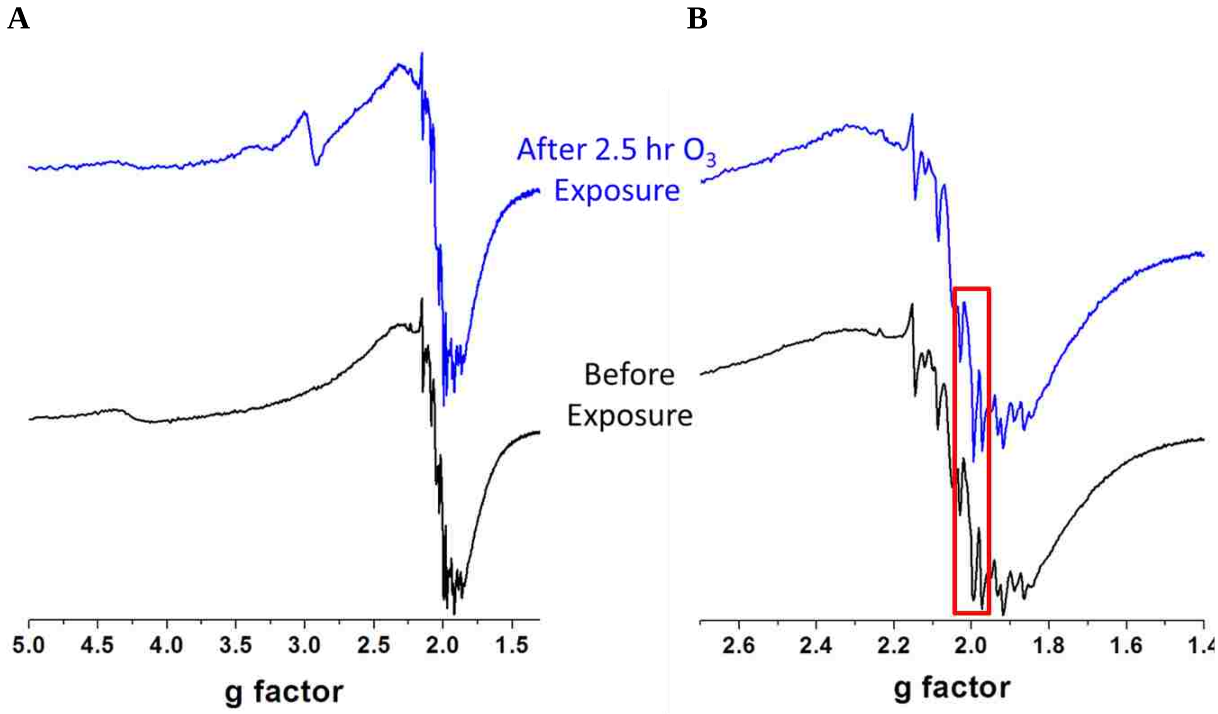

Figure 5.2 Effect of ozone on the $PM_{2.5}$ powder spectrum collected from 2/24/12. **A.** Inorganic radical EPR spectrum (1300 G - 5500 G) **B.** Organic radical in magnetic range 3420 G - 3500 G with Mn peaks present. The peaks in the red box are the organic signal.

was no significant change in the ΔH_{p-p} after exposure. The radical concentration slightly diminished from 1.90×10^{17} to 1.83×10^{17} radicals/g after 2 hr of exposure and 1.69×10^{17} radicals/g after 4 hr of exposure. The radical concentration from the control (open to lab air) also decreased from 1.96×10^{17} to 1.84×10^{17} radicals/g at the same time. Essentially, there was no appreciable change in the organic radical signal after exposure of $PM_{2.5}$ to ozone.

However, there was some interaction of ozone with the other paramagnetic species in $PM_{2.5}$; the Fe^{+3} g-factor at 4.2950 slightly diminished, Figure 5.2A. One relevant explanation here might be Fe^{3+} (as Fe_2O_3) is acting as a catalyst [19] to remove ozone resulting in a change of Fe^{3+} coordination (a strong rhombic distorted tetrahedral or octahedral position [12-16]). Because of this expected physical change of the Fe^{+3} environment, a small diminution in the signal will occur. In addition, a new signal at g = 2.9995 appears after exposure of ozone and the new peak is suggested to result from Fe in a complex matrix [20], Figure 2A.

Generally, the interaction mechanism of ozone with organics is complex. For instance,

Table 5.2 Concentration of soot in $PM_{2.5}$and diesel

Soot Concentration† (μg/m^3)	$PM_{2.5}$ Concentration† (μg/m^3)	Percentage of soot in $PM_{2.5}$
1.7	17.2	9.9%
1.9	26.5	7.2%
1.6	16.5	9.7%
4.1	22.9	18.1%
1.9	17.9	10.6%
Percent Concentration of Soot in Diesel[28, 30]		
47.9%		
48%		

†All values used were given or averages of all measurements [26, 27, 29, 31, 32]

interaction with unsaturated hydrocarbons induces formation of radicals through Criegee intermediates in the gas phase [21, 22] or during the formation of secondary organic aerosols [23]. In the latter case, formation of new, short lived radicals, such as alkyl, alkoxyl, and peroxyl, were detected using electrospray ionization/tandem mass spectrometry in the ozonolysis of α-pinene [23]. However, there is controversial information in the literature concerning direct interaction of ozone with PM, in particular soot and carbon black. One study observed ozone to decrease radicals found in soot [24], while another indicated the radical concentration to increase when ozone was exposed to carbon black [25]. In our study, the alteration of EPFRs in $PM_{2.5}$ was not observed from the interaction of ozone, Figure 5.2B. The main difference between this and the previous studies [24, 25] is a significantly diminished amount of soot detected in different $PM_{2.5}$ samples [26-32], Table 5.2. In addition, the EPFRs in these samples might be located in the inner layers of $PM_{2.5}$ [1]. Remaining in the inner layers, those radicals are inaccessible to oxidizers as also observed during exposure of $PM_{2.5}$ to NO (*vide infra*). The existence of these types of samples, abbreviated as “passive” (in term of •OH generation), was advocated earlier, CHAPTER IV on page 68.

5.3 •OH Generation After Exposure of $PM_{2.5}$ to Ozone

The effects of ozone exposure on $PM_{2.5}$ and concomitant •OH generation is displayed in Figure 5.3. Clearly, there was no significant change in the •OH generating capabilities between the exposed sample and its control, but the ozone exposed sample generated marginally more •OH.

However, other PM, notably soot and diesel exhaust particles (DEP) with a high content of soot (~48% [28, 29]), report greater oxidant yield after exposure to ozone [33, 34]. Even low

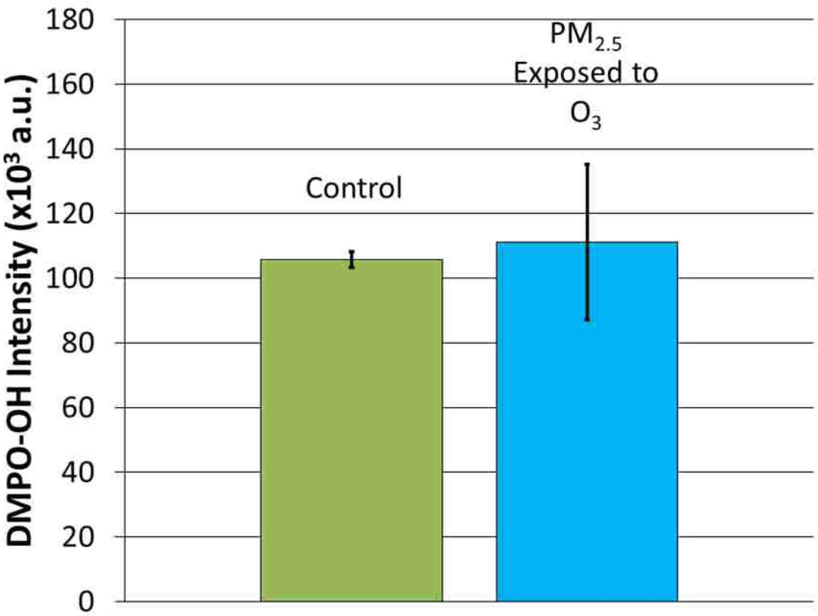

Figure 5.3 Effect of ozone exposure on •OH generation from $PM_{2.5}$. This sample was collected on 3/2/12. Both points were taken at the maximum •OH generation *i.e.* after 5 hours of incubation.

levels of ozone exposure increases the potency of DEP to induce lung injury [35]. In these cases, oxidation by ozone contributed to the organic carbon content (similarly to other work [25]) of the DEP by possibly forming quinones [36, 37] which may generate reactive oxygen species [7, 38]. Concerning to the present case, a much lower amount of soot in $PM_{2.5}$ (Table 5.2) in addition to the possibility of EPFRs internal location in $PM_{2.5}$ [1] might be the reasons nearly identical levels of •OH were generated in the control and exposed $PM_{2.5}$, Figure 5.3.

5.4 Effect of NO on Radical Signal and •OH Generation

Exposure to NO (starting from 2 torr) demonstrated no statistical effect on the radical EPR signal. The g_{app}, ΔH_{p-p}, and the intensity of the signal remained the same as the control ($PM_{2.5}$ powder exposed to air). Even exposing to high levels of NO (up to 395 torr) for 3 days at room temperature only slightly decreased the radical concentration, from 2.47×10^{17} radicals/g to

2.42×10^{17} radicals/g; however, the control also exhibited a slight decline, from 2.38×10^{17} radicals/g to 2.31×10^{17} radicals/g, in the radical concentration. This indicated, overall, there was no fluctuation in the radical signal intensity from exposure to NO. Subsequently, there was no effect from NO exposure on the $PM_{2.5}$'s ability to generate altered levels of •OH, Figure 5.4. These results are similar to the ozone exposure.

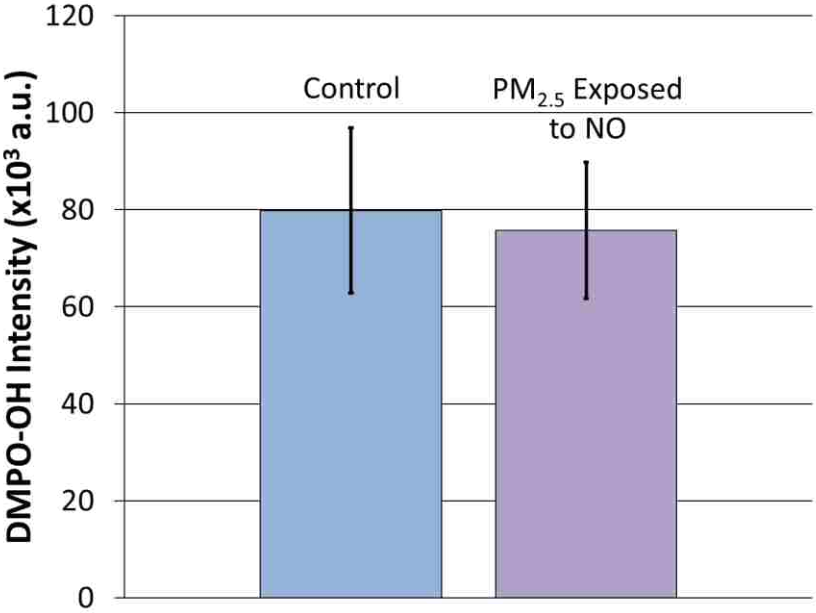

Figure 5.4 Effect of NO exposure on •OH generation from $PM_{2.5}$. This sample was collected 3/20/12. Both points were taken at the maximum •OH generation.

5.5 Effect of NO/NO_2 on Radical Signal

The effect of NO/NO_2 exposure on the wide magnetic range radical signal is displayed in Figure 5.5. After 30 min of exposure, the Fe^{3+} peak at a g-factor of 2.1343 (Fe^{3+} distributed in clusters [16, 17]) is sharpened. After an overnight exposure to NO_2, the Fe^{3+} peak at the g-factor of 2.1343 is significantly diminished. In the sample displayed in Figure 5.5A, there was no Fe^{3+} peak at a g-factor of 4.2950, but for the samples exhibiting the Fe^{+3} peak, introducing NO_2 to the PM completely eliminates the Fe^{3+} peak at g = 4.2950, Figure 5.5B. There was also a sharpening of the Mn signal in the same sample after exposure, Figure 5.5B. This implied a geometry change of Fe^{3+} and Mn after exposure, similar to the ozone exposure (*vide supra*, Figure 5.2A).

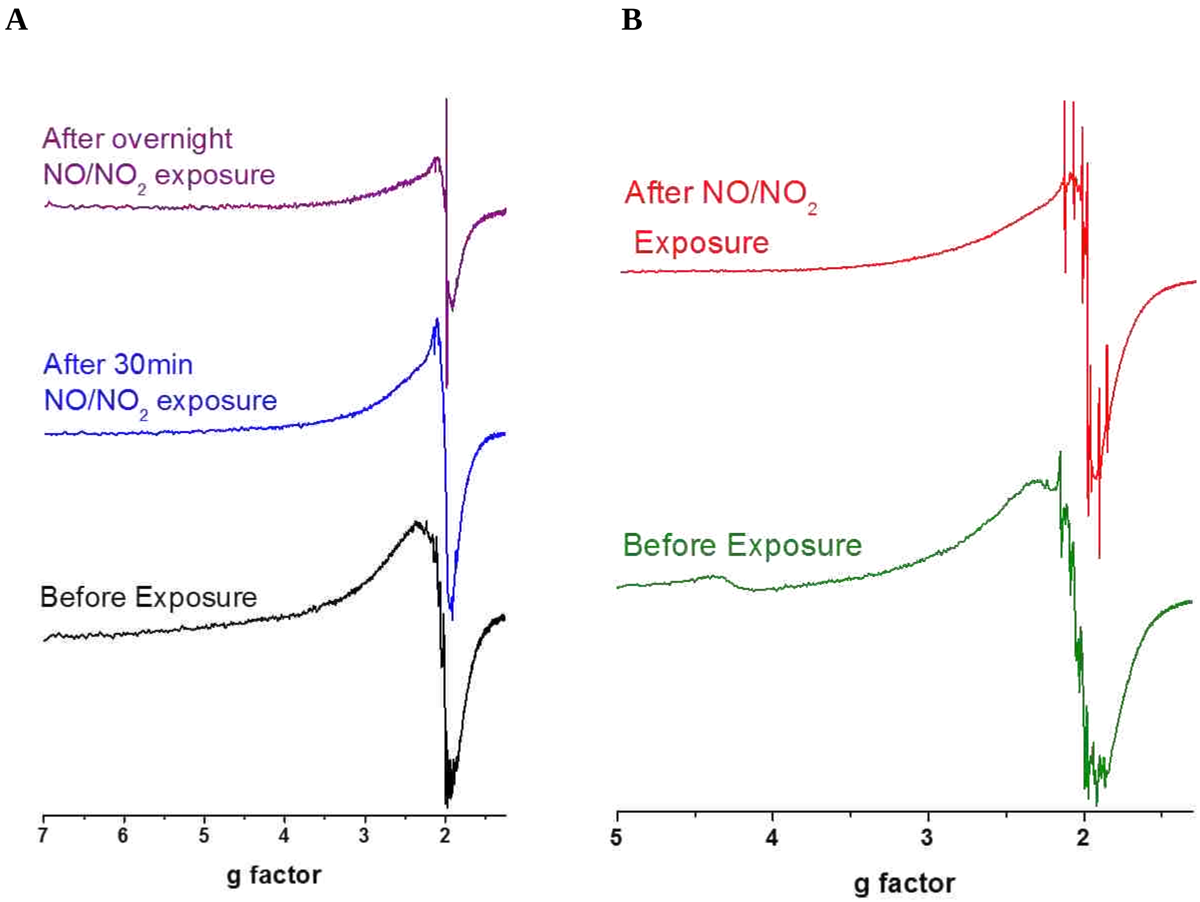

Figure 5.5 Effect of NO_2 on two different $PM_{2.5}$ samples. **A**. Effect of NO_2 on $PM_{2.5}$ EPFR spectrum collected from 3/14/12 illustrated in wide range magnetic field, 1500- 5500 G. **B**. Demonstration of NO_2 to eliminate the Fe^{3+} peak at a g-factor of 2.1343 for sample collected from 3/2/12. The extra peaks are from Mn.

The organic radical signal exhibited a noticeable difference after NO/NO_2 exposure, Figure 5.6, with a drastic increase in the organic radical concentration. Before exposure, the sample displayed 1.28×10^{17} radicals/g, and after only 15 min of NO/NO_2 exposure, the radical concentration intensified to 2.40×10^{17} radicals/g. Further exposures over a short time scale (1 hr) maintained approximately the same radical concentration. When exposed overnight, another large escalation to 8.33x10^{17} radicals/g was observed. This increase was confirmed by comparison to the control, only diminishing from 1.56x10^{17} to 1.39x10^{17} radicals/g. Subsequent evacuation and re-exposure of NO_2 to the same sample (8.33x10^{17} radicals/g) affected the organic signal little, marginally increasing to 8.45x10^{17} radicals/g with no variation in the other spectral features.

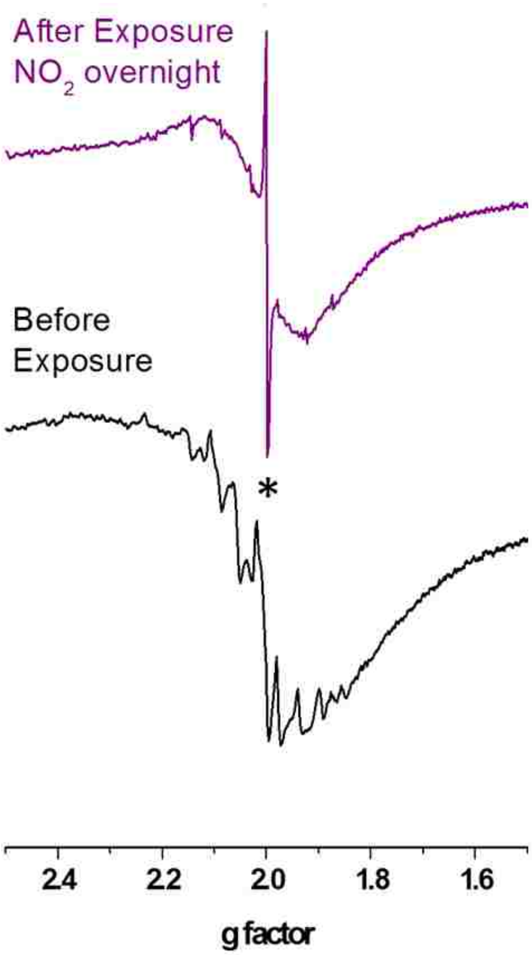

Figure 5.6 Effect of NO_2 exposure on the organic radical signal for $PM_{2.5}$ collected from 3/14/12 (same exposure as Figure 5.5A). The organic peak (assigned by asterisk) is overlaid on Mn signal.

Several suggestions may explain the different behavior of the $PM_{2.5}$ NO_2 exposure. The activity of NO_2 in the gas phase at low and ambient temperature is well documented, and the addition of NO_2 to tobacco smoke or mixtures of unsaturated hydrocarbons form alkyl and alkoxyl radicals [39-42]. There are few articles demonstrating heterogeneous interaction of NO_2 on other adsorbed substrates [43-45]. For catechol thin films, there was no reaction of NO_2 with catechol alone, and only when catechol was complexed with beznophenone did formation of 4-nitrocatechol occur [43]. Under dark conditions, the mechanism was implied to occur through hydrogen bonding of catechol with benzophenone stabilizing formation of the o-semiquinone radical [43]. However, when catechol was adsorbed on aerosol surrogates, formation of 4-nitrocatechol was observed without the addition of other substituents [45]. The unpaired electron on the surface was suggested to react with other paramagnetic species, such as NO_2 [46, 47].

NO is also relatively unreactive with organic species when compared to NO_2 [39]. This was observed with carbon blacks generating nitrated product formation from reactions of NO_2 but not NO [48]. Other correlations of NO_2 with nitrated and oxygenated PAHs were deemed significant (Spearman correlation $p < 0.10$) to an insignificant correlation with NO [49].

The large difference in activity between ozone and NO_2 is suggested by assuming an interaction of these components with soot constituents in $PM_{2.5}$. For simplicity, the rates of NO_2 addition to conjugated butadiene were compared to O_3 addition according to reaction 1 and reaction 2

$NO_2 + CH_2{=}CH\text{-}CH{=}CH_2 \rightarrow$ Products **reaction 1**

$O_3 + CH_2{=}CH\text{-}CH{=}CH_2 \rightarrow$ Products **reaction 2**

using known rate constants of $k1 = 1.87\text{x}10^4$ cm^3 / mol•s [50] and $k2 = 4.0\text{x}10^6$ cm^3 / mol•s [50] at room temperature in addition to concentrations of $[NO_2] \sim 100$ torr, $[O_3] = 2.76\text{x}10^{-6}$ torr. The ratio of the rate expression for reactions 1 and 2, R1/R2, was ~ 300. This indicated the formation rate from NO_2 exposure will be dominant over the ozone exposure because of the large concentration difference.

5.6 •OH Generation after Exposure of $PM_{2.5}$ to NO/NO_2

In all cases, NO/NO_2 exposed $PM_{2.5}$ demonstrated a lower affinity to generate •OH, Figure 5.7. At first, this fact appears to contradict previous results [1]. In this study, a direct dependence was observed between EPFR concentration and the •OH generation ability of $PM_{2.5}$ samples. Nevertheless, oxidants like ozone as well as NO_x drastically change the $PM_{2.5}$ environment (for example Figures 5.1 and 5.5, respectively), and this is observed here as a change in the pH of extracted $PM_{2.5}$ solutions. All NO_2 exposed $PM_{2.5}$ suspensions were observed to be more acidic than the control; the control maintained a constant pH of 7.0 - 7.5, while the pH for the NO_2 exposed $PM_{2.5}$ samples was dependent on the NO_2 concentration. For

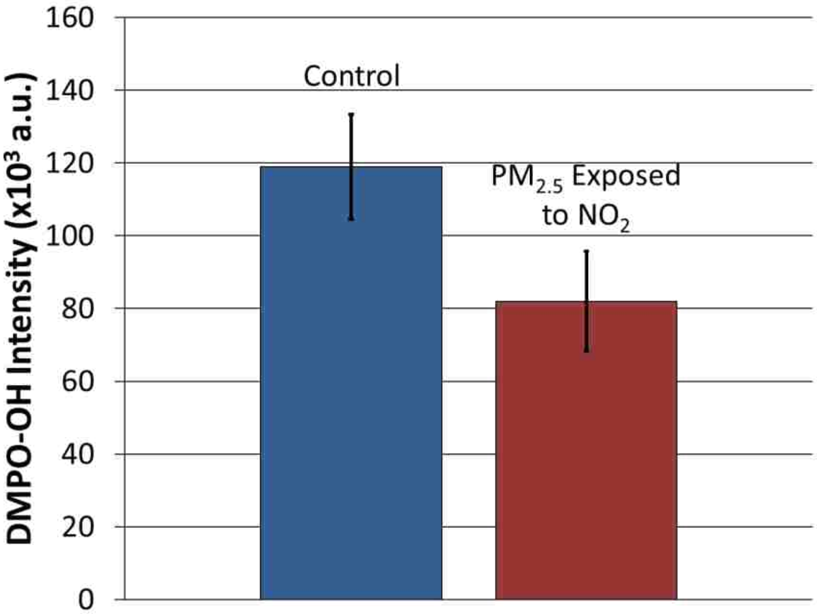

Figure 5.7 Effect of NO_2 exposure on •OH generation from $PM_{2.5}$ powder collected from 3/14/12.

example, when exposed to 354 torr NO_2, the resulting pH was 4.5, but when exposed to 36 torr for the same amount of time, the pH was 6.5. This might result from formation of nitric acid as a result of introducing NO_2 exposed $PM_{2.5}$ to an aqueous solution. Consequently, as the pH between the exposed sample and control were more closely matched, the generation of •OH would converge to the same adduct intensity.

The proposed catalytic cycle for •OH formation from EPFRs, as well as previous research [51], illustrates the importance of the solution pH [52-54]. In acidic solutions, there is diminished deprotonation from the surface bound EPFR (Figure 5.8), thus reducing formation of the superoxide anion and consequently •OH [52-54]. This behavior could explain why there were no increased health effects from exposures of NO_2 and PM [55, 56].

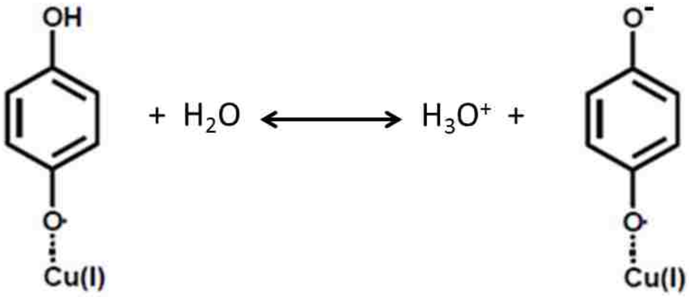

Figure 5.8 Deprotonation of the EPFR in water resulting in acid formation. Additional acid pushes reaction in the reverse direction.

5.7 References

1. Gehling, W., L. Khachatryan, and B. Dellinger, *Hydroxyl Radical Generation from Environmentall Persistent Free Radicals (EPFRs) in PM2.5.* Environ Sci Technol, 2013. **Submitted**.

2. Squadrito, G.L., et al., *Quinoid redox cycling as a mechanism for sustained free radical generation by inhaled airborne particulate matter.* Free Radical Biology and Medicine, 2001. **31** (9): p. 1132-1138.

3. Dellinger, B., et al., *Formation and stabilization of persistent free radicals.* Proceedings of the Combustion Institute, 2007. **31** (1): p. 521-528.

4. Lomnicki, S., et al., *Copper Oxide-Based Model of Persistent Free Radical Formation on Combustion-Derived Particulate Matter.* Environ. Sci. Technol., 2008. **42**: p. 4982-4988.

5. Valavanidis, A., K. Fiotakis, and T. Vlachogianni, *The Role of Stable Free Radicals, Metals and PAHs of Airborne Particulate Matter in Mechanisms of Oxidative Stress and Carcinogenicity.* , in *Urban Airborne Particulate Matter*, F. Zereini and C.L.S. Wiseman, Editors. 2011, Springer Berlin Heidelberg. p. 411-426.

6. Lachocki, T.M., D.F. Church, and W.A. Pryor, *Persistent free radicals in woodsmoke: an ESR spin trapping study.* Free radical biology & medicine, 1989. **7** (1): p. 17-21.

7. Pryor, W.A., *Cigarette smoke radicals and the role of free radicals in chemical carcinogenicity.* Environ Health Perspect, 1997. **105 Suppl 4**: p. 875-82.

8. Valavanidis, A., A. Salika, and A. Theodoropoulou, *Generation of hydroxyl radicals by urban suspended particulate air matter. The role of iron ions.* Atmospheric Environment, 2000. **34** (15): p. 2379-2386.

9. Valavanidis, A., et al., *Electron paramagnetic resonance study of the generation of reactive oxygen species catalysed by transition metals and quinoid redox cycling by inhalable ambient particulate matter.* Redox Report, 2005. **10** (1): p. 37-51.

10. Valavanidis, A., et al., *Determination of Selective Quinones and Quinoid Radicals in Airborne Particulate Matter and Vehicular Exhaust Particles.* Environmental Chemistry, 2006. **3** (2): p. 118-123.

11. Valavanidis, A., et al., *Persistent free radicals, heavy metals and PAHs generated in particulate soot emissions and residue ash from controlled combustion of common types of plastic.* J. Hazard. Mater., 2008. **156**: p. 277-284.

12. Castner, J.T., et al., *Note on the Paramagnetic Resonance of Iron in Glass.* The Journal of Chemical Physics, 1960. **32** (3): p. 668-673.

13. Griffith, J.S., *Theory of the isotropic g value of 4·27 found for some high-spin ferric ions.* Molecular Physics, 1964. **8** (3): p. 213-216.

14. Kedzie, R.W., D.H. Lyons, and M. Kestigian, *Paramagnetic Resonance of the Fe^{3+} Ion in CaWO_{4} (Strong Tetragonal Crystal Field).* Physical Review, 1965. **138** (3A): p. A918-A924.

15. Loveridge, D. and S. Parke, *Electron spin resonance of Fe3+, Mn2+, and Cr3+ in glasses.* Phys. Chem. Glasses, 1971. **12** (1): p. 19-27.

16. Ardelean, I., et al., *EPR and magnetic susceptibility studies of iron ions in 70TeO2·25B2O3·5PbO glass matrix.* Solid State Communications, 1997. **102** (4): p. 341-346.

17. Kumar, B., C. Chen, and S. Lin, *Effects of melting atmosphere on properties of a glass in the calcia-phosphorus pentoxide-iron sesquioxide system.* Phys. Chem. Glasses, 1992. **33** (5): p. 204-6.

18. Gehling, W., L. Khachatryan, and B. Dellinger, *Environmentally Persistent Free Radicals and Their Half-Lives in PM2.5.* Environ Sci Technol, 2013. **Submitted**.

19. Mehandjiev, D. and A. Naidenov, *Ozone Decomposition on α-Fe2O3 Catalyst.* Ozone: Science & Engineering, 1992. **14** (4): p. 277-282.

20. Davydov, R. and B.M. Hoffman, *EPR and ENDOR studies of Fe(II) hemoproteins reduced and oxidized at 77 K.* J Biol Inorg Chem, 2008. **13** (3): p. 357-69.

21. Alam, M.S., et al., *Total radical yields from tropospheric ethene ozonolysis.* Phys Chem Chem Phys, 2011. **13** (23): p. 11002-15.

22. Mysak, E.R., et al., *Competitive reaction pathways for functionalization and volatilization in the heterogeneous oxidation of coronene thin films by hydroxyl radicals and ozone.* Phys Chem Chem Phys, 2011. **13** (16): p. 7554-64.

23. Pavlovic, J. and P.K. Hopke, *Detection of radical species formed by the ozonolysis of α-pinene.* J. Atmos. Chem., 2010. **66**: p. 137-155.

24. Repine, J.E., et al., *Effects of fine carbonaceous particles containing high and low unpaired electron spin densities on lungs of female mice.* Transl Res, 2008. **152** (4): p. 185-93.

25. Peebles, B.C., et al., *Physicochemical and toxicological properties of commercial carbon blacks modified by reaction with ozone.* Environ Sci Technol, 2011. **45** (24): p. 10668-75.

26. Lena, T.S., et al., *Elemental carbon and PM2.5 levels in an urban community heavily impacted by truck traffic.* Environ. Health Perspect., 2002. **110** (10): p. 1009-1015.

27. Pang, Y., N.L. Eatough, and D.J. Eatough, *PM2.5 semivolatile organic material at Riverside, California: implications for the PM2.5 Federal Reference Method sampler.* Aerosol Sci. Technol., 2002. **36** (3): p. 277-288.

28. Sharma, M., A.K. Agarwal, and K.V.L. Bharathi, *Characterization of exhaust particulates from diesel engine.* Atmospheric Environment, 2005. **39** (17): p. 3023-3028.

29. Darrow, L.A., et al., *Ambient air pollution and birth weight in full-term infants in Atlanta, 1994-2004.* Environ. Health Perspect., 2011. **119** (5): p. 731-737.

30. Chiang, H.-L., Y.-M. Lai, and S.-Y. Chang, *Pollutant constituents of exhaust emitted from light-duty diesel vehicles.* Atmos. Environ., 2012. **47**: p. 399-406.

31. Lim, S., et al., *Ionic and carbonaceous compositions of PM10, PM2.5 and PM1.0 at Gosan ABC Superstation and their ratios as source signature.* Atmos. Chem. Phys., 2012. **12** (4): p. 2007-2024.

32. Wilhelm, M., et al., *Traffic-related air toxics and term low birth weight in Los Angeles County, California.* Environ Health Perspect, 2012. **120** (1): p. 132-8.

33. Li, Q., A. Wyatt, and R.M. Kamens, *Oxidant generation and toxicity enhancement of aged-diesel exhaust.* Atmospheric Environment, 2009. **43** (5): p. 1037-1042.

34. Holder, A.L., et al., *Increased cytotoxicity of oxidized flame soot.* Atmos. Pollut. Res., 2012. **3**: p. 25-31.

35. Madden, M.C., et al., *Effect of Ozone on Diesel Exhaust Particle Toxicity in Rat Lung.* Toxicology and Applied Pharmacology, 2000. **168** (2): p. 140-148.

36. Ntziachristos, L., et al., *Relationship between redox activity and chemical speciation of size-fractionated particulate matter.* Particle and fibre toxicology, 2007. **4**: p. 5.

37. Rattanavaraha, W., et al., *The reactive oxidant potential of different types of aged atmospheric particles: An outdoor chamber study.* Atmospheric Environment, 2011. **45** (23): p. 3848-3855.

38. Dellinger, B., et al., *Role of Free Radicals in the Toxicity of Airborne Fine Particulate Matter.* Chemical Research in Toxicology, 2001. **14** (10): p. 1371-1377.

39. Church, D.F. and W.A. Pryor, *Free-Radical Chemistry of Cigarette Smoke and Its Toxicological Implications.* Environmental Health Perspectives, 1985. **64**: p. 111-126.

40. Jonkman, L., et al., *Electron spin resonance of radicals formed in the reaction of nitrogen dioxide with olefins.* The Journal of Physical Chemistry, 1970. **74** (7): p. 1650-1652.

41. Jonkman, L., H. Muller, and J. Kommandeur, *Electron spin resonance study of nitroxides formed in the reaction of nitrogen dioxide and nitrogen oxide with styrenes.* Journal of the American Chemical Society, 1971. **93** (22): p. 5833-5838.

42. Cueto, R. and W.A. Pryor, *Cigarette smoke chemistry: conversion of nitric oxide to nitrogen dioxide and reactions of nitrogen oxides with other smoke components as studied by Fourier transform infrared spectroscopy.* Vibrational Spectroscopy, 1994. **7** (1): p. 97-111.

43. Nichols, B.R., et al., *Heterogeneous and Photochemical Reactions of Solid Benzophenone-Catechol Films with NO2.* J. Phys. Chem. C, 2009. **113**: p. 2111-2119.

44. Miet, K., et al., *Heterogeneous reactivity of pyrene and 1-nitropyrene with NO2: Kinetics, product yields and mechanism.* Atmospheric Environment, 2009. **43** (4): p. 837-843.

45. Woodill, L.A. and R.Z. Hinrichs, *Heterogeneous reactions of surface-adsorbed catechol with nitrogen dioxide: substrate effects for tropospheric aerosol surrogates.* Phys. Chem. Chem. Phys., 2010. **12** (36): p. 10766-10774.

46. Akhter, M.S., A.R. Chughtai, and D.M. Smith, *Reaction of hexane soot with nitrogen dioxide/nitrogen oxide (N2O4).* J. Phys. Chem., 1984. **88** (22): p. 5334-42.

47. Chughtai, A.R., J.M. Kim, and D.M. Smith, *The Effect of Air/Fuel Ratio on Properties and Reactivity of Combustion Soots.* Journal of Atmospheric Chemistry, 2002. **43** (1): p. 21-43.

48. Smith, D.M., et al., *Reaction of nitrogen oxides with black carbon: an FT-IR study.* Appl. Spectrosc., 1988. **42** (4): p. 674-80.

49. Wilson, N.K., T.R. McCurdy, and J.C. Chuang, *Concentrations and phase distributions of nitrated and oxygenated polycyclic aromatic hydrocarbons in ambient air.* Atmospheric Environment, 1995. **29** (19): p. 2575-2584.

50. NIST, *Chemical Kinetics Database 17 G.* Gaithersburg, 1998: p. MD.

51. Valavanidis, A., et al., *Influence of ozone on traffic-related particulate matter on the generation of hydroxyl radicals through a heterogeneous synergistic effect.* Journal of Hazardous Materials, 2009. **162** (2–3): p. 886-892.

52. Dellinger, B., et al., *Free radicals in tobacco smoke.* Mini-Rev. Org. Chem., 2011. **8**: p. 427-433.

53. Khachatryan, L., et al., *Environmentally Persistent Free Radicals (EPFRs). 1. Generation of Reactive Oxygen Species in Aqueous Solutions.* Environmental Science & Technology, 2011. **45** (19): p. 8559-66.

54. Khachatryan, L. and B. Dellinger, *Environmentally Persistent Free Radicals (EPFRs)-2. Are Free Hydroxyl Radicals Generated in Aqueous Solutions?* Environmental Science & Technology, 2011. **45** (21): p. 9232-9239.

55. Gong, H., Jr., et al., *Respiratory responses to exposures with fine particulates and nitrogen dioxide in the elderly with and without COPD.* Inhalation Toxicol., 2005. **17**: p. 123-132.

56. Huang, Y.C., et al., *Synergistic effects of exposure to concentrated ambient fine pollution particles and nitrogen dioxide in humans.* Inhal Toxicol, 2012. **24** (12): p. 790-7.

CHAPTER VI. SIMULATED SOLAR IRRADIATION OF EPFRs in $PM_{2.5}$

With an understanding of how oxygen, ozone, and NO_x can affect the EPFRs in $PM_{2.5}$, there is still one major contributor to common atmospheric processes, solar radiation. Therefore, the fourth objective was to investigate how simulated solar radiation affects EPFRs in $PM_{2.5}$ and the subsequent ability to generate hydroxyl radicals. These experiments were performed with the use of a Xenon lamp and an AM1.5 filter simulating the solar spectrum when the sun is 48° from zenith (directly above).

6.1 Initial EPR Measurements of $PM_{2.5}$

The initial EPR examination of all $PM_{2.5}$ powder after extraction from the filter displayed a single, unstructured organic peak exhibiting an average $\Delta H_{p\text{-}p}$ of 6 - 7 Gauss [1, 2]. The relatively wide peak in addition to a lack of hyperfine splitting implied multiple organic species of the same radical family present or broadening by organic-metal interactions [3-6]. These signals displayed initial g-factors of 2.0038 – 2.0043, suggesting a group of semiquinone radicals or more oxygenated radicals in a complex matrix [3-5, 7-12]. In addition to an organic peak, the presence of Fe^{3+} was detected at an approximate g-factor of 2.1 and attributed to Fe^{3+} distributed in clusters [13, 14]. The presence of Mn(I=5/2) was also noticed. These peaks were not observed to be effected from the irradiation.

The two $PM_{2.5}$ powders' (collected on binder free glass fiber filters for six weeks each) initial radical concentration is given in Table 6.1; however, this radical concentration did not remain constant before each simulated solar exposure. This is due to EPFRs in $PM_{2.5}$ decaying from exposure to air [1]. Between illumination experiments, the $PM_{2.5}$ powder was maintained in a sealed vial at -20 °C to slow this decay. Immediately before irradiation, all $PM_{2.5}$ exhibited an average initial radical concentration of 6.27 $x10^{16}$ radicals/g resulting from 5 - 8 mg of $PM_{2.5}$ powder used for each irradiation.

Table 6.1. Initial radical concentration for the two powdered $PM_{2.5}$ collected

Collection Period	Initial Radical Concentration (radicals/g)
April/May 2012	$1.85x10^{17}$
June/July 2012	$1.54x10^{17}$

6.2 Effect of Simulated Solar Exposure on the $PM_{2.5}$ EPFR Signal

The effect of simulated solar exposure, 45 minutes at 950 W/m^2, on the organic radical signal from freshly extracted $PM_{2.5}$ powder (loaded in an EPR tissue cell) is displayed in Figure 6.1. There was an average 4x increase in the organic radical signal after irradiation demonstrating the importance of solar radiation on forming new EPFRs. This resulted from an escalation in the relative intensity and an average broadening of the ΔH_{p-p} by 1.02 Gauss. The g-factor increased by an average of 0.0002 implying photo-oxidation of the sample during irradiation in ambient air [1]. Exposure beyond 45 min affected the signal little (c.f. Figures 6.2 and 6.4).

UV radiation is suggested to effect metal oxide surfaces by forming radical species which recombine to form more complex species [15]. Furthermore, irradiation of metal oxides, sand, ash, and sea salt generate radicals on the PM surface with various terpenes, hydrocarbons, and halocarbons [16]. This is in addition to enhancing the chemisorption of volatile organic compounds [16, 17]. In the case of aromatic hydrocarbons on metal oxides, these were observed to bind incomplete oxidation and degraded products to the metal oxide surface. These species were not identified until desorption from the surface at elevated temperatures [18], and this suggests irradiation forms very stable species on the surface of metal oxides in PM.

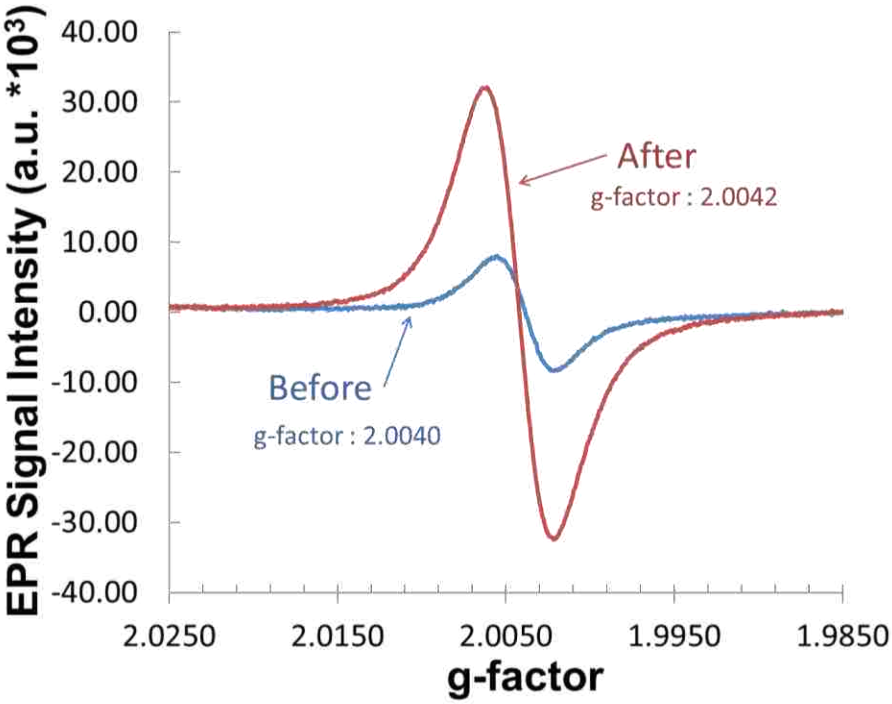

Figure 6.1. Effect of simulated solar irradiation on the organic radical signal from $PM_{2.5}$ powder collected from June/July of 2012. In the displayed case, the radical concentration increased three fold from 1.54 x10^{17} radicals/g to 4.54 x10^{17} radicals/g.

Polycyclic aromatic hydrocarbons (PAHs) are well documented to absorb sunlight in the visible and UV regions due to delocalized electrons in conjugated π systems [19, 20], and they undergo photolysis at the solid-air interface by a charge transfer mechanism [21]. In atmospheric conditions, photo-oxidized PAHs can subsequently degrade other organic compounds [19, 20]. This was confirmed from the photo-degradation of aliphatic hydrocarbons on oxidized PAHs [20]. In soot, photolysis decreased PAH concentrations [22, 23]. When exposing fresh soot to O_2 as well as simulated sunlight, formation of oxygen containing species, such as aromatic aldehydes, ketones, or quinones, was observed [19, 20, 24-27], and when the organic carbon was removed, there was a drastic decrease in photolysis activity [27]. This indicated the organic carbon fraction as a major contributor to photochemical aging [27].

In addition to metal oxides and PAHs, previous studies on the photochemistry of 4-chlorophenol supported on cellulose revealed the organic fraction absorbed photons upon irradiation [28]. After irradiation, there was a slow chemical decomposition resulting in the formation of the 4-chorophenoxy radical based on the product distribution. The same experiment on silica revealed benzoquinone and hydroquinone were the two major photo-degradation products [28].

Based on the above, we postulate the metal as well as organic fraction (hydroquinones, semiquinone, quinones, hydroxylated organics, etc.) in $PM_{2.5}$ will follow similar radical-mediated, photochemical pathways and form additional radicals (EPFRs) on the surface. The UV region is chemically active as the wavelengths match normal bond energies [29], and photolysis reactions can generate radical species by bond breaking [20]. The amount of metals, or generally the mineral fraction, in PM samples was suggested to determine the photochemical activity [30, 31], and $PM_{2.5}$ previously collected by us was demonstrated to contain a wide variety and concentration of metals [1, 2]. $PM_{2.5}$ is also well documented to contain quinones and aromatic carbonyls which, under irradiation, will oxidize and degrade PAHs in addition to other species adsorbed on the PM [20, 32, 33]. Given both metals and quinones as well as aromatic carbonyls are present in $PM_{2.5}$, this further strengthens the hypothesis of EPFRs forming on the surface of $PM_{2.5}$ due to irradiation.

6.3 Comparison of Simulated Solar Exposure Between the Collected Samples

The two $PM_{2.5}$ powders were irradiated after extraction and compared for trends, Figure 6.2. As displayed, both samples at this point in their decay demonstrated similar affinity towards simulated irradiation. The April/May and June/July increased from their initial (before exposure) organic radical concentration by 3.20 and 3.25, respectively. The appearance of the April/May sample accumulating additional radicals results from a slightly larger initial radical concentration.

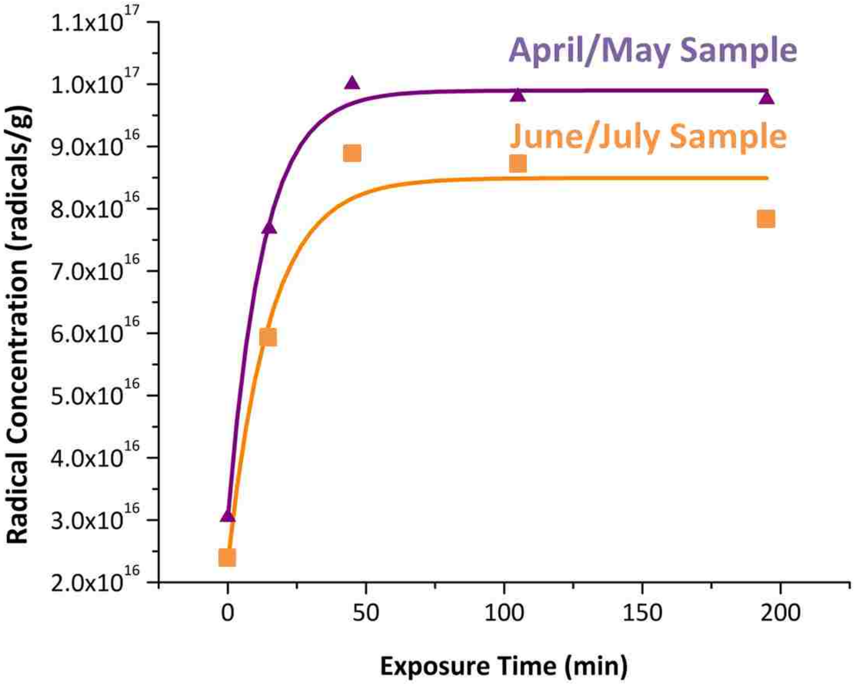

Figure 6.2. Comparison of simulated solar irradiation between the two $PM_{2.5}$ powders collected.

6.4 Decay of Irradiated EPFRs

To determine the persistence of these newly formed EPFRs, the $PM_{2.5}$ powder was allowed to age in ambient air after 1 hr of irradiation. This decay was monitored until approximately reaching the radical concentration before irradiation, and the resulting decay, relative to the initial radical concentration, is plotted in Figure 6.3. The first decay, designated as the "solar" decay, demonstrated a decay rate of 0.002 min^{-1} (0.12 hr^{-1}) corresponding to a 1/e half-life of 8 hours, while the second decay, designated as the "slower" decay, exhibited a decay rate of 0.00008 min^{-1} (0.00480 hr^{-1}) corresponding to a 1/e half-life of 9 days. Although the second decay is designated as the "slower" decay, it is much faster than the previously reported slow decay rate (0.0028 - 0.0005 hr^{-1} corresponding to an average 1/e half-life of 214 – 402 days) of non-irradiated $PM_{2.5}$ [1].

In the previous decay study, samples were collected for 24 hours from 9AM. The irradiation for this study corresponds to midday solar radiation levels. Therefore, this allowed

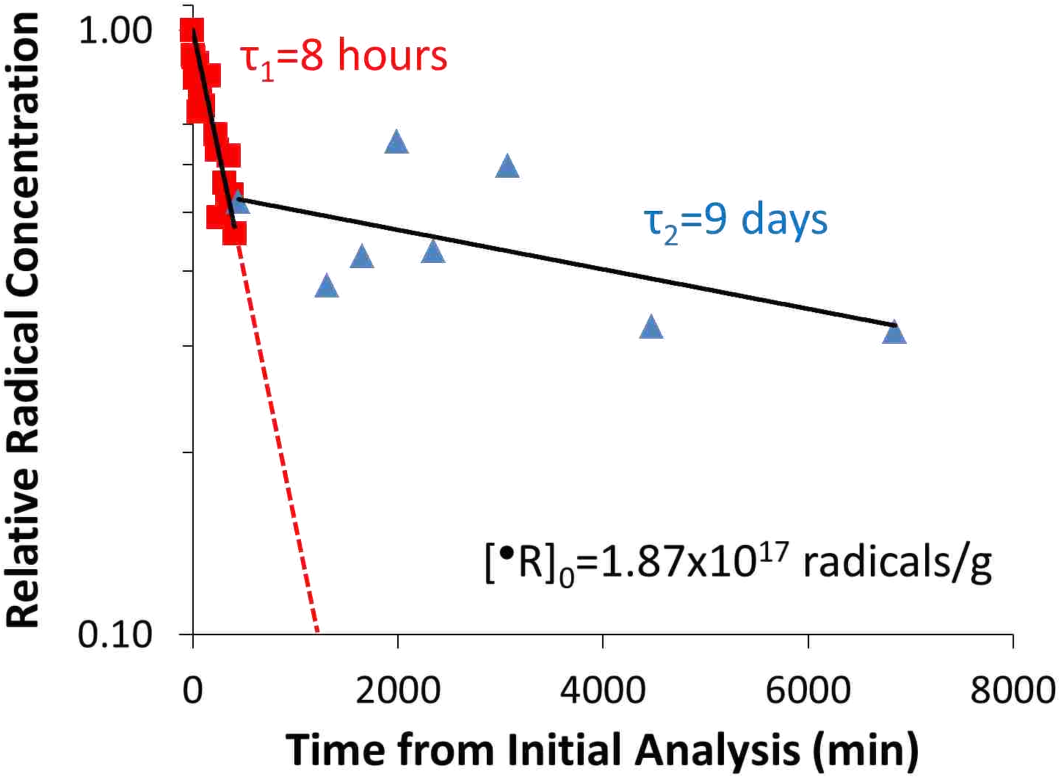

Figure 6.3. Decay of EPFRs after irradiation for $PM_{2.5}$ powder collected in June/July of 2012. All half-lives displayed are 1/e half-lives. The radical concentration before exposure was 4.95×10^{16} radicals/g.

the radicals generated from the solar irradiation ample time to decay before an initial radical measurement was acquired the next morning. Diurnal sample collection was attempted at the time of the first decay study, but due to small $PM_{2.5}$ collection, on the order of 200 μg, an accurate quantitative radical concentration was not established after the first 2 - 3 days.

6.5 Multiple Exposures on the Same Sample

Since $PM_{2.5}$ stays airborne for extended periods of time, multiple exposures from sunlight, although at longer times and lower average intensities, will occur. Thus, to mimic natural conditions, the same portion of the $PM_{2.5}$ powder was irradiated and allowed to decay in air until the next morning (~18 hours). After the first exposure, an additional exposure was performed and the procedure repeated. The first exposure displayed normal behavior with a 5.8x increase in the organic radical concentration from the initial value (Figure 6.4) and a shift in the g-factor from 2.0040 to 2.0043. When initially investigated the next day, the irradiated radical concentration dropped by 72% in this powder portion and the g-value decreased to 2.0041. When irradiated for the second time, the radical concentration increased by only 3.0x, a much lesser amount than the previous day, and the g-value shifted to 2.0043 again. This became even more reduced by the third exposure, demonstrating 62% reduction from the previous day's irradiation and a reduction of the g-value to 2.0041. This was followed by a 2.4x increase in the organic radical concentration and an increase in the g-value from 2.0041 to 2.0043 upon further irradiation.

The subsequent exposures' initial measurement not maintaining the initial radical concentration before exposure is explained by the radical decay. Considering the 1/e half-life for the longer decay is 9 days, 18 hours is not enough time for the irradiated radical concentration to decay to its original unexposed concentration. This suggests $PM_{2.5}$ will increase its baseline radical concentration everyday it is exposed to high levels of solar radiation.

The species responsible for radical concentration increasing after subsequent exposure is suggested to be quinones or other aromatic carbonyls present in PM [20, 32, 33], as they are documented photosensitizers [32, 33]. These species are also demonstrated as extremely persistent in an oxygen environment [1, 34] thereby allowing multiple photo-absorptions. There might be other multiple mechanisms, but due to the complexity of $PM_{2.5}$ and a lack of literature investigating these effects, they are not currently elucidated.

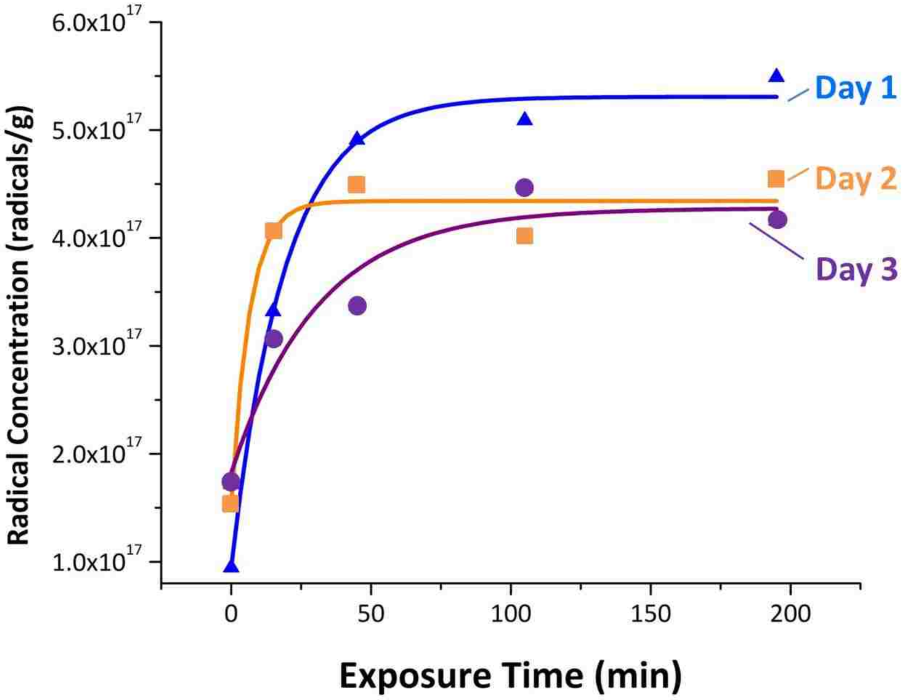

Figure 6.4 Demonstration of multiple simulated solar exposures on the same $PM_{2.5}$ powder portion collected from April/May of 2012. Subsequent exposures did not reach the radical concentration of the initial irradiation nor the initial concentration before exposure.

6.6 •OH Generation from Simulated Solar Irradiation

A comparison of •OH generations between an irradiated $PM_{2.5}$ sample to an unexposed sample is displayed in Figure 6.5. As observed in the figure, the irradiated sample generated more •OH than the unexposed sample. This increase may be due to the increased concentration of radicals participating in red-ox cycling thoroughly described in CHAPTER IV on page 68. These radicals represent organic radicals initially existing in $PM_{2.5}$ as well as the new radicals formed from the organic carbon [19, 20, 24-27] by solar irradiation. However, simulated solar irradiation may also drastically change the $PM_{2.5}$ surface environment. For example, a change might occur in the oxidation states of some transition metals, therefore permitting them to be Fenton active in generating •OH. There is also the possibility a change in both the radicals from organic carbon and metal fraction could augment the formation of •OH. Despite an uncertainty in the mechanisms dominant in •OH generation, this data suggests there are more adverse health effects gained from inhaling $PM_{2.5}$ in the afternoon hours during summer due to solar radiation.

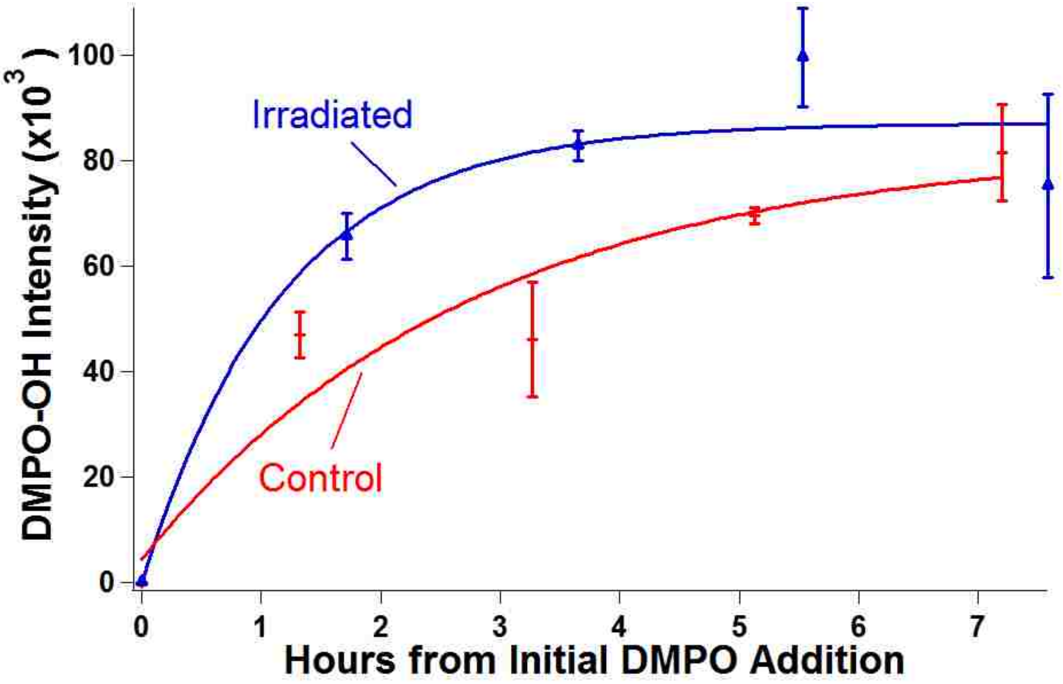

Figure 6.5. Generation of DMPO-OH adduct from an irradiated and control (non-irradiated) sample collected from April/May of 2012. The irradiated sample corresponded to a radical concentration of 2.53×10^{17} radicals/g. The control sample radical concentration was 1.23×10^{17} radicals/g.

6.7 References

1. Gehling, W., L. Khachatryan, and B. Dellinger, *Organic Radical Decay from Environmentally Persistent Free Radicals (EPFRs) in PM2.5.* Environ Sci Technol, 2013. **Submitted**.

2. Gehling, W., L. Khachatryan, and B. Dellinger, *Hydroxyl Radical Generation from Environmentall Persistent Free Radicals (EPFRs) in PM2.5.* Environ Sci Technol, 2013. **Submitted**.

3. Squadrito, G.L., et al., *Quinoid redox cycling as a mechanism for sustained free radical generation by inhaled airborne particulate matter.* Free Radical Biology and Medicine, 2001. **31** (9): p. 1132-1138.

4. Dellinger, B., et al., *Formation and stabilization of persistent free radicals.* Proceedings of the Combustion Institute, 2007. **31** (1): p. 521-528.

5. Lomnicki, S., et al., *Copper Oxide-Based Model of Persistent Free Radical Formation on Combustion-Derived Particulate Matter.* Environ. Sci. Technol., 2008. **42**: p. 4982-4988.

6. Valavanidis, A., K. Fiotakis, and T. Vlachogianni, *The Role of Stable Free Radicals, Metals and PAHs of Airborne Particulate Matter in Mechanisms of Oxidative Stress and Carcinogenicity.* , in *Urban Airborne Particulate Matter*, F. Zereini and C.L.S. Wiseman, Editors. 2011, Springer Berlin Heidelberg. p. 411-426.

7. Lachocki, T.M., D.F. Church, and W.A. Pryor, *Persistent free radicals in woodsmoke: an ESR spin trapping study.* Free radical biology & medicine, 1989. **7** (1): p. 17-21.

8. Pryor, W.A., *Cigarette smoke radicals and the role of free radicals in chemical carcinogenicity.* Environ Health Perspect, 1997. **105 Suppl 4**: p. 875-82.

9. Valavanidis, A., A. Salika, and A. Theodoropoulou, *Generation of hydroxyl radicals by urban suspended particulate air matter. The role of iron ions.* Atmospheric Environment, 2000. **34** (15): p. 2379-2386.

10. Valavanidis, A., et al., *Electron paramagnetic resonance study of the generation of reactive oxygen species catalysed by transition metals and quinoid redox cycling by inhalable ambient particulate matter.* Redox Report, 2005. **10** (1): p. 37-51.

11. Valavanidis, A., et al., *Determination of Selective Quinones and Quinoid Radicals in Airborne Particulate Matter and Vehicular Exhaust Particles.* Environmental Chemistry, 2006. **3** (2): p. 118-123.

12. Valavanidis, A., et al., *Persistent free radicals, heavy metals and PAHs generated in particulate soot emissions and residue ash from controlled combustion of common types of plastic.* J. Hazard. Mater., 2008. **156**: p. 277-284.

13. Kumar, B., C. Chen, and S. Lin, *Effects of melting atmosphere on properties of a glass in the calcia-phosphorus pentoxide-iron sesquioxide system.* Phys. Chem. Glasses, 1992. **33** (5): p. 204-6.

14. Ardelean, I., et al., *EPR and magnetic susceptibility studies of iron ions in 70TeO2·25B2O3·5PbO glass matrix.* Solid State Communications, 1997. **102** (4): p. 341-346.

15. Emeline, A.V., et al., *Photoinduced radical processes on the spinel (MgAl2O4) surface involving methane, ammonia, and methane/ammonia.* Langmuir, 2012. **28** (19): p. 7368-73.

16. Isidorov, V. and J. Jaroszynska, *Modeling of heterogeneous reactions of organic compounds in the atmosphere.* Wiad. Chem., 1998. **52** (7-8): p. 569-586.

17. Sassine, M., et al., *Kinetics of the tropospheric formaldehyde loss onto mineral dust and urban surfaces.* Atmospheric Environment, 2010. **44** (40): p. 5468-5475.

18. Isidorov, V., et al., *Photocatalysis on atmospheric aerosols: Experimental studies and modeling.* Catalysis Today, 1997. **39** (3): p. 233-242.

19. Mallakin, A., D.G. Dixon, and B.M. Greenberg, *Pathway of anthracene modification under simulated solar radiation.* Chemosphere, 2000. **40** (12): p. 1435-41.

20. Vione, D., et al., *Photochemical reactions in the tropospheric aqueous phase and on particulate matter.* Chem Soc Rev, 2006. **35** (5): p. 441-53.

21. Barbas, J.T., et al., *Spectroscopy and photochemistry of fluorene at a silica gel/air interface.* Journal of Photochemistry and Photobiology A: Chemistry, 1997. **109** (3): p. 229-236.

22. Kamens, R.M., et al., *The influence of humidity, sunlight, and temperature on the daytime decay of polyaromatic hydrocarbons on atmospheric soot particles.* Environ. Sci. Technol., 1988. **22** (1): p. 103-8.

23. Kim, D., et al., *Environmental aging of polycyclic aromatic hydrocarbons on soot and its effect on source identification.* Chemosphere, 2009. **76** (8): p. 1075-1081.

24. Barbas, J.T., M.E. Sigman, and R. Dabestani, *Photochemical Oxidation of Phenanthrene Sorbed on Silica Gel.* Environ. Sci. Technol., 1996. **30** (5): p. 1776-80.

25. Springob, C. and T. Wolff, *Photochemistry in porous materials. IV. Oxygen quenching of the fluorescence of fluoranthenes adsorbed on silica gel differing in pore size.* J. Photochem. Photobiol., A, 1996. **101** (1): p. 75-84.

26. Sigman, M.E., et al., *Mechanism of Pyrene Photochemical Oxidation in Aqueous and Surfactant Solutions.* Environmental Science & Technology, 1998. **32** (24): p. 3980-3985.

27. Han, C., et al., *Key role of organic carbon in the sunlight-enhanced atmospheric aging of soot by O2.* Proceedings of the National Academy of Sciences, 2012. **109** (52): p. 21250-21255.

28. Da Silva, J.P., et al., *Photochemistry of 4-chlorophenol on cellulose and silica.* Environ Sci Technol, 2003. **37** (20): p. 4798-803.

29. Finlayson-Pitts, B.J. and J.N. Pitts, *Chemistry of the Upper and Lower Atmosphere: Theory, Experiments, and Applications*. 1999: Academic. 1040 pp.

30. Dunstan, T.D.J., et al., *Adsorption and photodegradation of pyrene on magnetic, carbonaceous, and mineral subfractions of coal stack ash.* Environmental Science & Technology, 1989. **23** (3): p. 303-308.

31. Lackhoff, M. and R. Niessner, *Photocatalytic Atrazine Degradation by Synthetic Minerals, Atmospheric Aerosols, and Soil Particles.* Environmental Science & Technology, 2002. **36** (24): p. 5342-5347.

32. Jang, M. and S.R. McDow, *Benz[a]anthracene photodegradation in the presence of known organic constituents of atmospheric aerosols.* Environ. Sci. Technol., 1995. **29** (10): p. 2654-60.

33. Jang, M. and S.R. McDow, *Products of Benz[a]anthracene Photodegradation in the Presence of Known Organic Constituents of Atmospheric Aerosols.* Environmental Science & Technology, 1997. **31** (4): p. 1046-1053.

34. Pryor, W.A., *Biological effects of cigarette smoke, wood smoke, and the smoke from plastics: the use of electron spin resonance.* Free Radic Biol Med, 1992. **13** (6): p. 659-76.

CHAPTER VII. SUMMARY AND CONCLUSION

7.1 EPFRs and Their Half-Lives in $PM_{2.5}$

This study demonstrated the concentrations of EPFRs from a complex variety of point sources in an industrial corridor, and their decay followed pseudo-first order kinetics. A slight average increase of the g-factor by 0.0002 implied the EPFRs were oxidized during decay or an elimination of carbon centered radicals. Four patterns of decay were observed from the samples collected. The majority of the decays (47%) exhibited two consecutive decays with a fast decay displaying an average 1/e half-life of 7 days followed by a slow decay with an average half-life of 402 days. The second most abundant decay (24%) was a single slow decay exhibiting an average 1/e half-life of 214 days. The last two types of decays were no decay (18%) and a fast decay accompanied by no decay (11%) where the average 1/e half-life for the fast decay was 6. However, one of the decay categories may not actually be present, due to long residence times in the atmosphere eliminating radicals associated with the fast decay before analysis. Therefore, only 3 decays may exist, a fast decay, a slow decay, or no decay.

The two decays are implicated to result from the decay of two different radical species. The fast decay was suggested to result from decay of the phenoxyl radical. This was corroborated from other analysis where phenol was observed present in $PM_{2.5}$ and correlated well with the fast decay (p=0.60 n=7). The slow decay was attributed to decomposition of semiquinone type radicals to phenoxyl radicals[1]. The no decay pattern was explained by radicals entrapped in the bulk of $PM_{2.5}$ (or internal radicals) restricted in a solid matrix with the unpaired electrons delocalized over many conjugated or aromatic bonds[2-7].

Although there were no strong correlations with the metal data, a few interesting associations with the meteorological data were found. Correlations with photochemical processes (ozone, solar radiation, and UV radiation) were found to significantly correlate ($p=0.28$, $p=0.14$, $p=0.12$, respectively) with initial radical concentration and fast decay. Since the photochemical processes increased the radical concentration, their presence would slow down the fast decay rate as they are forming new radicals.

In order to assess the potentially negative health consequences of $PM_{2.5}$ in an easily understandable way, the EPFRs in cigarette tar were compared to those in airborne $PM_{2.5}$. Based on initial radical concentrations, a resident of the U.S. inhales enough radicals in $PM_{2.5}$ to be equivalent to smoking 0.3-0.9 cigarettes a day.

7.2 Hydroxyl Radical Generation from EPFRs in $PM_{2.5}$

Freshly captured $PM_{2.5}$ was demonstrated to generate hydroxyl radical without the need to add H_2O_2. The generation of hydroxyl radicals is believed to arise from a catalytic cycle involving EPFRs attached to a reduced metal species on the surface of $PM_{2.5}$. This cycle depends on the presence of oxygen, which is reduced by EPFRs to form the superoxide anion, H_2O_2, and ultimately form hydroxyl radicals.

Due to drastically different metal concentrations, the variation in hydroxyl radical formation could not be tested between samples. Instead, the suspended $PM_{2.5}$ was allowed to decay over time and a decrease in the hydroxyl radical formation was observed from when it was fresh. This decrease was attributed to a reduced presence of the organic radical. Other experiments demonstrated hydroxyl radical generation was dependent on the suspended particle concentration where higher particle concentrations exhibited increased generation of hydroxyl radicals.

The other steps in the cycle were confirmed in experiments where the suspension reduced formation of hydroxyl radicals by purging dissolved oxygen from solution with nitrogen; however, some $PM_{2.5}$ samples did not generate altered levels of hydroxyl radicals under the aforementioned conditions. This was believed due to the radicals being internal, rather than surface associated. Remaining internal, they are not accessible to react with O_2 or DMPO and thus unable to generate hydroxyl radicals.

7.3 Effects of NO_x and O_3 on EPFRs in $PM_{2.5}$ and Their Ability to Generate Hydroxyl Radicals

Collected $PM_{2.5}$ was extracted from a filter and the radical signal was observed to change after the extraction. This resulted in a significant reduction of the Fe^{3+} peak at the g-factor of 4.2950, from Fe^{3+} in a strong rhombic distorted tetrahedral or octahedral position[8-13]. There was also a partial elimination of the organic radical either from dissolved oxygen in solution or losing some PM fraction in the extraction process. When the extracted $PM_{2.5}$ powder was exposed to ozone, there was no effect on the organic radical signal or concomitant hydroxyl radical generation. This was believed to result from a reduced presence of soot in $PM_{2.5}$ as others observed exposed ozone to change the organic radical concentration for soot and carbon black[14, 15] as well as generate greater oxidant yields for DEP[16, 17] which has an inherently large amount of soot present. Ozone did, however, impact the transition metal environment by creating a new peak at a g-value of 2.9995. Even though this peak was not empirically elucidated, the presence of Fe in a complex matrix was suggested[18].

There was no effect from exposure to NO, and thus, no effect on the ability of the $PM_{2.5}$ to generate altered levels of hydroxyl radicals. This is suggested to result from the radical's internal nature in these particular samples. However, the exposure to NO_2 displayed a significant effect on the radical signal. After exposure to NO_2, there was a significant decrease in the ΔH_{p-p} and an immense growth in the organic radical concentration. This might arise from the formation of alkoxyl or alkyl radicals[19]. The diminished activity of ozone compared to NO_2 was explained by high concentrations of NO_2 (up to hundreds of torr) vs. 2.760×10^{-6} torr of ozone. When suspending the NO_2 exposed $PM_{2.5}$ in solution, the pH was found to become acidic from the formation of an acid and therefore diminished the ability of the $PM_{2.5}$ to generate hydroxyl radicals. This behavior was supported from the proposed catalytic cycle where acidic solutions diminish the deprotonation of the surface bound EPFR, thus reducing the formation of the superoxide anion and consequently the hydroxyl radical.

7.4 Simulated Solar Exposure of EPFRs in $PM_{2.5}$

The extracted $PM_{2.5}$ powder was exposed at an insolation of 950 W/m^2 corresponding to the maximum solar radiation Baton Rouge receives during midday in June. After 45 min exposure in ambient air, the organic radical concentration was observed to increase by three to four times the original radical concentration. Further irradiation demonstrated the radical concentration to remain relatively constant. Corresponding with the increase of the organic radical concentration was an average increase of the g-factor by 0.0002 implying photo-oxidation of the $PM_{2.5}$. We proposed the formation of new radicals on the surface derives from a combination of metal and organic factors inducing a radical-mediated photochemical pathway.

The newly formed radicals exhibited a two stage decay, a faster solar decay of 8 hr and a slower decay of 9 days. The slower decay here correlated well with the previously observed decay studies of EPFRs in $PM_{2.5}$. Multiple simulated solar exposures on the same portion of $PM_{2.5}$ was found to consistently generate more radicals but at reduced quantities for subsequent exposures. Spin trapping experiments demonstrated the irradiated sample to generate more hydroxyl radicals than the unexposed sample. Therefore, solar irradiation might be an important pathway for adverse health effects from EFPRs in $PM_{2.5}$.

7.5 Conclusion

These results demonstrate EPFRs were found in all collected $PM_{2.5}$, and subsequently, they can undergo important atmospheric and toxicological reactions. The long half-lives observed indicate EPFRs in ambient $PM_{2.5}$ are extremely stable to oxygen and follow similar behavior as previous studies on the model EPFR system. The spin trapping experiment demonstrates EPFRs in $PM_{2.5}$ can generate ROS, and this further strengthens the EPFR mechanism for $PM_{2.5}$'s toxicity. Reactions with ozone and NO demonstrate them, at least for these particular samples, to not impact the organic radical concentration or the altered generation of hydroxyl radicals. Exposure to NO_2 exhibited a large increase in the EPFR concentration but a drastic decrease in the formation of hydroxyl radicals. This observation might support some of the previous medical exposure studies of NO_2 and PM. In these studies, either minor differences or a slight antagonism between the two were observed[20, 21]. The simulated solar exposure consistently generated an increased concentration of EPFRs in $PM_{2.5}$ and confers an important pathway for EPFR formation in the atmosphere. This ROS generation after exposure implies any heavy exertion, such as running or biking, during midday in the summer may exacerbate any adverse health effects from inhaling $PM_{2.5}$.

7.6 Recommendations for Future Research

Based on the results of this investigation, the author suggests future research on EPFRs in ambient $PM_{2.5}$. Perhaps the most important is a more accurate analysis of $PM_{2.5}$'s organic fraction before and after different simulated atmospheric exposures. Due to the small masses used in these experiments, an accurate GC/MS analysis was quite difficult, because the quantities of the organics were in the detection limit region for the present instrumentation. If a specialized method for organic extraction of the $PM_{2.5}$ is not developed for the present instrumentation, then other methods should be explored, such as a time-of-flight mass spectrometer.

In regards to the simulated solar exposure, there are many studies to perform. Initial studies should confirm if photo-oxidation increases the organic carbon fraction in $PM_{2.5}$, and consequently, if this increase in organic carbon is the cause of a greater hydroxyl radical accumulation. Other intensities closely matching winter insolation should also be explored and compared to the impact from summer. In addition to these studies, a simpler exposure system should develop to only use single gases, such as O_2 or N_2, during irradiation.

There is also the need to understand how simultaneous atmospheric exposures, such as ozone and NO_x or NO_x and simulated solar irradiation, will affect $PM_{2.5}$. After simple combinations, the end result should culminate to a system where ozone, NO_x, and simulated sunlight are exposed at the same time. From there, simple VOCs, such as formaldehyde, are added into the system to observe if any additional radical generation results from uptake of the irradiated VOCs onto the $PM_{2.5}$ surface. Additionally, the resulting generation of hydroxyl radicals from these combined, simple or otherwise, exposures must be performed to understand if these exposures result in any additional adverse health effects.

7.7 References

1. Vejerano, E., S. Lomnicki, and B. Dellinger, *Formation and Stabilization of Combustion-Generated Environmentally Persistent Free Radicals on an Fe(III)2O3/Silica Surface.* Environ. Sci. Technol., 2011. **45**: p. 589-594.

2. Borg, D.C. *Oxygen free radicals and tissue injury: a reference outline*. 1993. Birkhaeuser.

3. Jankovic, J., et al., *Measurement of short-lived reactive species and long-lived free radicals in air samples from structural fires.* Appl. Occup. Environ. Hyg., 1993. **8**: p. 650-4.

4. Yordanov, N.D. and R. Mladenova, *EPR study of thermally generated free radicals in nuts.* Int. J. Food Sci. Technol., 2007. **42**: p. 1384-1389.

5. Lomnicki, S., et al., *Copper Oxide-Based Model of Persistent Free Radical Formation on Combustion-Derived Particulate Matter.* Environ. Sci. Technol., 2008. **42**: p. 4982-4988.

6. Valavanidis, A., et al., *Persistent free radicals, heavy metals and PAHs generated in particulate soot emissions and residue ash from controlled combustion of common types of plastic.* J. Hazard. Mater., 2008. **156**: p. 277-284.

7. Tian, L., et al., *Carbon-Centered Free Radicals in Particulate Matter Emissions from Wood and Coal Combustion.* Energy & Fuels, 2009. **23** (5): p. 2523-2526.

8. Castner, J.T., et al., *Note on the Paramagnetic Resonance of Iron in Glass.* The Journal of Chemical Physics, 1960. **32** (3): p. 668-673.

9. Griffith, J.S., *Theory of the isotropic g value of 4·27 found for some high-spin ferric ions.* Molecular Physics, 1964. **8** (3): p. 213-216.

10. Kedzie, R.W., D.H. Lyons, and M. Kestigian, *Paramagnetic Resonance of the Fe^{3+} Ion in CaWO_{4} (Strong Tetragonal Crystal Field).* Physical Review, 1965. **138** (3A): p. A918-A924.

11. Loveridge, D. and S. Parke, *Electron spin resonance of Fe3+, Mn2+, and Cr3+ in glasses.* Phys. Chem. Glasses, 1971. **12** (1): p. 19-27.

12. Ardelean, I., et al., *EPR and magnetic susceptibility studies of iron ions in 70TeO2·25B2O3·5PbO glass matrix.* Solid State Communications, 1997. **102** (4): p. 341-346.

13. Kumar, B., C. Chen, and S. Lin, *Effects of melting atmosphere on properties of a glass in the calcia-phosphorus pentoxide-iron sesquioxide system.* Phys. Chem. Glasses, 1992. **33** (5): p. 204-6.

14. Repine, J.E., et al., *Effects of fine carbonaceous particles containing high and low unpaired electron spin densities on lungs of female mice.* Transl Res, 2008. **152** (4): p. 185-93.

15. Peebles, B.C., et al., *Physicochemical and toxicological properties of commercial carbon blacks modified by reaction with ozone.* Environ Sci Technol, 2011. **45** (24): p. 10668-75.

16. Li, Q., A. Wyatt, and R.M. Kamens, *Oxidant generation and toxicity enhancement of aged-diesel exhaust.* Atmospheric Environment, 2009. **43** (5): p. 1037-1042.

17. Holder, A.L., et al., *Increased cytotoxicity of oxidized flame soot.* Atmos. Pollut. Res., 2012. **3**: p. 25-31.

18. Davydov, R. and B.M. Hoffman, *EPR and ENDOR studies of Fe(II) hemoproteins reduced and oxidized at 77 K.* J Biol Inorg Chem, 2008. **13** (3): p. 357-69.

19. Church, D.F. and W.A. Pryor, *Free-Radical Chemistry of Cigarette Smoke and Its Toxicological Implications.* Environmental Health Perspectives, 1985. **64**: p. 111-126.

20. Gong, H., Jr., et al., *Respiratory responses to exposures with fine particulates and nitrogen dioxide in the elderly with and without COPD.* Inhalation Toxicol., 2005. **17**: p. 123-132.

21. Huang, Y.C., et al., *Synergistic effects of exposure to concentrated ambient fine pollution particles and nitrogen dioxide in humans.* Inhal Toxicol, 2012. **24** (12): p. 790-7.

APPENDIX 1. SUPPORTING INFORMATION FOR EPFRS AND THEIR HALF-LIVES IN $PM_{2.5}$

A1.1 Complete List of Samples' Decay

Displayed below is a list of all samples according to their decay behavior in order from most abundant to least abundant. Samples displaying a fast decay followed by slow decay are given in Table A1.1; samples demonstrating a single slow decay in Table A1.2; samples with no decay in Table A1.3; samples exhibiting a fast decay followed by no decay are given in Table A1.4. Included at the end of each table are the averages, standard deviations, and number of samples for that category.

Table A1.1 Samples exhibiting a fast decay followed by a slow decay

Sample Date	Initial Radical Concentration (radicals/g $*10^{17}$)	Fast Decay Rate	$\tau_{(1/e)}$ Fast Decay (in Days)	Slow Decay Rate	$\tau_{(1/e)}$ Slow Decay (in Days)
11/3/2008	2.79	-0.07	0.60	-0.002	20.83
7/11/2009	2.26	-0.002	20.83	-0.0004	104.17
7/12/2009	0.366	-0.012	3.47	-0.0003	138.89
7/13/2009	9.22	-0.014	2.98	-0.0001	416.67
7/14/2009	0.232	-0.019	2.19	-0.0002	208.33
7/15/2009	4.23	-0.029	1.44	-0.0003	138.89
7/16/2009	2.15	-0.016	2.60	-0.00004	1041.67
7/17/2009	3.92	-0.047	0.89	-0.0005	83.33
7/20/2009	1.69	-0.007	5.95	-0.0008	52.08
7/21/2009	8.71	-0.016	2.60	-0.0008	52.08
7/22/2009	0.262	-0.031	1.34	-0.0009	46.30
7/26/2009	0.415	-0.006	6.94	-0.0004	104.17
7/27/2009	8.19	-0.013	3.21	-0.0002	208.33
7/31/2009	1.27	-0.006	6.94	-0.0005	83.33
8/1/2009	0.260	-0.008	5.21	-0.0007	59.52
8/2/2009	1.55	-0.017	2.45	-0.0001	416.67
8/4/2009	0.818	-0.003	13.89	-0.0008	52.08
8/5/2009	1.51	-0.014	2.98	-0.001	41.67
8/12/2009	2.18	-0.004	10.42	-0.0003	138.89

Table A1.1 continued

Date	Initial Radical Concentration (radicals/g $*10^{17}$)	Fast Decay Rate	$\tau_{(1/e)}$ Fast Decay (in Days)	Slow Decay Rate	$\tau_{(1/e)}$ Slow Decay (in Days)
8/13/2009	3.72	-0.006	6.94	-0.0003	138.89
8/15/2009	0.743	-0.014	2.98	-0.0001	416.67
8/18/2009	5.70	-0.004	10.42	-0.0005	83.33
8/19/2009	2.17	-0.018	2.31	-0.0008	52.08
8/21/2009	1.17	-0.018	2.31	-0.0006	69.44
8/22/2009	0.584	-0.002	20.83	-0.0002	208.33
8/24/2009	34.8	-0.004	10.42	-0.0004	104.17
8/25/2009	2.40	-0.014	2.98	-0.0005	83.33
8/26/2009	2.12	-0.015	2.78	-0.0003	138.89
8/27/2009	1.83	-0.008	5.21	-0.0009	46.30
8/28/2009	1.35	-0.014	2.98	-0.0009	46.30
8/30/2009	1.32	-0.008	5.21	-0.0007	59.52
8/31/2009	1.18	-0.004	10.42	-0.001	41.67
3/6/2010	0.620	-0.008	5.21	-0.00005	833.33
3/7/2010	7.12	-0.012	3.47	-0.00004	1041.67
3/8/2010	6.50	-0.007	5.95	-0.00005	833.33
3/9/2010	4.40	-0.01	4.17	-0.0005	83.33
3/10/2010	11.8	-0.004	10.42	-0.0006	69.44
3/14/2010	10.9	-0.004	10.42	-0.00003	1388.89
3/29/2010	10.5	-0.01	4.17	-0.000008	5208.33
3/30/2010	10.4	-0.012	3.47	-0.0001	416.67
4/4/2010	2.07	-0.032	1.30	-0.0008	52.08
4/9/2010	3.06	-0.002	20.83	-0.0001	416.67
4/29/2010	23.8	-0.051	0.82	-0.002	20.83
5/1/2010	2.07	-0.003	13.89	-0.0002	208.33
5/7/2010	2.05	-0.005	8.33	-0.0007	59.52
5/8/2010	7.04	-0.025	1.67	-0.001	41.67
5/14/2010	2.75	-0.002	20.83	-0.0002	208.33
5/2/2011	5.82	-0.017	2.45	-0.00009	462.96
5/5/2011	25.4	-0.016	2.60	-0.0001	416.67
5/24/2011	4.62	-0.002	20.83	-0.00001	4166.67
7/18/2011	3.25	-0.002	20.83	-0.0001	416.67
7/26/2011	6.68	-0.003	13.89	-0.0006	69.44
8/2/2011	5.20	-0.005	8.33	-0.0002	208.33
9/3/2011	3.94	-0.003	13.89	-0.0002	208.33

Table A1.1 continued

# Samples: 54					
Average	**5.02**	**0.0129**	**7.05**	**0.00047**	**402.38**
Standard Deviation	**6.51**	**0.0132**	**6.14**	**0.00043**	**902.63**

Table A1.2 Samples demonstrating a slow decay

Date	Initial Radical Concentration (radicals/g $*10^{17}$)	Slow Decay Rate	$\tau_{(1/e)}$ Slow Decay (in Days)
11/2/2008	0.898	-0.0009	46.30
11/4/2008	0.765	-0.002	20.83
11/6/2008	1.28	-0.002	20.83
11/8/2008	1.38	-0.004	10.42
11/11/2008	0.223	-0.003	13.89
11/12/2008	2.37	-0.005	8.33
11/13/2008	2.40	-0.006	6.94
11/14/2008	1.69	-0.01	4.17
11/16/2008	1.01	-0.004	10.42
11/17/2008	1.06	-0.001	41.67
11/18/2008	0.246	-0.009	4.63
11/19/2008	3.23	-0.011	3.79
7/28/2009	0.377	-0.0009	46.30
7/29/2009	0.295	-0.009	4.63
8/6/2009	0.753	-0.0002	208.33
8/7/2009	0.413	-0.0001	416.67
8/9/2009	0.202	-0.0001	416.67
8/21/2009	3.57	-0.004	10.42
8/23/2009	0.447	-0.0005	83.33
3/13/2010	6.90	-0.0001	416.67
5/3/2010	4.00	-0.001	41.67
5/15/2010	13.4	-0.002	20.83
5/4/2011	10.5	-0.00002	2083.33
7/17/2011	2.82	-0.00005	833.33
7/25/2011	4.04	-0.00007	595.24
8/9/2011	1.31	-0.0002	208.33
9/2/2011	2.99	-0.0002	208.33
# Samples: 27			
Average	**2.54**	**0.00283**	**214.31**
Standard Deviation	**3.16**	**0.00340**	**430.42**

Table A1.3 Samples with no decay

Date	Initial Radical Concentration (radicals/g $*10^{17}$)
11/1/2008	0.508
11/5/2008	0.343
11/7/2008	0.592
11/21/2008	0.347
11/22/2008	0.265
11/23/2008	0.338
8/8/2009	0.408
3/11/2010	11.7
4/1/2010	2.24
4/3/2010	1.48
4/5/2010	0.626
4/6/2010	0.597
4/7/2010	1.42
4/8/2010	2.24
4/10/2010	0.755
4/30/2010	1.94
5/5/2010	4.53
5/13/2010	1.43
5/13/2010	2.77
8/1/2011	5.54
8/8/2011	1.42
# Samples: 21	
Average	**1.98**
Standard Deviation	**2.63**

Table A1.4 Samples exhibiting a fast decay accompanied by no decay

Date	Initial Radical Concentration (radicals/g $*10^{17}$)	Fast Decay Rate	$\tau_{(1/e)}$ Fast Decay (in Days)
7/23/2009	5.05	-0.009	4.63
7/24/2009	2.30	-0.005	8.33
7/25/2009	0.785	-0.022	1.89
7/30/2009	1.90	-0.015	2.78
8/3/2009	0.687	-0.014	2.98
8/11/2009	6.67	-0.008	5.21
8/17/2009	1.73	-0.006	6.94
8/29/2009	0.592	-0.005	8.33
3/12/2010	7.07	-0.007	5.95
5/2/2010	1.27	-0.002	20.83
5/10/2010	6.90	-0.007	5.95
5/3/2011	19.9	-0.159	0.26
# Samples: 12			
Average	**4.57**	**0.0216**	**6.17**
Standard Deviation	**5.46**	**0.0436**	**5.25**

A1.2 Metals Analysis and Correlation

A list of metals found in $PM_{2.5}$ is given in Table A1.5. Samples were analyzed for Al, As, B, Ba, Ca, Cd, Co, Cr, Cu, Fe, K, Mg, Mn, Na, Ni, Pb, Si, and Zn after decays were measured. The listed metals were found in most samples with notable exceptions for As (observed in 7 of the 24 samples), B (observed in 4 of the 24 samples), and Cd (observed in 14 of the 24 samples). The most abundant metals averaged from all the samples were Si (133.28 ± 184.22 ppm), Na (122.34 ± 163.34 ppm), Ca (113.46 ± 114.15 ppm), Fe (65.38 ± 74.58 ppm), and Al (87.48 ± 133.33 ppm). This demonstrates a wide range of metal concentrations found in ambient $PM_{2.5}$ from day to day in Baton Rouge. Considering the large industrial activity in and around Baton Rouge, as well as being downwind from major industrial and manufacturing point sources in Houston, such deviations are expected.

To understand the role of metals in reference to the current study, correlations were calculated with the metal data against the initial radical concentration and the fast/slow decay rates for trends, Table A1.6. Boron was not correlated due to a lack of data points obtained from the metal analysis. The metal with the best correlation for all 3 factors was As, although this metal had the least amount of data points used for the correlation. Therefore, As might not have as strong a correlation as displayed.

Correlations of metals with the initial radical concentration conferred the strongest associations of the three parameters. The two strongest positive correlations, even though weak overall, came from Cr and Cu with a correlation factor of 0.153 and 0.162, respectively. The strongest negative correlations came from Na and Mg with a correlation factor of -0,372 and -0.309, respectively. Surprisingly, there was a negative correlation with Fe and Zn. Previous research performed in this laboratory has demonstrated EPFRs to form on the surface of Fe_2O_3 and ZnO, so it was expected for these metals to have an overall positive correlation [1, 2]. Overall, there were no strong correlations between the metal data and the initial radical concentration.

Table A1.5 List of metals found in $PM_{2.5}$ samples (in ppm) from ICP-AE analysis.

Collection Date	**Al**	**As**	**B**	**Ba**	**Ca**	**Cd**	**Co**	**Cr**	**Cu**	**Fe**	**K**	**Mg**	**Mn**	**Na**	**Ni**	**Pb**	**Si**	**Zn**
7/15/2009	499.89	0.000	0.00	9.86	541.39	0.000	0.000	0.13	5.65	251.52	137.28	119.77	6.45	0.0	2.52	3.54	0.00	11.86
8/15/2009	0.000	0.000	0.00	1.743	109.45	0.000	0.000	0.000	4.086	253.037	0.00	29.30	0.286	0.0	2.886	2.366	0.000	0.000
3/6/2010	19.605	0.000	2.05	2.430	66.3	0.044	0.024	0.080	2.912	25.089	51.52	7.6	0.660	28.8	0.222	0.754	52.469	8.995
3/7/2010	27.453	0.000	0.00	2.105	13.8	0.034	0.015	0.160	2.340	24.631	13.57	19.0	0.748	118.3	0.360	0.799	68.654	4.045
3/9/2010	10.943	0.097	0.00	1.173	69.641	0.000	0.003	0.061	1.516	9.789	21.773	4.540	0.349	1.988	1.038	0.161	30.417	2.009
3/11/2010	54.260	0.000	0.00	2.503	77.282	0.019	0.036	0.372	2.346	54.462	29.518	19.528	1.177	81.889	0.604	1.228	118.903	17.610
3/14/2010	21.755	0.059	0.00	2.489	80.397	0.033	0.022	0.087	3.187	27.298	23.199	6.627	0.709	10.209	0.204	0.562	52.626	8.919
3/29/2010	32.939	0.212	0.00	3.885	95.450	0.062	0.031	0.207	5.039	41.076	22.773	11.687	1.087	8.877	0.434	1.375	77.622	9.565
3/30/2010	29.207	0.063	0.00	1.677	86.571	0.036	0.025	0.173	2.219	27.125	34.267	11.596	0.955	16.491	0.400	0.756	76.470	9.652
4/13/2010	94.389	0.000	0.00	2.34	120.562	0.024	0.039	0.182	4.67	67.88	45.367	31.755	1.234	120.22	0.85	0.623	129.87	7.233
4/30/2010	230.68	0.000	0.00	1.80	56.1	0.00	0.0540	0.225	0.596	103.75	77.84	68.2	2.034	390.3	0.436	0.296	407.60	3.93
5/1/2010	458.189	0.000	1.583	3.494	127.576	0.00	0.169	0.468	1.022	229.344	114.570	142.436	5.270	609.323	0.433	0.264	874.227	3.498
5/2/2010	137.396	0.114	0.00	1.533	41.284	0.009	0.053	0.156	1.245	73.628	38.879	36.986	1.601	137.560	0.407	0.150	263.180	5.037
5/3/2010	42.379	0.212	2.573	2.306	92.152	0.027	0.027	0.109	2.620	36.075	21.719	18.300	1.276	39.784	0.201	0.683	90.797	9.853
5/5/2010	36.836	0.050	0.502	2.319	130.758	0.025	0.032	0.174	2.996	34.464	17.017	17.216	1.265	20.734	0.341	0.616	86.244	5.625
5/7/2010	87.41	0.000	0.00	1.74	150.7	0.0084	0.1020	0.182	3.844	45.24	60.38	35.7	1.299	160.2	0.447	0.285	170.51	6.33
5/10/2010	45.14	0.000	0.00	2.38	87.1	0.0062	0.0135	0.105	0.543	26.74	19.84	15.7	1.181	41.6	0.344	0.292	92.97	3.24
5/13/2010	36.20	0.000	0.00	1.20	89.1	0.000	0.0228	0.096	0.842	24.43	28.88	41.4	0.887	289.2	0.360	0.259	85.53	2.56
5/14/2010	36.215	0.000	0.00	1.018	69.7	0.000	0.013	0.097	0.647	23.324	19.93	37.8	0.681	231.6	0.668	0.228	93.468	2.622
5/2/2011	28.586	0.000	0.00	1.209	64.3	0.000	0.002	0.049	27.527	17.709	19.64	28.7	0.563	179.2	0.561	0.147	68.577	1.774
5/3/2011	16.861	0.000	0.00	1.189	22.0	0.000	0.003	0.113	4.874	15.652	6.37	5.1	0.627	7.7	0.398	0.462	36.632	4.149
5/4/2011	23.874	0.000	0.00	1.969	69.6	0.026	0.006	0.159	3.285	25.436	15.66	9.7	0.996	12.3	0.036	1.446	53.672	3.546
5/5/2011	35.15	0.000	0.00	2.95	112.0	0.0342	0.0457	0.254	5.886	49.82	18.20	12.9	2.594	18.2	0.509	0.873	83.22	8.71
5/24/2011	101.01	0.000	0.00	4.77	356.9	0.0944	0.0783	0.379	7.318	84.09	157.52	73.6	3.990	409.4	1.271	1.732	181.59	17.39

Table A1.6 Correlations of metal data with the initial radicals/g, fast decay, and slow decay.

	Al	**As**	**Ba**	**Ca**	**Cd**	**Co**	**Cr**	**Cu**	**Fe**	**K**	**Mg**	**Mn**	**Na**	**Ni**	**Pb**	**Si**	**Zn**
Initial radicals/g	-0.214	0.183	0.068	-0.081	0.054	-0.195	0.153	0.162	-0.239	-0.219	-0.309	-0.008	-0.372	-0.168	0.071	-0.259	-0.072
# samples	24	7	24	24	14	22	23	24	24	24	24	24	22	24	24	22	23
fast decay	-0.077	0.797	-0.069	-0.104	0.015	-0.271	-0.178	0.086	-0.096	-0.207	-0.161	-0.099	-0.246	0.008	0.028	-0.192	0.073
# samples	16	5	16	16	10	15	16	16	16	16	16	16	15	16	16	15	16
slow decay	0.064	0.628	-0.065	-0.005	-0.466	0.129	-0.186	-0.184	0.020	-0.072	0.051	-0.025	-0.012	0.042	-0.156	0.019	0.067
# samples	15	5	15	15	10	14	15	15	15	15	15	15	14	15	15	14	15
Range of metal (ppm)	10.94-499.89	0.050-0.212	1.02-9.86	13.8-541	0.006-0.094	0.002-0.078	0.061-0.379	0.596-27.53	9.79-253.04	6.37-157.52	5.1-142.44	0.29-6.45	7.7-609.3	0.036-1.271	0.147-3.54	30.42-874.227	1.77-17.61

Correlation with the slow and fast decay rates also exhibited weak or no correlations except for a strong negative correlation of Cd with the slow decay rate. This suggests the presence of organics bound to Cd lengthen the slow decay rate.

A1.3 Meteorological and Atmospheric Pollutant Correlations

Correlations of meteorological conditions and other pollutant information were performed from data obtained at the same DEQ ambient monitoring station as the sampler with the exception of solar and UV radiation data which came from a monitoring station one mile away, Table A1.7. This data was averaged over the 24 hours for which the samples were

Table A1.7 Pearson correlations of meteorological data with initial radicals/g, fast decay, and slow decay for samples collected between 7/12/09 to 8/31/09

	Solar radiation	**UV Radiation**	**Temperature**	**% Relative Humidity**	**SO_2**	**Total Hydrocarbons**
Initial radicals/g	0.139	0.119	-0.001	-0.198	-0.047	0.131
# Samples	46	46	46	46	46	46
Fast Decay	-0.446	-0.417	-0.454	0.448	-0.235	-0.169
# Samples	39	39	39	39	39	39
Slow Decay	0.113	0.134	-0.170	-0.003	-0.060	-0.062
# Samples	37	37	37	37	37	37

	Ozone	**NO**	**NO_2**	**NO_x**	**Methane**	**Non-methane organic carbon**
Initial radicals/g	0.278	0.223	0.191	0.236	0.156	0.039
# Samples	41	42	42	42	46	46
Fast Decay	-0.103	0.042	-0.072	-0.067	-0.200	0.000
# Samples	35	36	36	36	39	39
Slow Decay	-0.040	0.237	0.148	0.228	-0.033	-0.099
# Samples	33	34	34	34	37	37

collected (9AM to 9AM), Table A1.8, and used to correlate samples collected from 7/12/09 to 8/31/09 to determine if the collected conditions had any bearing on the radical properties.

The strongest correlation for the initial radical concentration resulted from ozone suggesting the importance of photochemical processes for EPFR formation in the atmosphere and supported by positive correlations with both solar and UV radiation. NO_x, NO, and NO_2 demonstrated positive correlations suggesting formation of EPFRs while $PM_{2.5}$ is suspended in the atmosphere. Methane and total hydrocarbons had weaker positive correlations yet significant when compared to the non-methane organic carbon. This is surprising and it was expected for the non-methane organic carbon to have a significant positive correlation as previous research has demonstrated non-methane organic carbon compounds form EPFRs when bound to a transition metal [1-4]. The only significant negative correlation observed was with relative humidity.

The correlation of the fast decay with relative humidity displayed the largest positive correlation. The correlations with the fast decay indicate the presence of ozone as well as solar and UV radiation to decrease the fast decay rate. Since the previous set of correlations demonstrated the ability of all three to increase radical concentration, their presence would also slow down the fast decay rate as they are forming new radicals. This explanation can also be applied with the negative correlations seen with NO_2 and NO_x. There were significant negative correlations with SO_2, methane, and total hydrocarbons.

The correlations with the slow decay are the weakest overall and less clear. The negative correlations from SO_2, non-methane organic carbon, and total hydrocarbons suggest these to decrease the slow decay rate but very subtly. Correlations with solar/UV radiation, NO, NO_2, and NO_x all demonstrate an increase the slow decay rate in complete contrast to the other correlations. This appears to advocate other pathways for the slow decay.

Table A1.8 Averaged meteorological and pollutant data for listed collection dates from 9AM to 9AM the following day.

Date	Solar (W/M^2)	UV (W/M^2)	Temp (°C)	RH (%)	SO_2 (ppb)	THC (ppm)	Ozone (ppb)	NO (ppb)	NO_2 (ppb)	NO_X (ppb)	Methane (ppmc)	NMOC (PPMC)
7/12/2009	238.17	12.08	25.46	86.04	0.10	2.34	32.43	3.13	8.21	10.29	2.25	0.10
7/13/2009	316.29	15.79	25.50	76.13	0.10	2.24	30.22	3.46	7.46	9.79	2.17	0.08
7/14/2009	220.67	11.83	23.79	77.46	0.13	2.32	23.00	4.13	15.21	17.83	2.18	0.15
7/15/2009	227.71	11.79	23.38	88.13	0.14	2.15	21.13	2.21	5.54	6.88	2.09	0.07
7/16/2009	212.58	11.67	22.96	86.42	0.10	2.23	14.79	3.25	9.21	11.25	2.11	0.14
7/17/2009	105.92	5.96	23.00	94.46	0.11	2.08	36.29	1.24	6.19	6.76	1.99	0.10
7/20/2009	287.54	15.17	24.50	70.67	0.93	2.10	36.08	2.36	7.45	8.73	2.06	0.05
7/21/2009	210.88	11.88	23.50	77.00	0.15	1.93	16.50	3.88	11.08	13.71	1.88	0.06
7/22/2009	110.29	6.13	23.83	89.29	0.20	1.37	24.67	3.96	14.79	17.21	1.37	0.02
7/23/2009	228.17	12.08	23.21	79.13	2.30	2.75	31.67	7.08	18.25	23.63	2.56	0.21
7/24/2009	314.29	15.79	22.63	64.50	1.97	2.13	42.33	1.64	6.41	7.05	2.06	0.09
7/25/2009	313.46	15.63	23.00	65.08	0.67	2.17	20.61	2.54	7.50	9.21	2.09	0.09
7/26/2009	217.13	11.29	23.38	83.46	0.34	2.19	13.79	3.63	9.38	11.92	2.09	0.11
7/27/2009	186.13	9.96	23.33	89.71	0.38	2.12	10.21	4.05	6.41	9.64	2.05	0.08
7/28/2009	169.04	9.46	23.29	86.67	0.40	2.10	11.50	3.46	5.38	8.04	2.03	0.08
7/29/2009	273.50	13.88	23.96	80.50	0.23	2.10	*	*	*	*	2.04	0.08
7/30/2009	200.54	10.88	26.79	85.71	0.30	2.05	*	*	*	*	1.97	0.09
7/31/2009	260.17	13.54	27.38	81.17	0.29	1.93	*	*	*	*	1.90	0.05
8/1/2009	257.79	13.29	27.25	77.96	0.29	2.22	*	*	*	*	2.13	0.10
8/2/2009	128.17	7.04	27.46	88.38	0.33	1.96	*	1.78	6.67	6.67	1.89	0.08
8/4/2009	274.13	13.96	25.92	73.67	0.48	2.18	17.17	3.08	11.00	13.50	2.04	0.15
8/5/2009	254.67	12.58	26.00	75.42	0.73	2.23	19.25	6.79	10.71	17.04	2.08	0.17
8/6/2009	269.88	13.29	25.88	81.96	0.17	2.22	47.46	0.38	10.83	10.75	2.09	0.14
8/7/2009	240.17	11.79	26.08	73.63	0.15	2.04	28.50	0.77	6.18	6.59	1.97	0.08
8/9/2009	213.75	11.04	26.17	89.75	0.12	2.29	16.39	2.83	8.83	11.21	1.89	0.24
8/8/2009	281.38	14.25	25.92	80.04	0.18	2.09	20.75	3.79	10.50	13.92	2.03	0.07
8/11/2009	232.79	11.92	26.21	81.17	0.14	2.03	33.78	1.00	8.71	9.42	1.98	0.06
8/12/2009	272.50	13.29	25.96	78.08	0.49	2.12	33.88	0.71	9.75	9.96	2.08	0.05
8/13/2009	215.13	11.08	25.96	75.21	0.16	2.12	33.25	1.29	10.75	11.58	2.03	0.10
8/15/2009	238.33	12.04	26.33	79.46	0.10	2.06	19.87	2.96	10.21	12.63	2.03	0.05
8/16/2009	170.96	8.79	26.57	86.63	0.10	2.02	20.22	2.65	8.96	11.30	1.97	0.06
8/17/2009	158.21	8.08	27.08	84.29	0.11	2.03	14.29	4.05	9.71	13.52	1.96	0.09
8/18/2009	186.50	9.54	26.67	84.46	0.18	2.07	17.57	2.79	8.17	10.58	2.00	0.07
8/19/2009	199.04	10.38	27.00	80.83	0.12	2.10	5.71	5.86	9.90	15.29	2.00	0.11
8/21/2009	102.33	5.58	26.75	92.92	0.15	2.03	31.13	1.18	8.64	9.27	1.96	0.08
8/22/2009	297.04	13.79	26.79	63.71	4.24	1.98	29.17	1.79	8.13	9.46	1.94	0.06
8/23/2009	301.54	14.21	26.54	59.71	0.60	2.01	29.25	2.29	9.71	11.42	1.95	0.07
8/24/2009	298.42	14.00	26.63	62.04	0.44	2.22	49.75	4.59	13.41	17.55	2.12	0.11
8/25/2009	265.13	12.13	25.92	65.88	2.83	2.30	48.61	5.95	14.45	19.73	2.18	0.14
8/26/2009	247.29	11.04	25.63	67.96	2.26	2.21	41.83	1.00	10.29	10.71	2.10	0.12
8/27/2009	253.67	11.67	26.42	65.83	1.21	2.35	30.58	2.67	14.25	16.25	2.23	0.14
8/28/2009	181.75	9.00	26.71	80.96	0.47	2.06	34.67	1.33	6.48	7.52	1.97	0.09
8/29/2009	215.42	10.88	26.63	80.46	0.31	1.95	34.74	1.21	5.79	6.50	1.92	0.05
8/30/2009	242.13	11.67	26.79	76.54	1.35	1.93	33.29	1.17	6.33	6.96	1.90	0.05
8/31/2009	208.83	10.46	26.67	65.63	0.52	1.96	38.25	1.23	9.09	9.77	1.91	0.06

***** no average was performed due to missing data points for that day
Solar is total solar radiation
UV is only UV radiation
RH is relative humidity
THC is total hydrocarbons
NMOC is nonmethane organic carbon

A1.4 References

1. Vejerano, E., S. Lomnicki, and B. Dellinger, *Formation and Stabilization of Combustion-Generated Environmentally Persistent Free Radicals on an Fe(III)2O3/Silica Surface.* Environ. Sci. Technol., 2011. **45**: p. 589-594.

2. Vejerano, E., S. Lomnicki, and B. Dellinger, *Lifetime of combustion-generated environmentally persistent free radicals on Zn(II)O and other transition metal oxides.* J. Environ. Monit., 2012. **14**: p. 2803-2806.

3. Lomnicki, S., et al., *Copper Oxide-Based Model of Persistent Free Radical Formation on Combustion-Derived Particulate Matter.* Environ. Sci. Technol., 2008. **42**: p. 4982-4988.

4. Vejerano, E., S.M. Lomnicki, and B. Dellinger, *Formation and Stabilization of Combustion-Generated, Environmentally Persistent Radicals on Ni(II)O Supported on a Silica Surface.* Environ. Sci. Technol., 2012. **46**: p. 9406-9411.

APPENDIX 2. SUPPORTING INFORMATION FOR HYDROXYL RADICAL GENERATION FROM EPFRs IN $PM_{2.5}$

A2.1 Chelex Treatment of $PM_{2.5}$ Samples

In an attempt to more closely match previous studies[1-4], Chelex was utilized for elimination of any trace metals present in the ultrahigh purity (UP) H_2O. The manufacturer batch method for preparation was adjusted to accommodate the smaller volume employed. This involved adding approximately 1.3 g of Chelex resin to 10 mL PBS solution and mixing rigorously for 1 hour. The PBS solutions with resin were left overnight before use and filtered from solution using a Fisherbrand P5 filter paper.

After multiple attempts, the Chelex treatment did not reduce the DMPO-OH signal as expected[2-6]. Instead, the DMPO-OH signals increased by an average of 140%. Similar phenomena was previously observed suggesting another pathway where Chelex participates in the reaction[1]. To avoid any extra confounding factors, Chelex was not used in this study.

A2.2 Effect of Chelating Agents

Using a 0.1 mM solution of DFO corresponded to a 72% reduction of the DMPO-OH signal from the $PM_{2.5}$ suspension and this suggests an important role for Fe in the catalysis of H_2O_2 to $^{\bullet}OH$. Previous studies, regardless of assay type, had conflicting results from DFO. Some reports observed a substantial or nearly complete elimination of the ROS signal[7-9]. These studies used samples stored for long periods of time (from months to years) or were completely relying on the generation of $^{\bullet}OH$ from H_2O_2. Therefore, these investigations were biased in favor of DFO to completely eliminate the signal by metal complexation.

Other reports only reduced the signal suggesting other pathways[10-15]. Recognizing DFO is very selective towards iron leaves the possibility of the other redox metals in the $PM_{2.5}$ to catalyze an exogenous Fenton reaction. Although the amount of the other redox active metals is minor when compared to iron, they are still present on the surface to catalyze the exogenous Fenton reaction.

Accompanying the complexation of metals, DFO was observed to scavenge the tetrachlorosemiquinone anion radical[16]. Such elimination would suggest a role in scavenging for other semiquinone type radicals. Either from metal complexation or eliminating the semiquinone radicals, the addition of DFO reduced the adduct intensity in these experiments.

DETAPAC exhibited unpredictable behavior in $PM_{2.5}$ solutions. Particularly, using DETAPAC in this work reduced the $^{\bullet}OH$ signal intensity by 53% while, in contrast, a previous study exhibited a higher $^{\bullet}OH$ signal[17].

Based on these observations, the above reagents were not included in the spin trapping experiments for $PM_{2.5}$. Instead, a comparative method[18, 19], where the same sample was utilized under different conditions (air vs. N_2 purging, fresh vs. aged), was chosen to monitor the $^{\bullet}OH$ generating capacity of ambient $PM_{2.5}$ particles collected from Louisiana industrial corridor.

A2.3 Metal Dependence

Previous studies report a metal association for ROS generation in PM, such as As[20], Ba[21], Cd[20], Co[5, 6, 22], Cr[6, 21, 22], Cu[9, 15, 21-27], Fe[5-7, 22-25, 28, 29], Mn[6, 22, 30], Ni[5, 20], V[20, 30], Zn[23, 30, 31], and Zr[21]. Most of the studies listed above included the presence of reducing agents or H_2O_2 thereby favoring the metal mediated generation of $^{\bullet}OH$. In addition to total metals, correlations suggested associations with soluble Fe[7, 8, 31, 32]. Soluble transition metals from PM are suggested important due to their bioavailability[3, 6, 14, 30]. The soluble Fe oxidation state in $PM_{2.5}$ also displayed no significant changes over 40 days[33]. However, particle bound transition metals (or the particle itself) also demonstrated increased ROS generation when compared to the soluble metals present[26, 34].

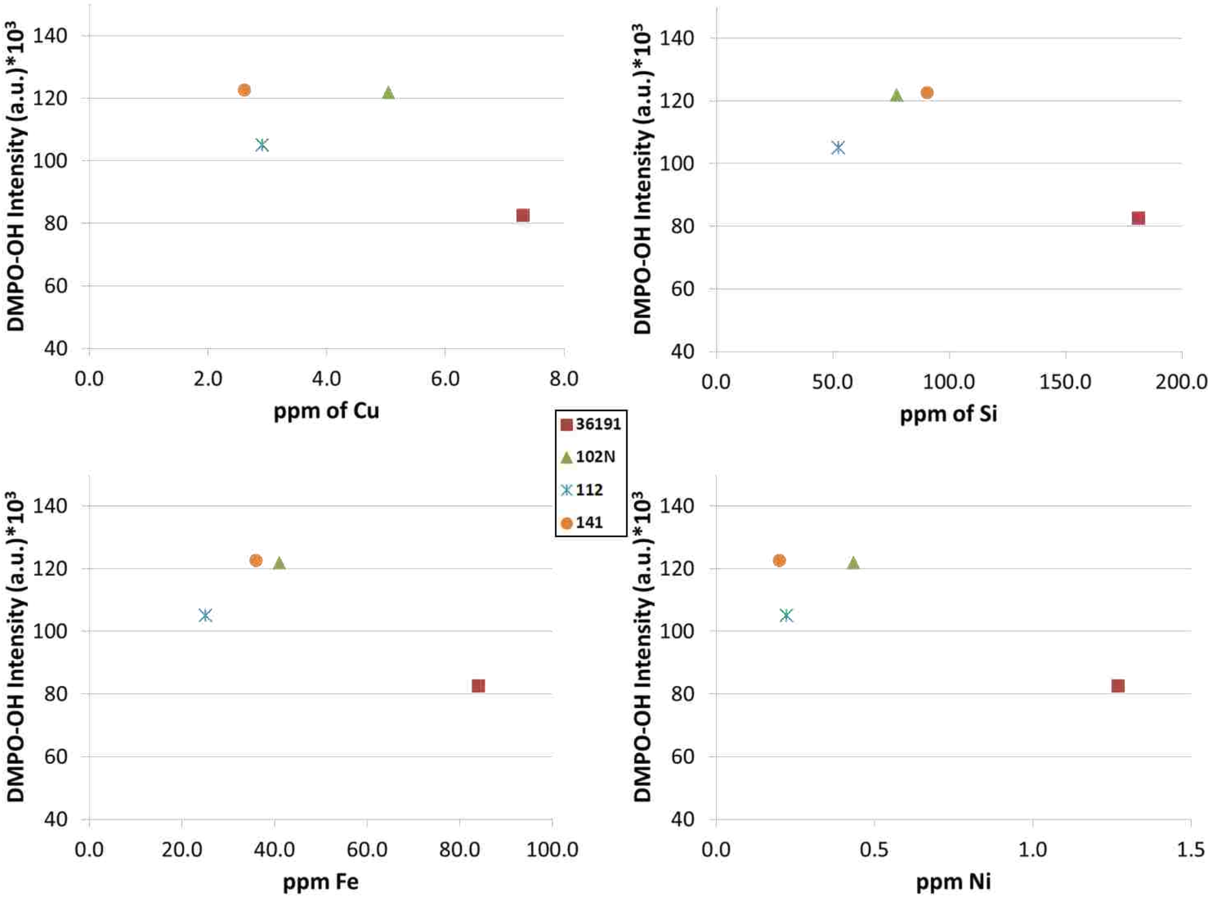

Figure A2.1 Demonstration of no correlation between DMPO-OH intensity and metal concentration from some "active" samples (the metals are shown on the graph).

Straightforward dependencies between metal content and DMPO-OH concentration were not observed in this study; although, only the total metals from a nitric acid digestion were studied. There was no investigation into the soluble metals. Using only the "active" samples, there was no correlation between the DMPO-OH intensity and individual, Figure S1, or total metals (not presented but similar behavior as Figure S1). When applying the "passive" samples as well, there were still no correlations from the metals data (data not shown).

A2.4 References

1. Li, B.; Blough, N. V.; Gutierrez, P. L., *Trace detection of hydroxyl radicals during the redox cycling of low concentrations of diaziquone: a new approach.* Free Radical Biol. Med., 2000. **29**: p. 548-556.

2. Vidrio, E.; Jung, H.; Anastasio, C., *Generation of hydroxyl radicals from dissolved transition metals in surrogate lung fluid solutions.* Atmospheric Environment, 2008. **42** (18): p. 4369-4379.

3. DiStefano, E.; Eiguren-Fernandez, A.; Delfino, R. J.; Sioutas, C.; Froines, J. R.; Cho, A. K., *Determination of metal-based hydroxyl radical generating capacity of ambient and diesel exhaust particles.* Inhalation Toxicology, 2009. **21** (8-11): p. 731-738.

4. Shen, H.; Anastasio, C., *A comparison of hydroxyl radical and hydrogen peroxide generation in ambient particle extracts and laboratory metal solutions.* Atmospheric Environment, 2012. **46** (0): p. 665-668.

5. Shafer, M. M.; Perkins, D. A.; Antkiewicz, D. S.; Stone, E. A.; Quraishi, T. A.; Schauer, J. J., *Reactive oxygen species activity and chemical speciation of size-fractionated atmospheric particulate matter from Lahore, Pakistan: an important role for transition metals.* Journal of Environmental Monitoring, 2010. **12** (3): p. 704-715.

6. Verma, V.; Shafer, M. M.; Schauer, J. J.; Sioutas, C., *Contribution of transition metals in the reactive oxygen species activity of PM emissions from retrofitted heavy-duty vehicles.* Atmospheric Environment, 2010. **44** (39): p. 5165-5173.

7. Valavanidis, A.; Salika, A.; Theodoropoulou, A., *Generation of hydroxyl radicals by urban suspended particulate air matter. The role of iron ions.* Atmospheric Environment, 2000. **34** (15): p. 2379-2386.

8. Valavanidis, A.; Fiotakis, K.; Vlachogianni, T., *The Role of Stable Free Radicals, Metals and PAHs of Airborne Particulate Matter in Mechanisms of Oxidative Stress and Carcinogenicity*, in *Urban Airborne Particulate Matter*, F. Zereini and C.L.S. Wiseman, Editors. 2011, Springer Berlin Heidelberg. p. 411-426.

9. Shen, H.; Anastasio, C., *Formation of hydroxyl radical from San Joaquin Valley particles extracted in a cell-free surrogate lung fluid.* Atmos. Chem. Phys., 2011. **11** (18): p. 9671-9682.

10. Donaldson, K.; Brown, D. M.; Mitchell, C.; Dineva, M.; Beswick, P. H.; Gilmour, P.; MacNee, W., *Free radical activity of PM10: iron-mediated generation of hydroxyl radicals.* Environ Health Perspect, 1997. **105 Suppl 5**: p. 1285-9.

11. Eiguren-Fernandez, A.; Shinyashiki, M.; Schmitz, D. A.; DiStefano, E.; Hinds, W.; Kumagai, Y.; Cho, A. K.; Froines, J. R., *Redox and electrophilic properties of vapor- and*

particle-phase components of ambient aerosols. Environmental Research, 2010. **110** (3): p. 207-212.

12. Frikke-Schmidt, H.; Roursgaard, M.; Lykkesfeldt, J.; Loft, S.; Nojgaard, J. K.; Moller, P., *Effect of vitamin C and iron chelation on diesel exhaust particle and carbon black induced oxidative damage and cell adhesion molecule expression in human endothelial cells.* Toxicol Lett, 2011. **203** (3): p. 181-9.

13. Jung, H.; Guo, B.; Anastasio, C.; Kennedy, I. M., *Quantitative measurements of the generation of hydroxyl radicals by soot particles in a surrogate lung fluid.* Atmospheric Environment, 2006. **40** (6): p. 1043-1052.

14. Antonini, J. M.; Taylor, M. D.; Leonard, S. S.; Lawryk, N. J.; Shi, X.; Clarke, R. W.; Roberts, J. R., *Metal composition and solubility determine lung toxicity induced by residual oil fly ash collected from different sites within a power plant.* Mol. Cell. Biochem., 2004. **255**: p. 257-265.

15. Briede, J. J.; De Kok, T.; Hogervorst, J. G. F.; Moonen, E. J. C.; Den Camp, C.; Kleinjans, J. C. S., *Development and application of an electron spin resonance spectrometry method for the determination of oxygen free radical formation by particulate matter.* Environmental Science & Technology, 2005. **39** (21): p. 8420-8426.

16. Zhu, B.-Z.; Zhao, H.-T.; Kalyanaraman, B.; Frei, B., *Metal-independent production of hydroxyl radicals by halogenated quinones and hydrogen peroxide: an ESR spin trapping study.* Free Radical Biology and Medicine, 2002. **32** (5): p. 465-473.

17. Burkitt, M.J., *Esr Spin Trapping Studies Into of Nature of the Oxidizing Species Formed in the Fenton Reaction: Pitfalls Associated With of Use Of 5,5-Dimethyl-1-Pyrroline-n-Oxide in the Detection of the Hydroxyl Radical.* Free Radical Research, 1993. **18** (1): p. 43-57.

18. Khachatryan, L.; Vejerano, E.; Lomnicki, S.; Dellinger, B., *Environmentally Persistent Free Radicals (EPFRs). 1. Generation of Reactive Oxygen Species in Aqueous Solutions.* Environmental Science & Technology, 2011. **45** (19): p. 8559-66.

19. Khachatryan, L.; Dellinger, B., *Environmentally Persistent Free Radicals (EPFRs)-2. Are Free Hydroxyl Radicals Generated in Aqueous Solutions?* Environmental Science & Technology, 2011. **45** (21): p. 9232-9239.

20. Verma, V.; Ning, Z.; Cho, A. K.; Schauer, J. J.; Shafer, M. M.; Sioutas, C., *Redox activity of urban quasi-ultrafine particles from primary and secondary sources.* Atmospheric Environment, 2009. **43** (40): p. 6360-6368.

21. Ntziachristos, L.; Froines, J. R.; Cho, A. K.; Sioutas, C., *Relationship between redox activity and chemical speciation of size-fractionated particulate matter.* Particle and fibre toxicology, 2007. **4**: p. 5.

22. Baulig, A.; Poirault, J. J.; Ausset, P.; Schins, R.; Shi, T.; Baralle, D.; Dorlhene, P.; Meyer, M.; Lefevre, R.; Baeza-Squiban, A.; Marano, F., *Physicochemical characteristics and biological activities of seasonal atmospheric particulate matter sampling in two locations of Paris.* Environ Sci Technol, 2004. **38** (22): p. 5985-92.

23. Kunzli, N.; Mudway, I. S.; Gotschi, T.; Shi, T.; Kelly, F. J.; Cook, S.; Burney, P.; Forsberg, B.; Gauderman, J. W.; Hazenkamp, M. E.; Heinrich, J.; Jarvis, D.; Norback, D.; Payo-Losa, F.; Poli, A.; Sunyer, J.; Borm, P. J., *Comparison of oxidative properties, light absorbance, total and elemental mass concentration of ambient PM2.5 collected at 20 European sites.* Environ Health Perspect, 2006. **114** (5): p. 684-90.

24. Vidrio, E.; Phuah, C. H.; Dillner, A. M.; Anastasio, C., *Generation of Hydroxyl Radicals from Ambient Fine Particles in a Surrogate Lung Fluid Solution.* Environmental Science & Technology, 2009. **43** (3): p. 922-927.

25. Wang, Y.; Arellanes, C.; Curtis, D. B.; Paulson, S. E., *Probing the source of hydrogen peroxide associated with coarse mode aerosol particles in southern California.* Environ Sci Technol, 2010. **44** (11): p. 4070-5.

26. Shi, T. M.; Schins, R. P. F.; Knaapen, A. M.; Kuhlbusch, T.; Pitz, M.; Heinrich, J.; Borm, P. J. A., *Hydroxyl radical generation by electron paramagnetic resonance as a new method to monitor ambient particulate matter composition.* Journal of Environmental Monitoring, 2003. **5** (4): p. 550-556.

27. Shi, T.; Knaapen, A. M.; Begerow, J.; Birmili, W.; Borm, P. J. A.; Schins, R. P. F., *Temporal variation of hydroxyl radical generation and 8-hydroxy-2'-deoxyguanosine formation by coarse and fine particulate matter.* Occup. Environ. Med., 2003. **60**: p. 315-321.

28. Jeng, H.A., *Chemical composition of ambient particulate matter and redox activity.* Environmental Monitoring and Assessment, 2010. **169** (1-4): p. 597-606.

29. Park, S.; Nam, H.; Chung, N.; Park, J. D.; Lim, Y., *The role of iron in reactive oxygen species generation from diesel exhaust particles.* Toxicology in Vitro, 2006. **20** (6): p. 851-857.

30. See, S. W.; Wang, Y. H.; Balasubramanian, R., *Contrasting reactive oxygen species and transition metal concentrations in combustion aerosols.* Environmental Research, 2007. **103** (3): p. 317-324.

31. Cheung, K. L.; Ntziachristos, L.; Tzamkiozis, T.; Schauer, J. J.; Samaras, Z.; Moore, K. F.; Sioutas, C., *Emissions of Particulate Trace Elements, Metals and Organic Species from Gasoline, Diesel, and Biodiesel Passenger Vehicles and Their Relation to Oxidative Potential.* Aerosol Science and Technology, 2010. **44** (7): p. 500-513.

32. Valavanidis, A.; Fiotakis, K.; Bakeas, E.; Vlahogianni, T., *Electron paramagnetic resonance study of the generation of reactive oxygen species catalysed by transition metals and quinoid redox cycling by inhalable ambient particulate matter.* Redox Report, 2005. **10** (1): p. 37-51.

33. Majestic, B. J.; Schauer, J. J.; Shafer, M. M., *Application of synchrotron radiation for measurement of iron red-ox speciation in atmospherically processed aerosols.* Atmos. Chem. Phys., 2007. **7**: p. 2475-2487.

34. Daher, N.; Ning, Z.; Cho, A. K.; Shafer, M.; Schauer, J. J.; Sioutas, C., *Comparison of the Chemical and Oxidative Characteristics of Particulate Matter (PM) Collected by Different Methods: Filters, Impactors, and BioSamplers.* Aerosol Science and Technology, 2011. **45** (11): p. 1294-1304.

APPENDIX 3. AMERICAN CHEMICAL SOCIETY'S POLICY ON THESES AND DISSERTATIONS (FORM)

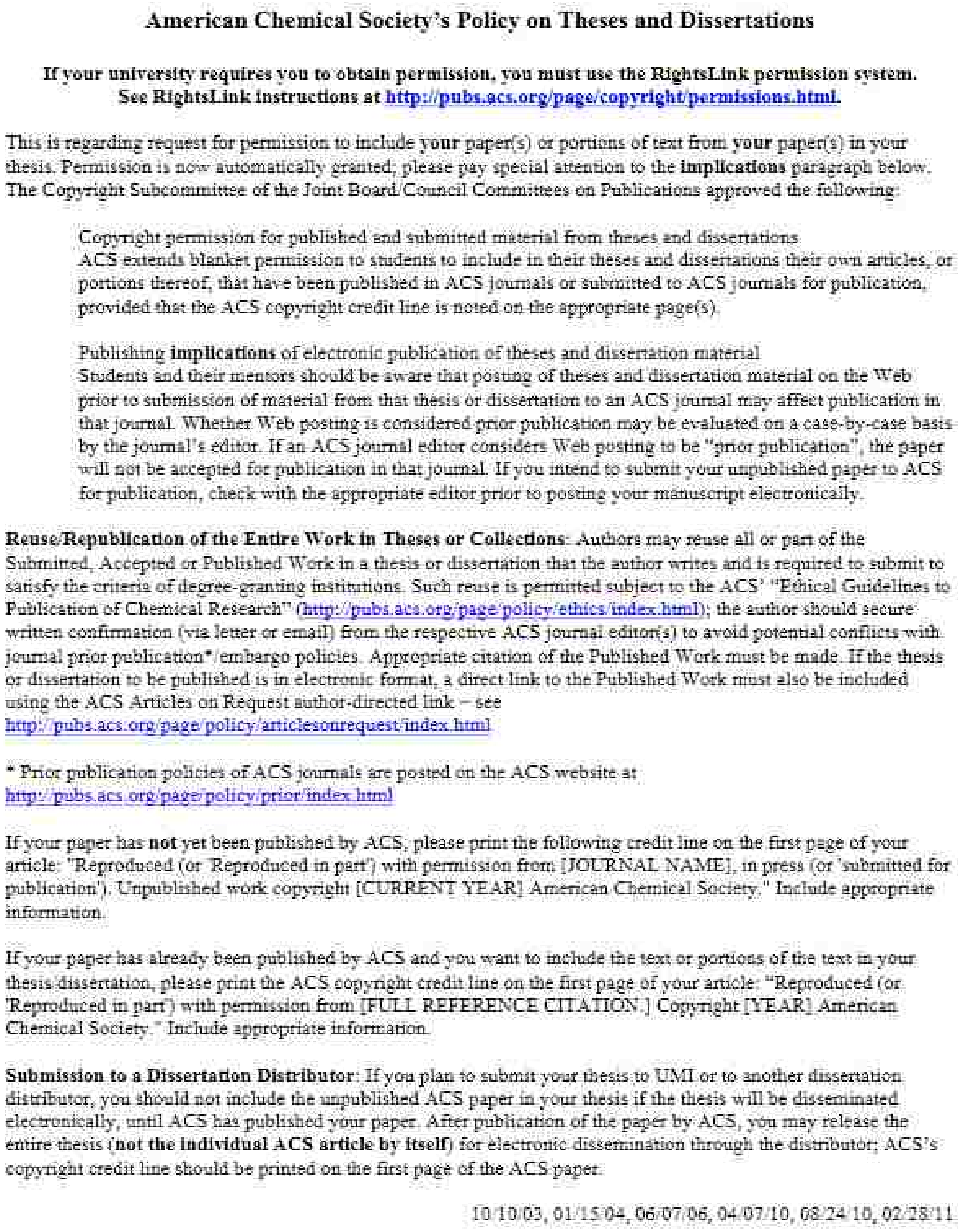

American Chemical Society's Policy on Theses and Dissertations

If your university requires you to obtain permission, you must use the RightsLink permission system. See RightsLink instructions at http://pubs.acs.org/page/copyright/permissions.html.

This is regarding request for permission to include **your** paper(s) or portions of text from **your** paper(s) in your thesis. Permission is now automatically granted; please pay special attention to the **implications** paragraph below. The Copyright Subcommittee of the Joint Board/Council Committees on Publications approved the following:

> Copyright permission for published and submitted material from theses and dissertations
> ACS extends blanket permission to students to include in their theses and dissertations their own articles, or portions thereof, that have been published in ACS journals or submitted to ACS journals for publication, provided that the ACS copyright credit line is noted on the appropriate page(s).
>
> Publishing **implications** of electronic publication of theses and dissertation material
> Students and their mentors should be aware that posting of theses and dissertation material on the Web prior to submission of material from that thesis or dissertation to an ACS journal may affect publication in that journal. Whether Web posting is considered prior publication may be evaluated on a case-by-case basis by the journal's editor. If an ACS journal editor considers Web posting to be "prior publication", the paper will not be accepted for publication in that journal. If you intend to submit your unpublished paper to ACS for publication, check with the appropriate editor prior to posting your manuscript electronically.

Reuse/Republication of the Entire Work in Theses or Collections: Authors may reuse all or part of the Submitted, Accepted or Published Work in a thesis or dissertation that the author writes and is required to submit to satisfy the criteria of degree-granting institutions. Such reuse is permitted subject to the ACS' "Ethical Guidelines to Publication of Chemical Research" (http://pubs.acs.org/page/policy/ethics/index.html); the author should secure written confirmation (via letter or email) from the respective ACS journal editor(s) to avoid potential conflicts with journal prior publication*/embargo policies. Appropriate citation of the Published Work must be made. If the thesis or dissertation to be published is in electronic format, a direct link to the Published Work must also be included using the ACS Articles on Request author-directed link – see
http://pubs.acs.org/page/policy/articlesonrequest/index.html

* Prior publication policies of ACS journals are posted on the ACS website at
http://pubs.acs.org/page/policy/prior/index.html

If your paper has **not** yet been published by ACS, please print the following credit line on the first page of your article: "Reproduced (or 'Reproduced in part') with permission from [JOURNAL NAME], in press (or 'submitted for publication'). Unpublished work copyright [CURRENT YEAR] American Chemical Society." Include appropriate information.

If your paper has already been published by ACS and you want to include the text or portions of the text in your thesis/dissertation, please print the ACS copyright credit line on the first page of your article: "Reproduced (or 'Reproduced in part') with permission from [FULL REFERENCE CITATION.] Copyright [YEAR] American Chemical Society." Include appropriate information.

Submission to a Dissertation Distributor: If you plan to submit your thesis to UMI or to another dissertation distributor, you should not include the unpublished ACS paper in your thesis if the thesis will be disseminated electronically, until ACS has published your paper. After publication of the paper by ACS, you may release the entire thesis (**not the individual ACS article by itself**) for electronic dissemination through the distributor; ACS's copyright credit line should be printed on the first page of the ACS paper.

10/10/03, 01/15/04, 06/07/06, 04/07/10, 08/24/10, 02/28/11

APPENDIX 4. COPYRIGHTS PERMISSION FORMS

Environ Health Perspect. 2006 June; 114(6): 810–817.
PMCID: PMC1480527
Published online 2006 January 25. doi: 10.1289/ehp.8629
Commentaries & Reviews

Origin and Health Impacts of Emissions of Toxic By-Products and Fine Particles from Combustion and Thermal Treatment of Hazardous Wastes and Materials

Stephanie A. Cormier,[1] Slawo Lomnicki,[2] Wayne Backes,[3] and Barry Dellinger[2]

Author information ► Article notes ► Copyright and License information ▼

This article has been cited by other articles in PMC.

Abstract

High-temperature, controlled incineration and thermal treatment of contaminated soils, sediments, and wastes at Superfund sites are often preferred methods of remediation of contaminated sites under the and related legislation. Although these methods may be executed safely, formation of toxic combustion or reaction by-products is still a cause of concern. Emissions of polycyclic aromatic hydrocarbons (PAHs); chlorinated hydrocarbons (CHCs), including polychlorinated dibenzo-p-dioxins and dibenzofurans; and toxic metals (e.g., chromium VI) have historically been the focus of combustion and health effects research. However, fine particulate matter (PM) and ultrafine PM, which have been documented to be related to cardiovascular disease, pulmonary disease, and cancer, have more recently become the focus of research. Fine PM and ultrafine PM are effective delivery agents for PAHs, CHCs, and toxic metals. In addition, it has recently been realized that brominated hydrocarbons (including brominated/chlorinated dioxins), redox-active metals, and redox-active persistent free radicals are also associated with PM emissions from combustion and thermal processes. In this article, we discuss the origin of each of these classes of pollutants, the nature of their association with combustion-generated PM, and the mechanisms of their known and potential health impacts.

Keywords: cardiovascular health, environmental health, fine and ultrafine particulate matter, persistent free radicals, respiratory health, thermal remediation

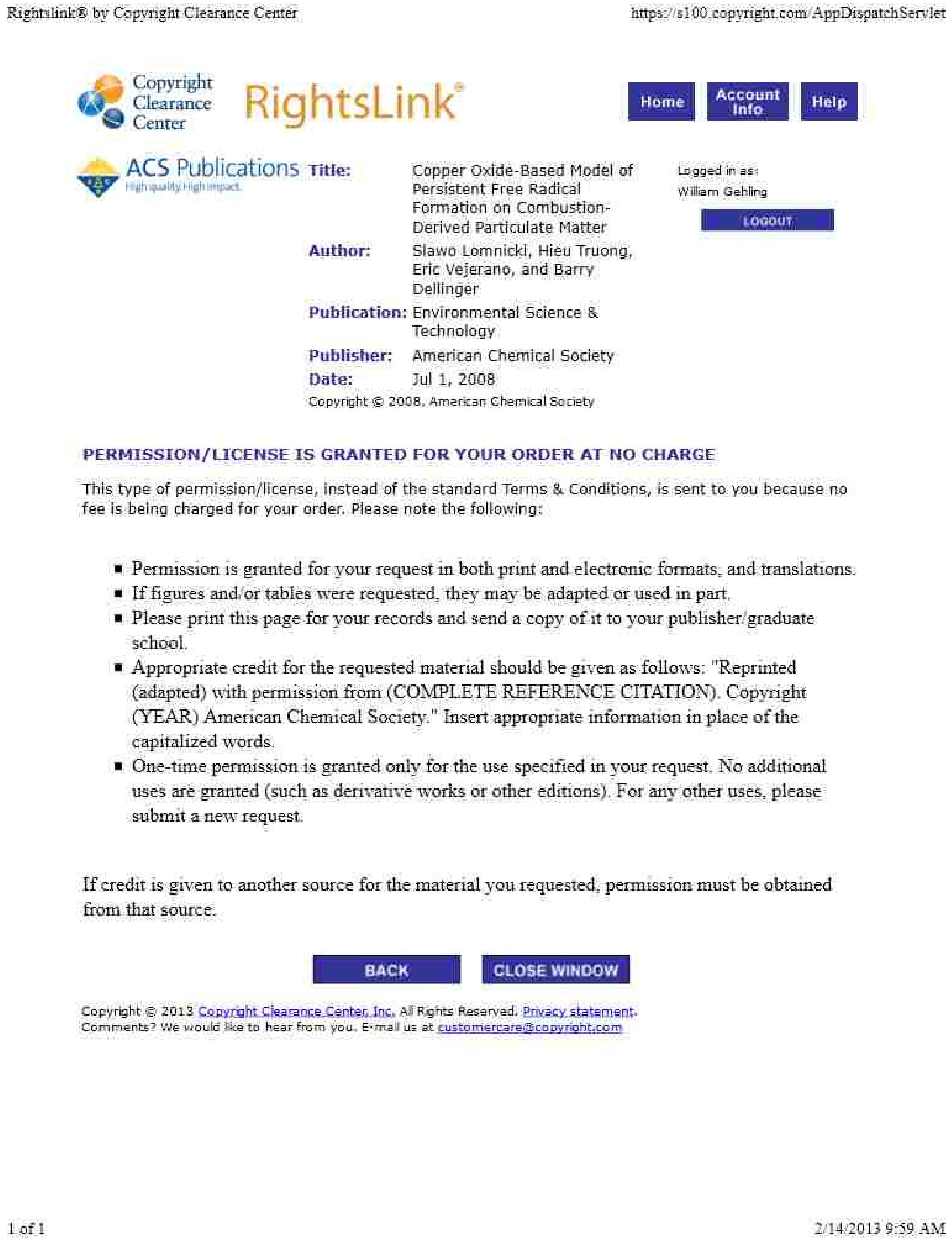

Rightslink® by Copyright Clearance Center https://s100.copyright.com/AppDispatchServlet

Copyright Clearance Center RightsLink®

ACS Publications
High quality. High impact.

Title:	Copper Oxide-Based Model of Persistent Free Radical Formation on Combustion-Derived Particulate Matter
Author:	Slawo Lomnicki, Hieu Truong, Eric Vejerano, and Barry Dellinger
Publication:	Environmental Science & Technology
Publisher:	American Chemical Society
Date:	Jul 1, 2008

Copyright © 2008, American Chemical Society

Logged in as:
William Gehling

PERMISSION/LICENSE IS GRANTED FOR YOUR ORDER AT NO CHARGE

This type of permission/license, instead of the standard Terms & Conditions, is sent to you because no fee is being charged for your order. Please note the following:

- Permission is granted for your request in both print and electronic formats, and translations.
- If figures and/or tables were requested, they may be adapted or used in part.
- Please print this page for your records and send a copy of it to your publisher/graduate school.
- Appropriate credit for the requested material should be given as follows: "Reprinted (adapted) with permission from (COMPLETE REFERENCE CITATION). Copyright (YEAR) American Chemical Society." Insert appropriate information in place of the capitalized words.
- One-time permission is granted only for the use specified in your request. No additional uses are granted (such as derivative works or other editions). For any other uses, please submit a new request.

If credit is given to another source for the material you requested, permission must be obtained from that source.

Copyright © 2013 Copyright Clearance Center, Inc. All Rights Reserved. Privacy statement.
Comments? We would like to hear from you. E-mail us at customercare@copyright.com

1 of 1 2/14/2013 9:59 AM

ELSEVIER LICENSE
TERMS AND CONDITIONS

Feb 14, 2013

This is a License Agreement between William M Gehling ("You") and Elsevier ("Elsevier") provided by Copyright Clearance Center ("CCC"). The license consists of your order details, the terms and conditions provided by Elsevier, and the payment terms and conditions.

All payments must be made in full to CCC. For payment instructions, please see information listed at the bottom of this form.

Supplier	Elsevier Limited The Boulevard,Langford Lane Kidlington,Oxford,OX5 1GB,UK
Registered Company Number	1982084
Customer name	William M Gehling
Customer address	Department of Chemistry
	Baton Rouge, LA 70803
License number	3087700223231
License date	Feb 14, 2013
Licensed content publisher	Elsevier
Licensed content publication	Proceedings of the Combustion Institute
Licensed content title	The role of combustion-generated radicals in the toxicity of PM2.5
Licensed content author	Barry Dellinger,William A. Pryor,Bafael Cueto,Giuseppe L. Squadrito,Walter A. Deutsch
Licensed content date	2000
Licensed content volume number	28
Licensed content issue number	2
Number of pages	7
Start Page	2675
End Page	2681
Type of Use	reuse in a thesis/dissertation
Portion	figures/tables/illustrations
Number of figures/tables /illustrations	1
Format	electronic
Are you the author of this Elsevier article?	No

Will you be translating?	No
Order reference number	
Title of your thesis/dissertation	Environmentally Persistent Free Radicals (EPFRs) in PM2.5: Their Contribution to Hydroxyl Radical Formation and Atmospheric Transformation
Expected completion date	May 2013
Estimated size (number of pages)	150
Elsevier VAT number	GB 494 6272 12
Permissions price	0.00 USD
VAT/Local Sales Tax	0.0 USD / 0.0 GBP
Total	0.00 USD
Terms and Conditions	

INTRODUCTION

1. The publisher for this copyrighted material is Elsevier. By clicking "accept" in connection with completing this licensing transaction, you agree that the following terms and conditions apply to this transaction (along with the Billing and Payment terms and conditions established by Copyright Clearance Center, Inc. ("CCC"), at the time that you opened your Rightslink account and that are available at any time at http://myaccount.copyright.com).

GENERAL TERMS

2. Elsevier hereby grants you permission to reproduce the aforementioned material subject to the terms and conditions indicated.

3. Acknowledgement: If any part of the material to be used (for example, figures) has appeared in our publication with credit or acknowledgement to another source, permission must also be sought from that source. If such permission is not obtained then that material may not be included in your publication/copies. Suitable acknowledgement to the source must be made, either as a footnote or in a reference list at the end of your publication, as follows:

"Reprinted from Publication title, Vol /edition number, Author(s), Title of article / title of chapter, Pages No., Copyright (Year), with permission from Elsevier [OR APPLICABLE SOCIETY COPYRIGHT OWNER]." Also Lancet special credit - "Reprinted from The Lancet, Vol. number, Author(s), Title of article, Pages No., Copyright (Year), with permission from Elsevier."

4. Reproduction of this material is confined to the purpose and/or media for which permission is hereby given.

5. Altering/Modifying Material: Not Permitted. However figures and illustrations may be altered/adapted minimally to serve your work. Any other abbreviations, additions, deletions and/or any other alterations shall be made only with prior written authorization of Elsevier Ltd. (Please contact Elsevier at permissions@elsevier.com)

6. If the permission fee for the requested use of our material is waived in this instance, please be advised that your future requests for Elsevier materials may attract a fee.

7. Reservation of Rights: Publisher reserves all rights not specifically granted in the combination of (i) the license details provided by you and accepted in the course of this licensing transaction, (ii) these terms and conditions and (iii) CCC's Billing and Payment terms and conditions.

8. License Contingent Upon Payment: While you may exercise the rights licensed immediately upon issuance of the license at the end of the licensing process for the transaction, provided that you have disclosed complete and accurate details of your proposed use, no license is finally effective unless and until full payment is received from you (either by publisher or by CCC) as provided in CCC's Billing and Payment terms and conditions. If full payment is not received on a timely basis, then any license preliminarily granted shall be deemed automatically revoked and shall be void as if never granted. Further, in the event that you breach any of these terms and conditions or any of CCC's Billing and Payment terms and conditions, the license is automatically revoked and shall be void as if never granted. Use of materials as described in a revoked license, as well as any use of the materials beyond the scope of an unrevoked license, may constitute copyright infringement and publisher reserves the right to take any and all action to protect its copyright in the materials.

9. Warranties: Publisher makes no representations or warranties with respect to the licensed material.

10. Indemnity: You hereby indemnify and agree to hold harmless publisher and CCC, and their respective officers, directors, employees and agents, from and against any and all claims arising out of your use of the licensed material other than as specifically authorized pursuant to this license.

11. No Transfer of License: This license is personal to you and may not be sublicensed, assigned, or transferred by you to any other person without publisher's written permission.

12. No Amendment Except in Writing: This license may not be amended except in a writing signed by both parties (or, in the case of publisher, by CCC on publisher's behalf).

13. Objection to Contrary Terms: Publisher hereby objects to any terms contained in any purchase order, acknowledgment, check endorsement or other writing prepared by you, which terms are inconsistent with these terms and conditions or CCC's Billing and Payment terms and conditions. These terms and conditions, together with CCC's Billing and Payment

terms and conditions (which are incorporated herein), comprise the entire agreement between you and publisher (and CCC) concerning this licensing transaction. In the event of any conflict between your obligations established by these terms and conditions and those established by CCC's Billing and Payment terms and conditions, these terms and conditions shall control.

14. Revocation: Elsevier or Copyright Clearance Center may deny the permissions described in this License at their sole discretion, for any reason or no reason, with a full refund payable to you. Notice of such denial will be made using the contact information provided by you. Failure to receive such notice will not alter or invalidate the denial. In no event will Elsevier or Copyright Clearance Center be responsible or liable for any costs, expenses or damage incurred by you as a result of a denial of your permission request, other than a refund of the amount(s) paid by you to Elsevier and/or Copyright Clearance Center for denied permissions.

LIMITED LICENSE

The following terms and conditions apply only to specific license types:

15. **Translation**: This permission is granted for non-exclusive world **English** rights only unless your license was granted for translation rights. If you licensed translation rights you may only translate this content into the languages you requested. A professional translator must perform all translations and reproduce the content word for word preserving the integrity of the article. If this license is to re-use 1 or 2 figures then permission is granted for non-exclusive world rights in all languages.

16. **Website**: The following terms and conditions apply to electronic reserve and author websites:
Electronic reserve: If licensed material is to be posted to website, the web site is to be password-protected and made available only to bona fide students registered on a relevant course if:
This license was made in connection with a course,
This permission is granted for 1 year only. You may obtain a license for future website posting,
All content posted to the web site must maintain the copyright information line on the bottom of each image,
A hyper-text must be included to the Homepage of the journal from which you are licensing at http://www.sciencedirect.com/science/journal/xxxxx or the Elsevier homepage for books at http://www.elsevier.com , and
Central Storage: This license does not include permission for a scanned version of the material to be stored in a central repository such as that provided by Heron/XanEdu.

17. **Author website** for journals with the following additional clauses:

All content posted to the web site must maintain the copyright information line on the bottom of each image, and the permission granted is limited to the personal version of your paper. You are not allowed to download and post the published electronic version of your article (whether PDF or HTML, proof or final version), nor may you scan the printed edition to create an electronic version. A hyper-text must be included to the Homepage of the journal from which you are licensing at http://www.sciencedirect.com/science/journal/xxxxx . As part of our normal production process, you will receive an e-mail notice when your article appears on Elsevier's online service ScienceDirect (www.sciencedirect.com). That e-mail will include the article's Digital Object Identifier (DOI). This number provides the electronic link to the published article and should be included in the posting of your personal version. We ask that you wait until you receive this e-mail and have the DOI to do any posting.

Central Storage: This license does not include permission for a scanned version of the material to be stored in a central repository such as that provided by Heron/XanEdu.

18. **Author website** for books with the following additional clauses:
Authors are permitted to place a brief summary of their work online only.
A hyper-text must be included to the Elsevier homepage at http://www.elsevier.com . All content posted to the web site must maintain the copyright information line on the bottom of each image. You are not allowed to download and post the published electronic version of your chapter, nor may you scan the printed edition to create an electronic version.

Central Storage: This license does not include permission for a scanned version of the material to be stored in a central repository such as that provided by Heron/XanEdu.

19. **Website** (regular and for author): A hyper-text must be included to the Homepage of the journal from which you are licensing at http://www.sciencedirect.com/science/journal/xxxxx. or for books to the Elsevier homepage at http://www.elsevier.com

20. **Thesis/Dissertation**: If your license is for use in a thesis/dissertation your thesis may be submitted to your institution in either print or electronic form. Should your thesis be published commercially, please reapply for permission. These requirements include permission for the Library and Archives of Canada to supply single copies, on demand, of the complete thesis and include permission for UMI to supply single copies, on demand, of the complete thesis. Should your thesis be published commercially, please reapply for permission.

21. **Other Conditions**:

v1.6

If you would like to pay for this license now, please remit this license along with your payment made payable to "COPYRIGHT CLEARANCE CENTER" otherwise you will be invoiced within 48 hours of the license date. Payment should be in the form of a check or money order referencing your account number and this invoice number RLNK500956930.

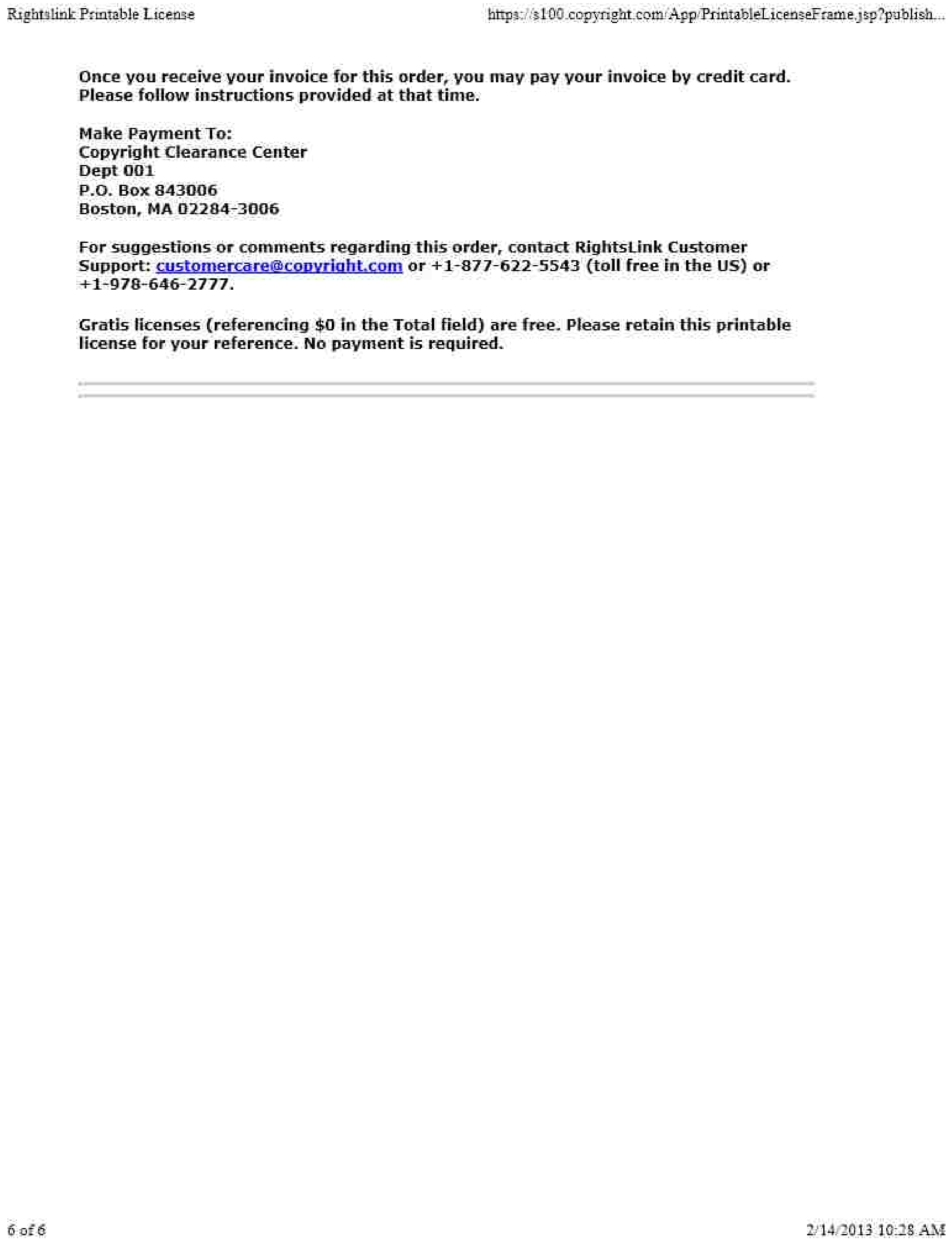

Once you receive your invoice for this order, you may pay your invoice by credit card. Please follow instructions provided at that time.

Make Payment To:
Copyright Clearance Center
Dept 001
P.O. Box 843006
Boston, MA 02284-3006

For suggestions or comments regarding this order, contact RightsLink Customer Support: customercare@copyright.com or +1-877-622-5543 (toll free in the US) or +1-978-646-2777.

Gratis licenses (referencing $0 in the Total field) are free. Please retain this printable license for your reference. No payment is required.

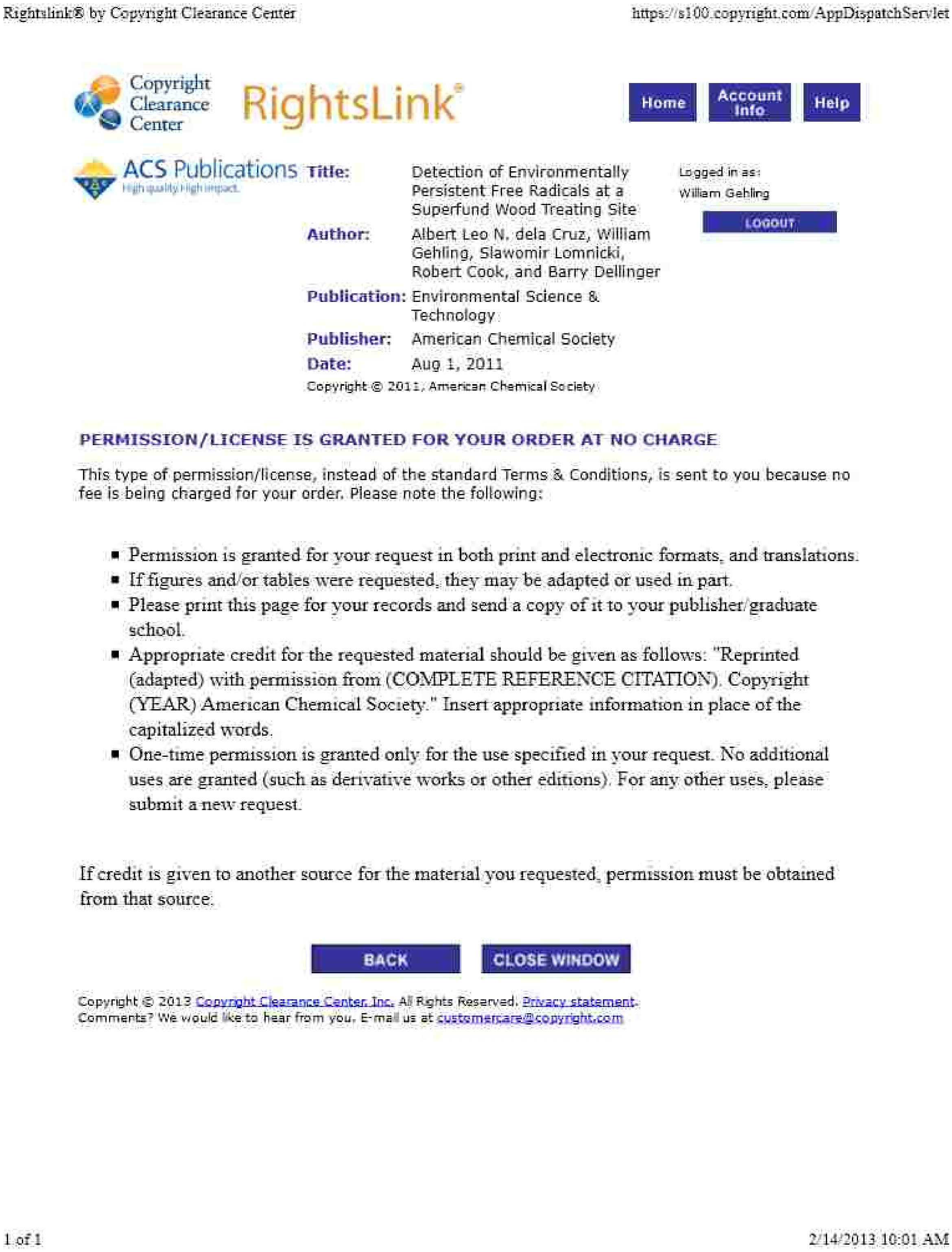

Rightslink® by Copyright Clearance Center https://s100.copyright.com/AppDispatchServlet

Title:	Detection of Environmentally Persistent Free Radicals at a Superfund Wood Treating Site
Author:	Albert Leo N. dela Cruz, William Gehling, Slawomir Lomnicki, Robert Cook, and Barry Dellinger
Publication:	Environmental Science & Technology
Publisher:	American Chemical Society
Date:	Aug 1, 2011

Copyright © 2011, American Chemical Society

Logged in as:
William Gehling

PERMISSION/LICENSE IS GRANTED FOR YOUR ORDER AT NO CHARGE

This type of permission/license, instead of the standard Terms & Conditions, is sent to you because no fee is being charged for your order. Please note the following:

- Permission is granted for your request in both print and electronic formats, and translations.
- If figures and/or tables were requested, they may be adapted or used in part.
- Please print this page for your records and send a copy of it to your publisher/graduate school.
- Appropriate credit for the requested material should be given as follows: "Reprinted (adapted) with permission from (COMPLETE REFERENCE CITATION). Copyright (YEAR) American Chemical Society." Insert appropriate information in place of the capitalized words.
- One-time permission is granted only for the use specified in your request. No additional uses are granted (such as derivative works or other editions). For any other uses, please submit a new request.

If credit is given to another source for the material you requested, permission must be obtained from that source.

Copyright © 2013 Copyright Clearance Center, Inc. All Rights Reserved. Privacy statement.
Comments? We would like to hear from you. E-mail us at customercare@copyright.com

1 of 1 2/14/2013 10:01 AM

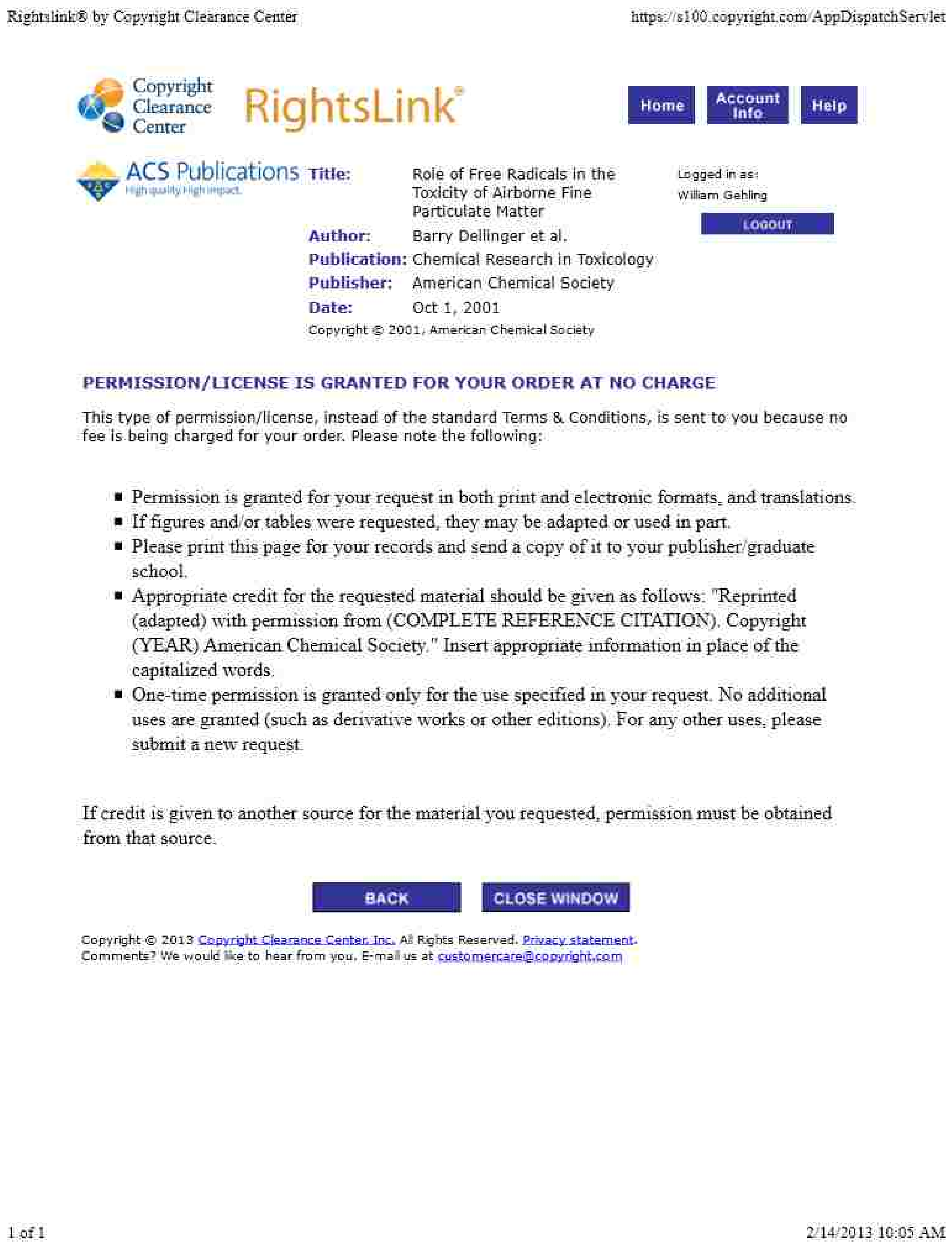

Rightslink® by Copyright Clearance Center https://s100.copyright.com/AppDispatchServlet

Title: Role of Free Radicals in the Toxicity of Airborne Fine Particulate Matter

Author: Barry Dellinger et al.

Publication: Chemical Research in Toxicology

Publisher: American Chemical Society

Date: Oct 1, 2001

Copyright © 2001, American Chemical Society

Logged in as:
William Gehling

PERMISSION/LICENSE IS GRANTED FOR YOUR ORDER AT NO CHARGE

This type of permission/license, instead of the standard Terms & Conditions, is sent to you because no fee is being charged for your order. Please note the following:

- Permission is granted for your request in both print and electronic formats, and translations.
- If figures and/or tables were requested, they may be adapted or used in part.
- Please print this page for your records and send a copy of it to your publisher/graduate school.
- Appropriate credit for the requested material should be given as follows: "Reprinted (adapted) with permission from (COMPLETE REFERENCE CITATION). Copyright (YEAR) American Chemical Society." Insert appropriate information in place of the capitalized words.
- One-time permission is granted only for the use specified in your request. No additional uses are granted (such as derivative works or other editions). For any other uses, please submit a new request.

If credit is given to another source for the material you requested, permission must be obtained from that source.

Copyright © 2013 Copyright Clearance Center, Inc. All Rights Reserved. Privacy statement.
Comments? We would like to hear from you. E-mail us at customercare@copyright.com

1 of 1 2/14/2013 10:05 AM

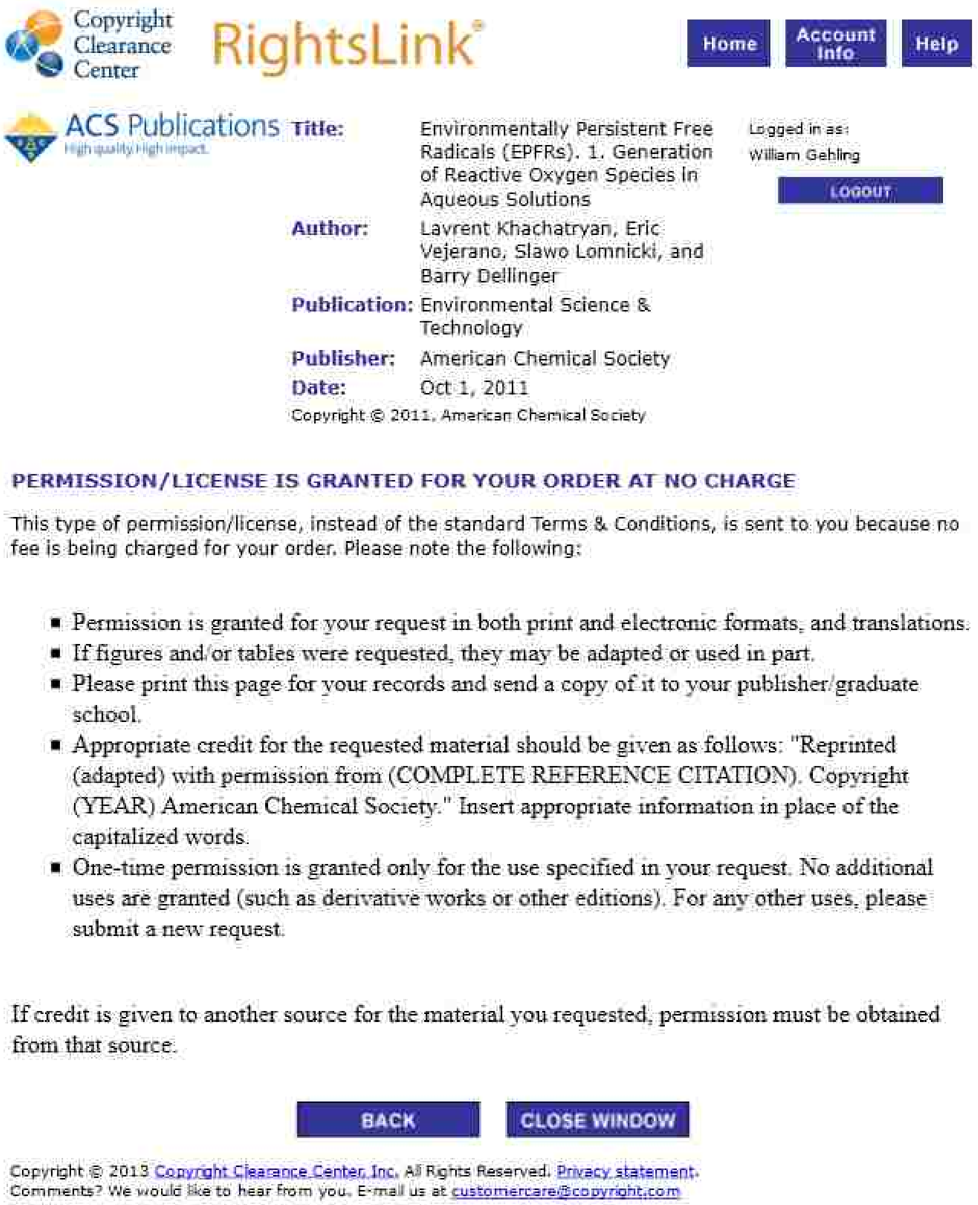

Title: Environmentally Persistent Free Radicals (EPFRs). 1. Generation of Reactive Oxygen Species in Aqueous Solutions

Author: Lavrent Khachatryan, Eric Vejerano, Slawo Lomnicki, and Barry Dellinger

Publication: Environmental Science & Technology

Publisher: American Chemical Society

Date: Oct 1, 2011

Copyright © 2011, American Chemical Society

Logged in as:
William Gehling

PERMISSION/LICENSE IS GRANTED FOR YOUR ORDER AT NO CHARGE

This type of permission/license, instead of the standard Terms & Conditions, is sent to you because no fee is being charged for your order. Please note the following:

- Permission is granted for your request in both print and electronic formats, and translations.
- If figures and/or tables were requested, they may be adapted or used in part.
- Please print this page for your records and send a copy of it to your publisher/graduate school.
- Appropriate credit for the requested material should be given as follows: "Reprinted (adapted) with permission from (COMPLETE REFERENCE CITATION). Copyright (YEAR) American Chemical Society." Insert appropriate information in place of the capitalized words.
- One-time permission is granted only for the use specified in your request. No additional uses are granted (such as derivative works or other editions). For any other uses, please submit a new request.

If credit is given to another source for the material you requested, permission must be obtained from that source.

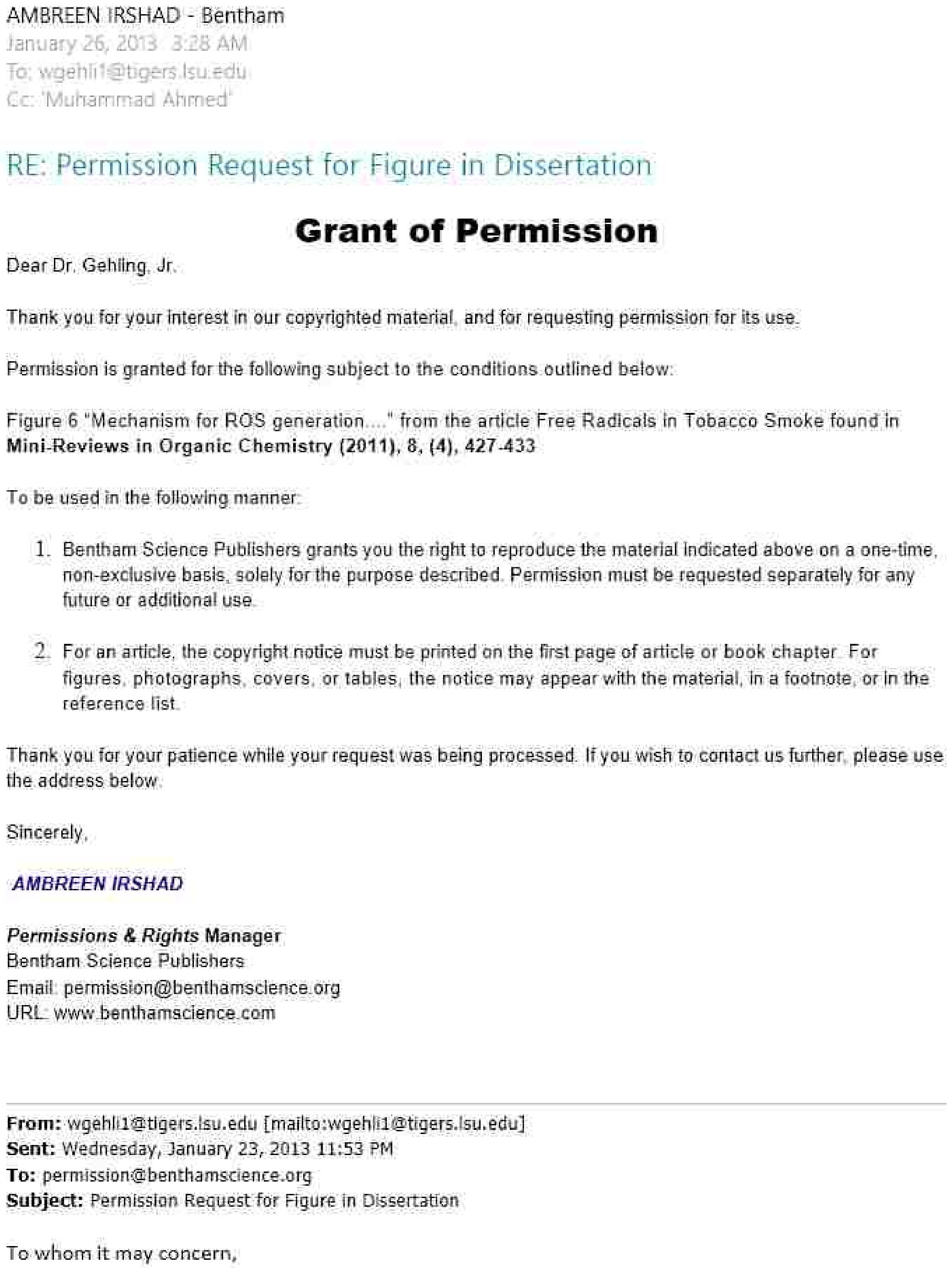

AMBREEN IRSHAD - Bentham
January 26, 2013 3:28 AM
To: wgehli1@tigers.lsu.edu
Cc: 'Muhammad Ahmed'

RE: Permission Request for Figure in Dissertation

Grant of Permission

Dear Dr. Gehling, Jr.

Thank you for your interest in our copyrighted material, and for requesting permission for its use.

Permission is granted for the following subject to the conditions outlined below:

Figure 6 "Mechanism for ROS generation...." from the article Free Radicals in Tobacco Smoke found in **Mini-Reviews in Organic Chemistry (2011), 8, (4), 427-433**

To be used in the following manner:

1. Bentham Science Publishers grants you the right to reproduce the material indicated above on a one-time, non-exclusive basis, solely for the purpose described. Permission must be requested separately for any future or additional use.
2. For an article, the copyright notice must be printed on the first page of article or book chapter. For figures, photographs, covers, or tables, the notice may appear with the material, in a footnote, or in the reference list.

Thank you for your patience while your request was being processed. If you wish to contact us further, please use the address below.

Sincerely,

AMBREEN IRSHAD

Permissions & Rights **Manager**
Bentham Science Publishers
Email: permission@benthamscience.org
URL: www.benthamscience.com

From: wgehli1@tigers.lsu.edu [mailto:wgehli1@tigers.lsu.edu]
Sent: Wednesday, January 23, 2013 11:53 PM
To: permission@benthamscience.org
Subject: Permission Request for Figure in Dissertation

To whom it may concern,

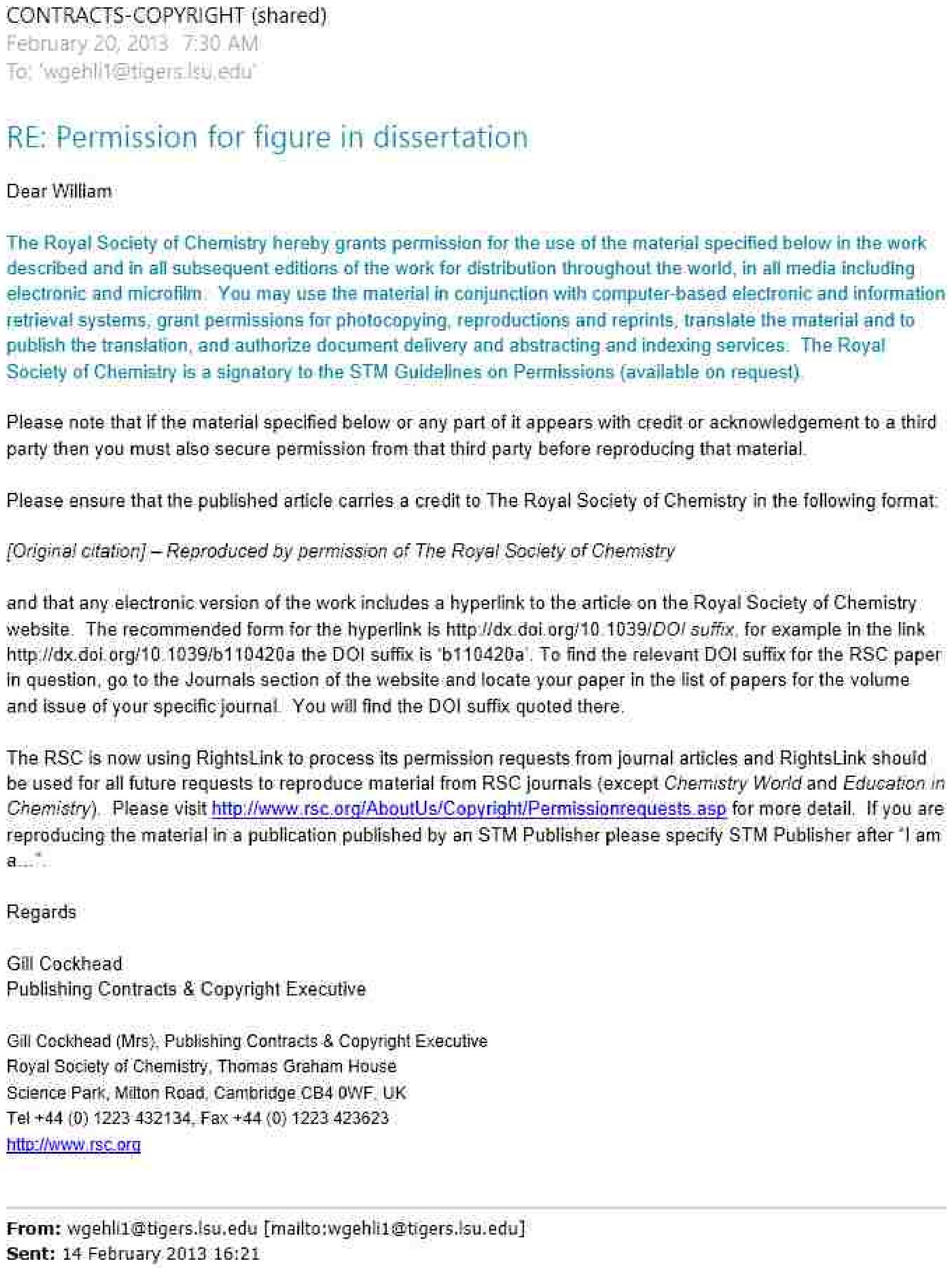

CONTRACTS-COPYRIGHT (shared)
February 20, 2013 7:30 AM
To: 'wgehli1@tigers.lsu.edu'

RE: Permission for figure in dissertation

Dear William

The Royal Society of Chemistry hereby grants permission for the use of the material specified below in the work described and in all subsequent editions of the work for distribution throughout the world, in all media including electronic and microfilm. You may use the material in conjunction with computer-based electronic and information retrieval systems, grant permissions for photocopying, reproductions and reprints, translate the material and to publish the translation, and authorize document delivery and abstracting and indexing services. The Royal Society of Chemistry is a signatory to the STM Guidelines on Permissions (available on request).

Please note that if the material specified below or any part of it appears with credit or acknowledgement to a third party then you must also secure permission from that third party before reproducing that material.

Please ensure that the published article carries a credit to The Royal Society of Chemistry in the following format:

[Original citation] – Reproduced by permission of The Royal Society of Chemistry

and that any electronic version of the work includes a hyperlink to the article on the Royal Society of Chemistry website. The recommended form for the hyperlink is http://dx.doi.org/10.1039/*DOI suffix*, for example in the link http://dx.doi.org/10.1039/b110420a the DOI suffix is 'b110420a'. To find the relevant DOI suffix for the RSC paper in question, go to the Journals section of the website and locate your paper in the list of papers for the volume and issue of your specific journal. You will find the DOI suffix quoted there.

The RSC is now using RightsLink to process its permission requests from journal articles and RightsLink should be used for all future requests to reproduce material from RSC journals (except *Chemistry World* and *Education in Chemistry*). Please visit http://www.rsc.org/AboutUs/Copyright/Permissionrequests.asp for more detail. If you are reproducing the material in a publication published by an STM Publisher please specify STM Publisher after "I am a...".

Regards

Gill Cockhead
Publishing Contracts & Copyright Executive

Gill Cockhead (Mrs), Publishing Contracts & Copyright Executive
Royal Society of Chemistry, Thomas Graham House
Science Park, Milton Road, Cambridge CB4 0WF, UK
Tel +44 (0) 1223 432134, Fax +44 (0) 1223 423623
http://www.rsc.org

From: wgehli1@tigers.lsu.edu [mailto:wgehli1@tigers.lsu.edu]
Sent: 14 February 2013 16:21

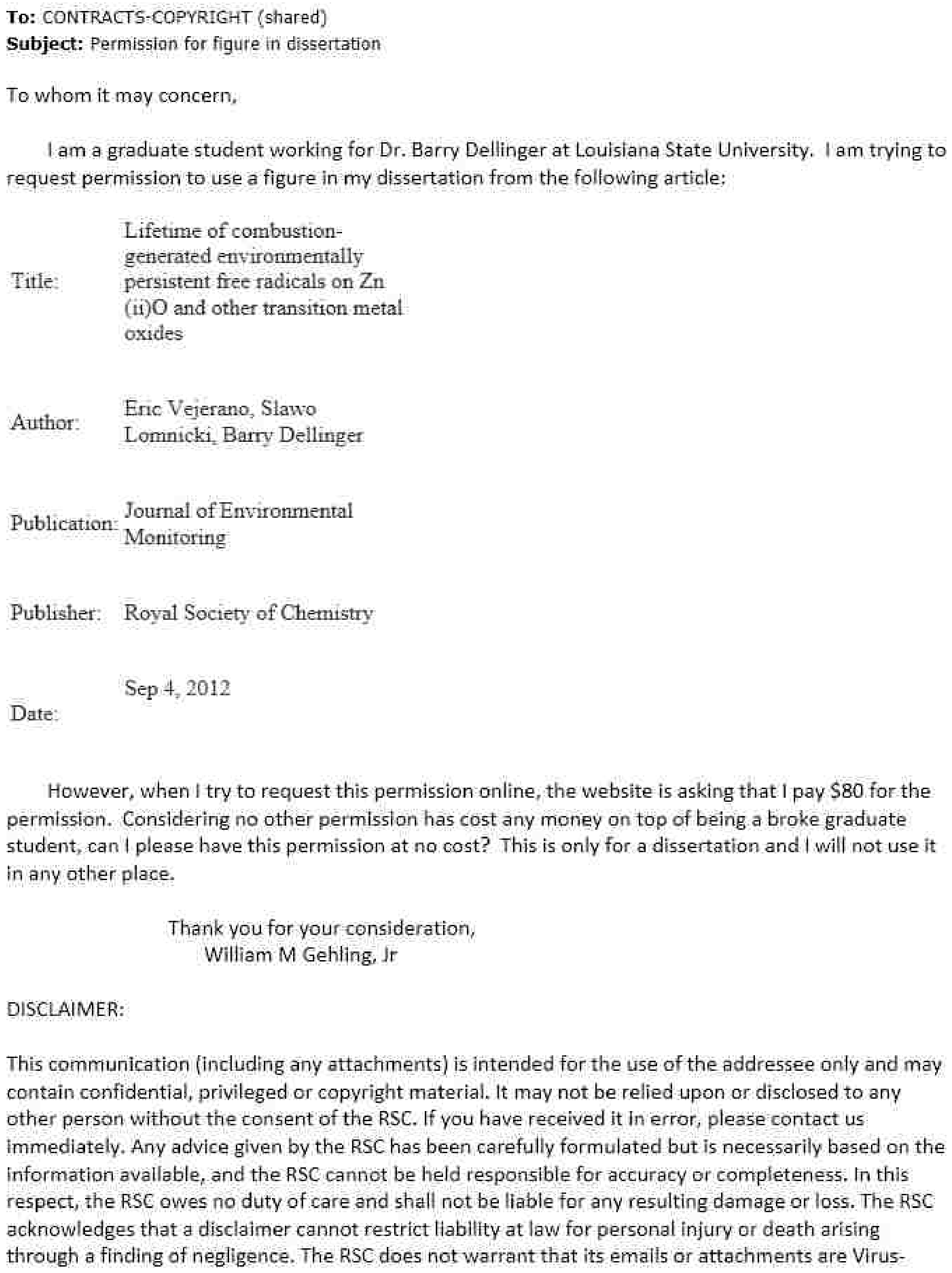

To: CONTRACTS-COPYRIGHT (shared)
Subject: Permission for figure in dissertation

To whom it may concern,

I am a graduate student working for Dr. Barry Dellinger at Louisiana State University. I am trying to request permission to use a figure in my dissertation from the following article:

Title:	Lifetime of combustion-generated environmentally persistent free radicals on Zn (ii)O and other transition metal oxides
Author:	Eric Vejerano, Slawo Lomnicki, Barry Dellinger
Publication:	Journal of Environmental Monitoring
Publisher:	Royal Society of Chemistry
Date:	Sep 4, 2012

However, when I try to request this permission online, the website is asking that I pay $80 for the permission. Considering no other permission has cost any money on top of being a broke graduate student, can I please have this permission at no cost? This is only for a dissertation and I will not use it in any other place.

Thank you for your consideration,
William M Gehling, Jr

VITA

William Micheal Gehling, Jr. was born 1980 in Baton Rouge, Louisiana. He completed his Bachelor of Science in chemistry from Northwestern State University in May 2003. Thereafter, he worked in the environmental regulatory field as an analytical/instrumental chemist and a radiochemist before pursuing his graduate studies. He pursued his doctoral degree in physical environmental chemistry at Louisiana State University in Baton Rouge on August 2006. His research was under the mentorship of Dr. Barry Dellinger, Professor, Patrick F. Taylor Chair, and Director of the LSU Superfund Research Center. He will receive his Doctor of Philosophy degree in May 2013.